THE ROLE OF INSULIN RECEPTOR SUBSTRATE 2 IN BETA CELL FUNCTION

A thesis submitted to the University of London
for the degree of Doctor of Philosophy
by

HELEN HEFFRON

Department of Medicine
University College London
Rayne Institute
5 University Street
London, WC1E 6JJ.

August 2006

ProQuest LLC
789 East Eisenhower Parkway
P.O. Box 1346
Ann Arbor, MI 48106-1346

Abstract.

Insulin receptor substrate (Irs) 2 plays complex roles in the regulation of glucose homeostasis, energy balance and CNS development. To address the tissue-specific role of Irs2 signalling events, conditional Irs2-deficient mice were generated. *Irs2lox/lox* mice were crossed with mice expressing *Cre recombinase* under the control of the rat insulin II gene promoter (*RIPCre* mice). Deletion of *Irs2* occurred in pancreatic β cells and in a population of hypothalamic neurons thus generating *RIPCreIrs2KO* mice. *RIPCreIrs2KO* mice displayed impaired glucose tolerance, reduced beta cell mass and islet number but remained hyperinsulinaemic. Over time some recovery in islet mass was seen with islets not expressing *Cre* repopulating the islets.

Furthermore *RIPCreIrs2KO* mice developed a prominent hypothalamic phenotype with hyperphagia, obesity, increased body length and hyperleptinaemia. *RIPCreIrs2KO* mice were sensitive to leptin treatment and displayed a normal metabolic rate. Characterisation of the hypothalamic neurons that express Cre recombinase revealed that they did not express pro-opiomelanocortin or neuropeptide Y. These findings therefore demonstrate a critical role for intrinsic Irs2 signalling pathways in β-cell and hypothalamic function and give insights into novel hypothalamic neuronal populations involved in the regulation of energy homeostasis.

Deleting *STAT3* in the same tissues (*RIPCreSTAT3KO*) resulted in a mouse with no β cell phenotype but which developed obesity. This obesity was not due to hyperphagia and was possibly due to an increase in activity, although this has not been confirmed.

In addition to this, *RIPCreSTAT3KO* mice were sensitive to leptin treatment. These findings therefore demonstrate that STAT3 signalling pathways are not needed for normal β-cell mass and function but that STAT3 in the hypothalamus plays an important role in body weight maintenance.

ACKNOWLEDGEMENTS

I would like to thank Professor Dominic Withers for his guidance throughout the duration of this work and also for giving me the opportunity to work in his laboratory. I would also like to thank the BBSRC and AstraZeneca for funding this work.

I would like to thank all members of the Withers lab, past and present, for all their help over the years. In particular I would like to thank Dr David Bedford and Dr Marcus Simmgen for all their help in the beginning, and Dr Melanie Clements, Hind Al-Qassab and Steve Lingard for making my bay such a nice place to work.

I would like to thank Dr Dave Smith at AstraZeneca for all his help and for providing me with the opportunity to carry out the gene expression studies, thanks go to all members of the CVGI group for making me so welcome, and in particular to Alison Davies for all her help and for introducing me to the joys of the 384 well plate.

I also thank Dr Kerensa Heffron for allowing me to stay in her home for the last three years and for all her support and advice.

I wish to thank Ann Heffron for all her support and encouragement, and for reminding me that no matter how badly my work was going, hers was going worse and at least I had heating!

Finally, I would like to thank my parents for their support and understanding over the last three years. This thesis is dedicated to them

1. INTRODUCTION

1.1 Type 2 diabetes: a worldwide epidemic

Diabetes is currently the most common endocrine disease worldwide. The number of people diagnosed with diabetes has risen rapidly in the last two decades, and this number is predicted to rise further (Figure 1). In the year 2003, 194.2 million people worldwide were diabetic with this figure predicted to rise to 332.8 million people worldwide by 2030 (Figure 1). This increase is almost entirely due to the rise in type 2 diabetes, which accounts for 90% of all cases (Zimmet *et al.*, 2001). One of the main risk factors for development of type 2 diabetes is obesity. The incidence of obesity is increasing in both developed and developing countries. For example in the UK currently over two thirds of men and half of women are overweight or obese (Peeters *et al.*, 2003), and in the USA 65% of the adult population are overweight or obese (Cheng, 2005).

The recent rise in the incidence of childhood obesity has resulted in the age of onset of type 2 diabetes falling. This has major implications for future health care costs, with type 2 diabetes increasing the risk of developing cardiovascular disease. It is predicted that by the year 2011, 10% of the NHS budget will be spent on treating patients with type 2 diabetes (Diabetes UK).

However, despite significant progress in our understanding of the mechanisms by which energy homeostasis is regulated, the precise pathophysiological relationships between obesity, insulin resistance and type 2 diabetes are not completely understood.

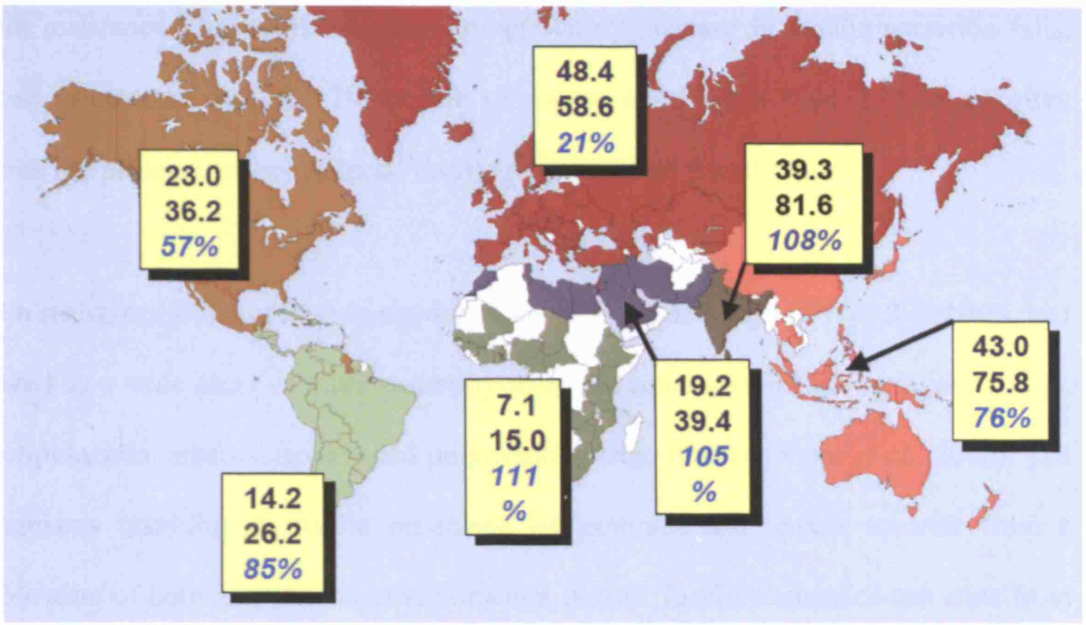

Figure 1. Global prediction for diabetes rates.

Top figure: number of people with diabetes in 2003, lower figure: predicted number of people with diabetes in 2030, percentage increase in blue. (Wild et al., 2004)

1.2 Overview of insulin resistance, type 2 diabetes and obesity

Type 2 diabetes is a complex metabolic disorder characterised by a triad of: 1) resistance to insulin action on glucose uptake in peripheral tissues, especially skeletal muscle and adipose tissue, 2) impaired insulin action to inhibit hepatic glucose production and 3) dysregulated insulin secretion. Insulin resistance is one of the earliest pathophysiological abnormalities in type 2 diabetes, and is frequently seen in non-diabetic relatives of diabetic subjects. However, insulin resistance does not necessarily lead to overt hyperglycaemia, because normally β-cells are capable of secreting sufficient amounts of insulin to offset the defects in insulin action. β-cell compensation in the face of insulin resistance occurs due to both an increase in the production of insulin by individual β-

cells, and also an overall increase in β-cell mass resulting in a state of compensated insulin resistance. However, once this compensatory increase in insulin secretion fails, glucose intolerance follows. Hence the development of overt type 2 diabetes often requires the presence of two defects: insulin resistance and β-cell failure.

Insulin resistance is therefore a fundamental factor in the aetiology of type 2 diabetes, and is linked to a wide array of other pathophysiological conditions including: hypertension, hyperlipidaemia, atherosclerosis, and polycystic ovarian disease (Kahn *et al.*, 2000). The mechanisms resulting in insulin resistance are complex and appear to arise from a combination of both genetic and environmental factors. Insulin resistance can arise from changes in the expression of proteins or genes that are targets of insulin action, cross talk from other hormonal systems (Saltiel *et al.*, 2001), metabolic abnormalities (O'Rahilly *et al.*, 2005; Saltiel *et al.*, 2001) or, more rarely, defects in insulin signal transduction via the insulin receptor (Saltiel *et al.*, 2001). In most cases, type 2 diabetes is a polygenic disease with complex inheritance patterns (O'Rahilly *et al.*, 2005). A strong genetic component is suggested by the concordance between monozygotic twins and increased prevalence in first-degree relatives of affected individuals. Environmental factors, especially diet, physical activity and age, interact with genetic predisposition to affect disease prevalence.

Obesity is a major risk factor for insulin resistance and therefore type 2 diabetes. The precise mechanisms whereby obesity causes insulin resistance are complex and not completely understood. However, a number of pathophysiological processes are thought to be involved. The elevated free fatty acid (FFA) levels and their metabolites, seen in

obesity are known to impair insulin action in skeletal muscle by acting negatively upon elements of the insulin-signalling pathway (Frederich *et al.*, 1995; Friedman, 2002).

It has also become clear that the excess FFAs seen in obesity may also impair pancreatic islet function and thus contribute to the beta cell defect seen in type 2 diabetes (Unger *et al.*, 2001; Zraika *et al.*, 2002).

In addition to this, adipose tissue production of cytokines, such as tumour necrosis factor α inhibits insulin signalling. Although leptin levels are increased in obesity, there is evidence that prolonged hyperglycaemia reduces leptin levels (Yildiz *et al.*, 2005), and that leptin treatment reduces plasma glucose and insulin levels in leptin-deficient patients with diabetes (Yildiz *et al.*, 2005).

Adiponectin has also been implicated in insulin resistance and is produced by adipose tissue at very high concentrations. Unlike other adipokines, adiponectin production is inversely proportional to adipose tissue mass (Whitehead *et al.*, 2006). Adiponectin has been shown to be reduced in obese and insulin resistant states and the adiponectin knockout mouse displays insulin resistance and glucose intolerance (Maeda *et al.*, 2002).

Adiponectin also has a strong anti-inflammatory role, with adopinectin levels being inversely proportional to inflammatory markers, including C-reactive peptide (CRP) (Whitehead *et al.*, 2006). The adiponectin knockout mouse shows increased atherogenesis and an increased vascular smooth muscle proliferation in response to injury, which can be prevented by administration of adiponectin (Ouchi *et al.*, 2003).

Another recently discovered adipokine that may contribute to the pathogensis of type 2 diabetes is serum retinol binding protein 4 (RBP4). Expression of RBP4 was found to be increased in the insulin-resistant adipose tissue specific GLUT4 knockout mouse and serum RBP4 levels are increased in insulin-resistant mice and humans (Yang *et al.*, 2005). It was shown that increasing RBP4 serum levels caused systemic insulin resistance and that insulin action could be improved by reducing RBP4 (Yang *et al.*, 2005) suggesting that RBP4 is, at least partially, responsible for obesity-induced insulin resistance and is a potential therapeutic target.

In addition to this, low grade inflammation is a significant feature of the metabolic syndrome, with elevated levels of inflammatory markers Interleukin-6 and C-reactive protein seen in obese adolescents (Weiss *et al.*, 2004).

Fatty acids, in the short term, induce insulin secretion by their action on the GPR40 receptor in the β-cell membrane (Itoh *et al.*, 2003). Activation of the GPR40 receptor promotes insulin secretion in response to glucose. However, as obesity develops adipocytes become resistant to the effects of insulin, leading to an increase in plasma FFA levels (Medina-Gomez *et al.*, 2005).

Therefore, it is clear that understanding the mechanisms that regulate glucose homeostasis, insulin sensitivity and whole body energy storage will have an important role in our understanding of the pathophysiology of type 2 diabetes.

1.3 Acute regulation of peripheral glucose homeostasis by insulin

1.3.1 Pancreatic islet function and glucose uptake

Plasma glucose levels are tightly regulated between 4 and 7 mM in normal individuals (DeFronzo, 1997). This narrow range is governed by a balance between glucose absorption from the gut, hepatic glucose production and uptake of glucose by peripheral tissues and organs. The balance between the utilization and production of glucose is maintained at equilibrium by the opposing actions of insulin and glucagon. As the result of a meal blood glucose levels rise and insulin is released from β-cells within the islets of Langerhans, stimulating glucose transport into muscle and fat via GLUT4 glucose transporter mechanisms (Kahn *et al.*, 2000). When glucose levels fall, glucagon is released from the α-cells and promotes the release of glucose stores and newly synthesised glucose into the bloodstream. Insulin and glucagon therefore act to ensure that glucose homeostasis is maintained throughout a wide variety of physiological states.

1.3.2 Insulin and gene expression

In addition to the acute effects upon glucose uptake, insulin also regulates metabolism at the level of gene transcription and translation, regulating processes such as gluconeogenesis and lipogenesis. For example, at the transcriptional level acute insulin treatment decreases messenger RNAs encoding gluconeogenic enzymes such as phosphoenolpyruvate carboxykinase, and increases mRNAs encoding lipogenic enzymes via the action of the transcription factor SREBP1c (Shimomura *et al.*, 2000).

1.4 Insulin receptor signalling cascade

Insulin action on glucose uptake in muscle and fat results from a cascade of signalling events from the insulin receptor, culminating in translocation of the major insulin responsive glucose transporter (GLUT-4) from intracellular vesicles to the plasma membrane (Holman *et al.*, 1997; Myers *et al.*, 1996); (Fig 2). Insulin binds to its cell surface receptor, stimulating receptor autophosphorylation and activation of its intrinsic kinase activity. This results in tyrosine phosphorylation of several cytosolic docking proteins, the best characterised of which are the insulin receptor substrate (Irs) proteins. There are at least four closely related insulin receptor substrate proteins (Irs1-4) which have different signalling functions. Findings from transgenic mouse models suggest that many of the cellular responses to insulin, especially those that are associated with somatic growth and carbohydrate metabolism, are largely mediated through Irs1 and Irs2. Once phosphorylated, Irs proteins bind to various effector molecules including the regulatory subunit of phosphoinositol 3-kinase via Src homology 2 (SH2) domains. Recruitment of its catalytic subunit, results in activation of phosphoinositol 3-kinase, which is necessary for insulin action on glucose transport, glycogen synthase, protein synthesis, antilipolysis, and suppression of hepatic gluconeogenesis through regulation of phosphoenolpyruvate carboxykinase (PEPCK) gene expression (Shepherd *et al.*, 1998). One of the key downstream targets of insulin-activated PI3K is protein kinase B (PKB, also known as AKT), a protein that has been implicated in the control of cell survival and metabolism.

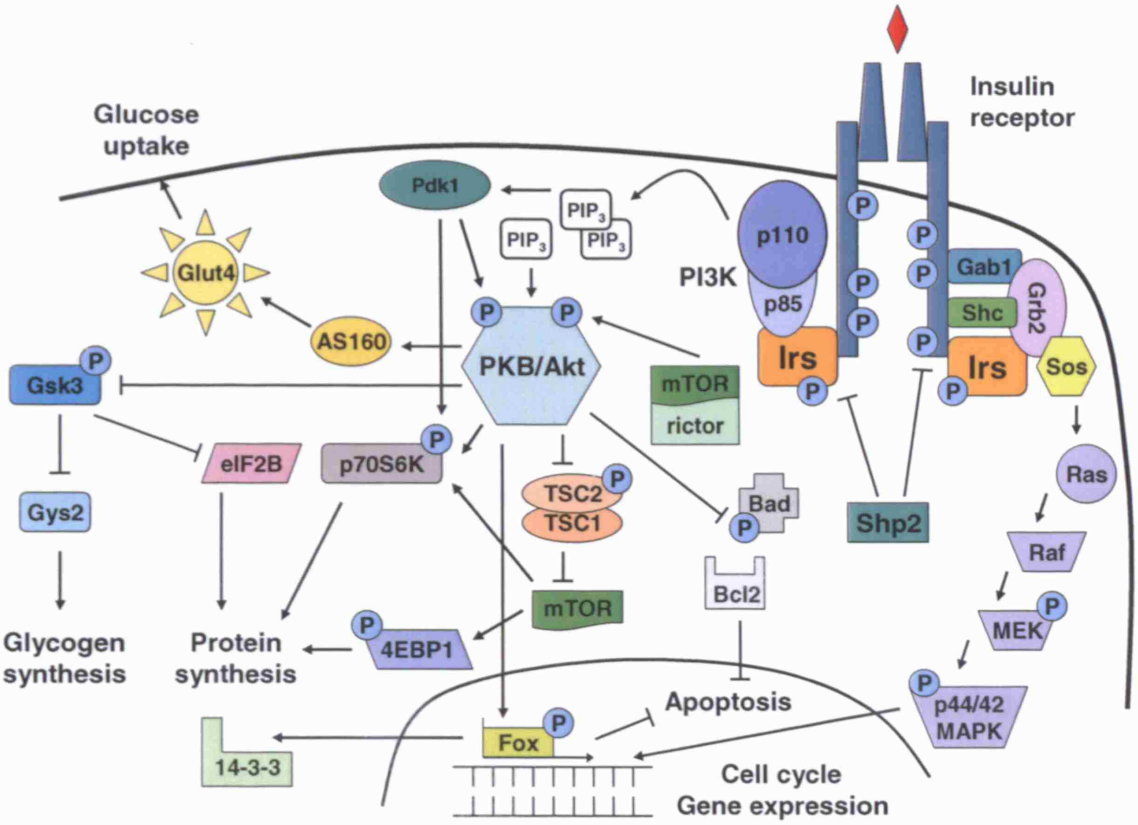

Figure 2. Insulin signalling cascade.

Following ligand binding, the activated insulin receptor recruits insulin receptor substrate (Irs) and other molecules (Grb2, Gab1, Shc). These scaffold proteins initiate a signalling cascade via Sos-Ras-Raf-MEK to activate p44/42 MAPK, which regulates gene transcription related to cell proliferation and apoptosis.

p110 recruitment to Irs-bound p85 activates PI3K and generates PIP_3 molecules. This leads to Pdk1-mediated PKB/Akt activation, which diversifies the insulin signal. Glucose transport is enhanced by AS160-mediated Glut4 translocation, and glycogen synthesis is stimulated by Gsk3 inhibition. PKB/Akt increases protein synthesis directly by activating p70S6 kinase and indirectly through TSC1:TSC2 complex phosphorylation, the mTOR-4EBP1 pathway, and the Gsk3-associated de-repression of eIF2B.

PKB/Akt phosphorylates nuclear Fox transcription factors, leading to their exclusion from the nucleus. Fox proteins control gene expression, elements of the cell cycle and influence apoptosis. PKB/Akt also regulates apoptosis through Bcl2-related proteins.

1.4.1 PI3K

The heterodimeric enzyme phosphatidylinositol 3-kinase (PI3K) catalyses the generation of 3-phosphorylated inositides (3-PIs) derived from the cell membrane. The multiple isoforms of PI3K have been classified into three classes, with class I the main type involved in insulin signalling. It consists of a p110 catalytic subunit whose activity is most commonly regulated by a p85 subunit although p55 subunits also exist (Vanhaesebroeck *et al.*, 2000).

Each of the phosphorylated IRS proteins has been found to associate with the p85 adapter subunit (Fantin *et al.*, 2000), thereby recruiting the p110 subunit to the plasma membrane where the activated PI3K can phosphorylate its phospholipid substrate. Phosphatidylinositol (3,4,5) triphosphate (PIP3) is the main product transducing the insulin signal further to the AGC superfamily of serine/threonine kinases through binding to their PH domain (Cantrell, 2001).

These play a central role in the insulin signal diversification to downstream pathways relating to carbohydrate metabolism and lipolysis, as well as to gene expression, transcription and protein turnover (Shepherd *et al.*, 1998).

Deletion of the p85α isoform increases insulin sensitivity in mice by increasing the activity of the p110 catalytic subunit, therefore increasing glucose transport into skeletal muscle and adipose tissue (Terauchi *et al.*, 1999). Deleting all of the isoforms leads to liver necrosis, hypoglycaemia, and perinatal death (Fruman *et al.*, 2000).

1.4.2 Akt

Mice with attenuated Akt acitivity in pancreatic islets display glucose intolerance coupled with defective insulin secretion (Bernal-Mizrachi *et al.*, 2004). *In vitro* studies on islets of these mice showed defects in Ca^{2+}-dependent insulin exocytosis.

It was also shown that these mice had defects in the adaptation of ß-cells to obesity-induced insulin resistance (Bernal-Mizrachi *et al.*, 2004) and this was found to be due to defective insulin exocytosis, as the capacity to increase ß-cell mass in response to insulin resistance was not impaired.

Activated Akt plays an important and diverse role in glucose homeostasis, three separately encoded proteins of which are known, Akt1/PKBα, Akt2/PKBβ, and Akt3/PKBγ.

The Akt2/PKBβ isoform mediates the insulin-dependent translocation of GLUT-4 molecules from intracellular storage vesicles into the plasma membrane (Bae *et al.*, 2003), thus facilitating glucose influx into the cell and lowering plasma glucose levels. Conversely, its absence leads to insulin resistance and hyperglycaemia (Cho *et al.*, 2001).

1.4.3 PDK

In addition to binding to Akt, 3-PI also binds to phosphoinositide-dependent kinase-1 (PDK1) (Cantrell, 2001). The intracellular location of unstimulated PDK1 remains controversial (Cantrell, 2001).

PDK1 also stimulates protein-70 S6 kinase (p70S6K) and exerts effects on cell growth and protein synthesis (Williams *et al.*, 2000). PDK1 therefore functions as a 'master switch' for a wide range of physiological processes (Mora *et al.*, 2004). Global deletion of PDK1 is embryonic lethal due to brain and neural crest abnormalities (Lawlor *et al.*, 2002). However, liver-specific deficiency was associated with defects in glucose homeostasis and premature death due to liver failure (Mora *et al.*, 2004).

1.4.4 p70 S6 Kinase

Another effector of the PI3 kinase signalling pathway, which is also sensitive to glucose is p70 S6 Kinase-1 (p70S6K1). p70S6K1 deficient mice have been generated. These mice do not show peripheral insulin resistance but have marked defects in glucose stimulated insulin secretion and in pancreatic insulin levels due to a decrease in β-cell size (Pende *et al.*, 2000; Um *et al.*, 2004). p70S6K-1 deficient mice were also resistant to diet-induced obesity, with this found to be due to an increase in β-oxidation resulting in reduced fat stores (Um *et al.*, 2004). When fed a high-fat diet, p70S6K-1 deficient mice do show hyperglycaemia and an increase in circulating FFAs, which results in insulin receptor desensitisation. However, these mice remain sensitive to insulin and their PI3K signalling is unaffected. This is due to the loss of an p70S6K-mediated negative feedback loop, in which under normal conditions activation of p70S6K results in serine phosphorylation of Irs1, inhibiting the PI3K pathway (Um *et al.*, 2004).

1.5 Glucose Stimulated Insulin Secretion (GSIS)

Insulin secretion by β-cells in response to an increase in glucose concentration is a very tightly controlled process. GSIS is biphasic and involves two main signalling pathways:

1. K_{ATP} channel dependent and 2. K_{ATP} independent pathways (Straub *et al.*, 2002). In the K_{ATP} dependent pathway the glucose transporter GLUT2 mediates uptake of glucose into the β-cell where it is phosphorylated by glucokinase. Oxidative phosphorylation of glucose leads to a rise in the intracellular ATP/ADP ratio causing K_{ATP} channels to close. The subsequent membrane depolarisation opens voltage-gated calcium channels and the influx of calcium triggers the release of insulin (Figure 3).

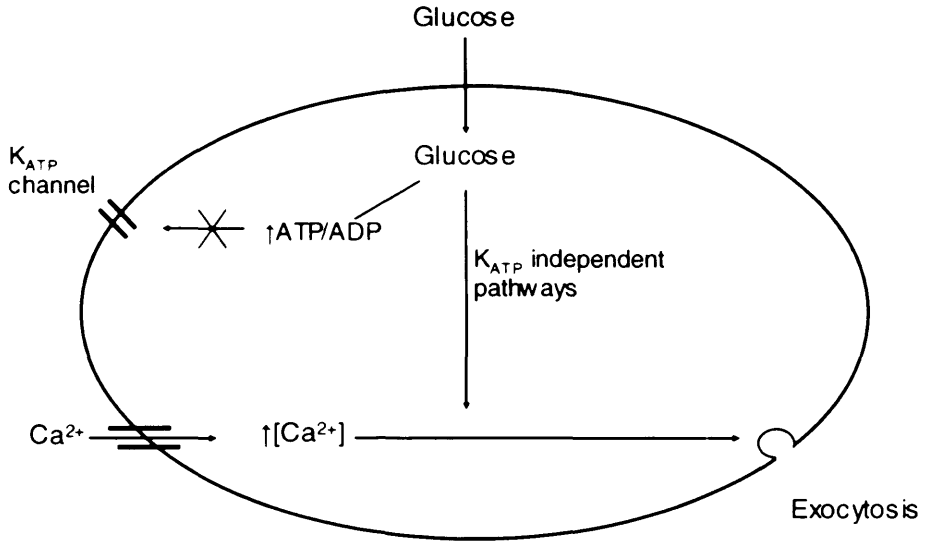

Figure 3. Glucose stimulated insulin secretion.

Glucose is taken up into the cell. Oxidative phosphorylation of glucose raises the ATP/ADP ratio and closes K_{ATP} channels. The resulting membrane depolarisation causes influx of Ca^{2+} which stimulates insulin exocytosis.

Activation of the K_{ATP} dependent pathway leads to a rapid release of insulin and forms the first phase of insulin secretion.

K_{ATP} channel independent pathways are responsible for the second phase insulin secretion, and act by augmenting the response to increased intracellular [Ca^{2+}], but the mechanisms for this are unknown

Typically, the first phase of insulin secretion only involves the release of a small percentage of insulin granules from the readily released pool of granules. The rest of the granules form the docked pool and the reserve pool, with these granules being released during the second phase of insulin secretion.

1.6 β-Cell growth

Under conditions of peripheral insulin resistance, pancreatic β-cells are able to mount a compensatory hyperinsulinaemic response, with an increase in both β-cell number and size. However, there is some controversy over where these new β-cells originate from.

There are 3 main ways in which β-cell number can be increased: either by a reduction in apoptosis (1) or by generation of new β-cells either via proliferation of existing cells (2) or by neogenesis from ductal precursor cells (3) (fig.4). However, the relative contribution of each of these mechanisms to the β-cell population is unclear.

It has recently been demonstrated, using lineage tracing and a cre/loxP system that pre-existing β-cells are the major source of new cells during life, and indeed that no new islets are formed by stem cells during adult life (Dor *et al.*, 2004). However this study does not definitively prove that new islets are not formed under condition that would induce regeneration, such as partial pancreatectomy.

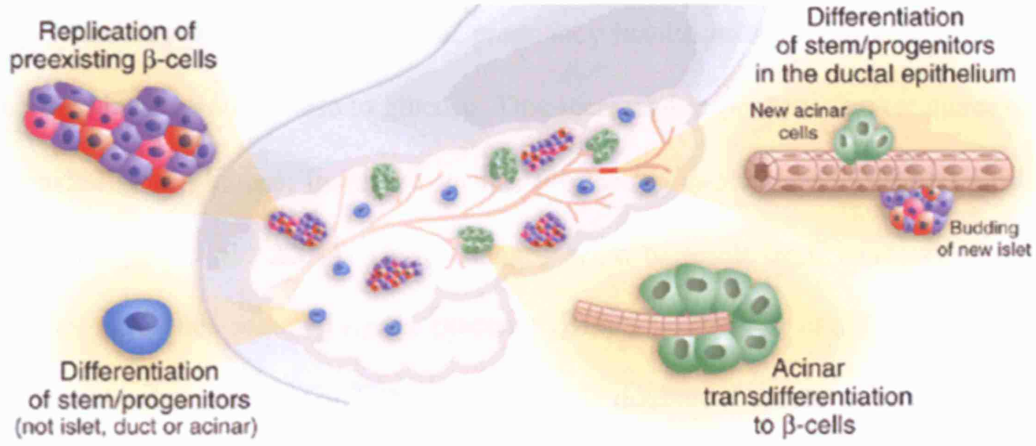

Figure 4. The pancreas as a source of new β-cells.

The pancreas is thought to be the main source of new β-cells through one of several possible mechanisms: Replication of pre-existing β-cells; differentiation of progenitor cells within the ductal epithelium; transdifferentiation of acinar cells and differentiation of stem cells. Adapted from Bonner-weir et al. 2005.

1.7 Pancreatic plasticity

Endocrine pancreas plasticity, the ability of the pancreas to change the β-cell mass in response to changes in insulin demand, is important in maintaining glucose homeostasis under a range of both physiological and pathological conditions.

1.7.1 Pregnancy

The best illustration of pancreatic plasticity occurs during pregnancy. In mammals, maternal metabolism changes to optimise nutrient delivery to the developing foetus during pregnancy. In the later stages of pregnancy insulin resistance is accompanied by an increase in insulin response to glucose. This increased response is due to: increased β-cell sensitivity to glucose; increased insulin production and changes to β-cell structure (Bernard-Kargar *et al.*, 2001). These changes seem to result from increased levels of pregnancy hormones secreted by the placenta (Bernard-Kargar *et al.*, 2001). It has been shown that by the end of pregnancy β-cell mass is doubled, but returns to normal by 10 days post-partum. This decrease in β-cell mass is due to both a decrease in cell volume and an increase in apoptosis (Scaglia *et al.*, 1995).

1.7.2 Obesity

In 75-80% of obese subjects glucose homeostasis is normal, despite peripheral insulin resistance. As in pregnancy, this is due to an increase in insulin secretion by individual β-cells and also by an overall increase in β-cell mass. However, the factors involved in increasing β-cell mass in obesity are not fully understood.

1.8 Apoptosis

Apoptosis, the genetically and metabolically determined process of cell death is important in normal cell turnover and homeostasis. A variety of factors can trigger apoptosis. Several models of type 2 diabetes have shown that the failure to compensate for insulin resistance is due to an increase in apoptosis in the β-cell rather then a decrease in proliferation (Butler *et al.*, 2003b; Pick *et al.*, 1998). In some cases inhibitors of RNA or protein synthesis can suppress apoptosis, suggesting that expression of these proteins trigger apoptosis. It is known that type 1 diabetes is accompanied by death of β-cells, but it is not clear whether this is a primary cause, and what the exact mechanism of cell death in diabetes is.

1.8.1 Glucose

Studies on isolated β-cells have shown that glucose promotes cell survival by blocking apoptosis (Hoorens *et al.*, 1996). It has been shown that β-cells undergo apoptosis when RNA or protein synthesis is blocked (Hoorens *et al.*, 1996), suggesting a constitutively active program of apoptosis. Exposure to high concentrations of glucose increases the number of active β-cells and decreases the rate of apoptosis. In addition to this, a prolonged period of reduced glucose sensitivity increases the rate of apoptosis. This study suggests that glucose activates β-cells to synthesise inhibitors of RNA and protein synthesis, thereby inhibiting the apoptotic process.

However, it has also been shown that the high concentrations of glucose seen in diabetes causes an increase in apoptosis through its effects on calcium channels (Bernard-Kargar *et al.*, 2001; Chandra *et al.*, 2001).

1.8.2 Free fatty acids (FFAs)

In the diabetic Zucker rat, the islets contain 100-fold higher levels of FFA's then those found in lean rats. In addition to this, culturing islets in FFA resulted in increased apoptosis accompanied by an increase in production of ceramide and nitric oxide (NO) (Mandrup-Poulsen, 2001).

1.8.3 Cytokines

Cytokines, such as interleukins, mediate cell death in both rodents and humans. Exposure to interleukin β (IL-1β) and interferon γ (IFN-γ) induces the gene coding for inducible nitric oxide synthase (iNOS). The resulting nitric oxide contributes to β-cell necrosis and apoptosis in rodents and apoptosis in humans (Eizirik *et al.*, 2001; Rhodes, 2005). Nitric oxide has also been implicated as a mediator of free fatty acid (FFA) induced cell death in type 2 diabetes (Shimabukuro *et al.*, 1998)

1.9 Increasing β-cell mass

There is currently much controversy surrounding which mechanism is most important in the compensatory response to insulin resistance.

1.9.1 β-cell neogenesis

During foetal development, ductal stem cells give rise to both endocrine and exocrine cells. During post-natal development, differentiation of endocrine cells from ductal epithelium continues. It has been proposed that changes in neogenesis could be associated

with diabetes. One study looking at insulin positive ductal cells in post-mortem pancreatic tissue did indeed show an increase in ductal insulin-positive cells in subjects with type 2 diabetes compared to non-diabetic controls (Jones *et al.*, 2001). In addition to this, it appears that in humans with type 2 diabetes β-cell neogenesis is upregulated while β-cell replication is unchanged (Butler *et al.*, 2003a)

Another study, which implied a role for neogenesis in adaptation to increased insulin demand, used rats fed a high sucrose diet. After 6 months these rats showed a reduced β-cell volume compared to control rats. Although these rats showed a decreased rate of apoptosis and an increase in β-cell replication, the rate of neogenesis was unchanged in comparison with wild-type rats (Del Zotto *et al.*, 2004). This suggests that the failure of these rats to adapt to an increased insulin demand was due to a failure to increase the rate of β-cell neogenesis.

1.9.2 β-cell replication

There is much evidence that β-cell proliferation plays an important role in pancreatic plasticity. I will now review some of the pathways that regulate β-cell replication.

1.9.2.1 Insulin-like Growth Factor 1 (IGF-1)

Both IGF-1 and the IGF-1 receptor are expressed in pancreatic β-cells. Mice lacking IGF-1 specifically in the pancreas show resistance to streptozotocin-induced diabetes, showing increased insulin production and a reduction in apoptosis (Lu *et al.*, 2004). These mice also show a delay in the onset of type 2 diabetes when fed a high-fat diet. This was

explained by an increase in islet area and by increased insulin production (Lu *et al.*, 2004). Thus, it appears that IGF-1 normally inhibits cell growth in the islet, but it is unclear which of these effects are mediated through the IGF-1 receptor and which are due to insulin receptor activation by IGF-1.

However mice lacking the IGF-1 receptor specifically in the β-cell show normal β-cell growth and development but have impaired glucose tolerance and glucose stimulated insulin secretion (Kulkarni *et al.*, 2002). This suggests that the IGF-1 receptor is important in control of β-cell function but not growth.

IGF-1 has also been shown to directly increase β-cell growth by inducing phosphorylation of extracellular-regulated kinase 1/2 (ERK1/2), glycogen synthase kinase-2 (GSK-3) and protein kinase B (PKB) (Lingohr *et al.*, 2002) It has also been demonstrated that this IGF-1 mediated proliferation was greatly increased in cells overexpressing Irs2 (Lingohr *et al.*, 2002), suggesting that IGF-1 acts by recruiting Irs2/PI3K signalling pathways.

1.9.2.2 Glucose

Glucose infusion in rats has also been shown to increase β-cell mass (Bouwens *et al.*, 2005) and glucose is also known to promote cell survival by suppressing apoptosis (Hoorens *et al.*, 1996).

1.9.2.3 Insulin receptor

Pancreatic ß-cell deletion of the insulin receptor in mice results in hyperglycaemia (Otani, 2004) and impaired glucose tolerance (Kulkarni *et al.*, 1999). These mice showed defects in insulin secretion, and it was shown that insulin content of islets in the knockout mouse was reduced. Consistent with this reduction in insulin output, these mice had an ~ 50% reduction in ß-cell mass (Otani *et al.*, 2004), shown to be due to a reduction in islet size (Kulkarni *et al.*, 1999).

1.9.2.4 IGF-1 Receptor

Mice lacking the IGF-1 receptor in ß-cells were glucose intolerant and also displayed a loss of first phase insulin secretion in response to glucose (Kulkarni *et al.*, 2002). However, these mice showed no abnormalities in islet size or number and β-cell mass is normal in these lines.

1.9.2.5 Combined insulin and IGF-1 receptor

Mice lacking both functional insulin and IGF-1 receptors in the ß-cell had normal islets at birth, but by three weeks of age had developed diabetes. This is in contrast to the single receptor knockouts described above. These double knockout mice were significantly hyperglycaemic and glucose intolerant with an almost complete reduction in first phase insulin secretion.

At 5 days of age no abnormalities in islet mass or architecture were seen in the double knockout, suggesting that insulin and IGF-1 receptor signalling are not vital for early islet development or function. However, by 2 weeks of age, these double knockout mice

showed a marked decrease in islet mass due to an increase in apoptosis, with a slight reduction in proliferation also seen (Ueki *et al.*, 2006). Therefore, insulin and IGF-1 signalling play an important role in maintaining ß-cell mass.

1.9.2.6 Insulin receptor substrate 2 (Irs2)

It has previously been shown that global *Irs2* null mice develop diabetes due to a decrease in β-cell mass and a failure in insulin secretion (Withers *et al.*, 1998). β-cell specific expression of Irs2 in *Irs2* null mice promotes β-cell growth and survival and protects against diabetes (Hennige *et al.*, 2003). This effect was more pronounced when Irs2 was expressed at a higher level. It was also demonstrated that, when transplanted, the transgenic islets overexpressing Irs2 were more effective at curing diabetes then transplantation of wild-type islets (Hennige *et al.*, 2003).

1.9.2.7 Cyclins

Cyclins promote cell replication by activating cyclin-dependent kinases which promote progression through the G_1 phase of the cell cycle. It has recently been shown that Cyclins D1 and D2 are necessary for β-cell growth and development. *CyclinD2* knockout mice show normal β-cell replication at a young age but by 3 months of age the rate of replication is decreased in comparison with control mice. This decrease in replication rate is also accompanied by a decrease in β-cell area (Kushner *et al.*, 2005). These mice did not develop progressive diabetes due to compensation by CyclinD1. This was supported by the observation that *CyclinD2*$^{-/-}$ *D1*$^{+/-}$ mice have severe defects in glucose homeostasis due to undetectable islet growth (Kushner *et al.*, 2005).

1.9.2.8 Signal Transducers and Activators of Transcription (STAT)

As discussed above, cyclins are important in adapting islet mass to reflect the metabolic needs . However, the factors regulating Cyclin D2 expression remain unclear although STAT5 has been shown to regulate the Cyclin D2 promoter (Friedrichsen *et al.*, 2003). Studies on β-cell lines have demonstrated that reduction in STAT5 reduces expression of Cyclin D2. In addition to this, induction of a constitutively active STAT5 stimulates transcription of Cyclin D2 and promotes cell proliferation (Friedrichsen *et al.*, 2003). Therefore it seems that STAT5 drives β-cell proliferation via Cyclin D2. It is not known however whether the STAT5 pathway is the major pathway determining β-cell mass, or if Cyclin D2 is the major target for STAT5.

It has also been shown using cells lines overexpressing STAT3, that STAT3 also increases proliferation of β-cells (Tsukiyama *et al.*, 2006). This proliferation was achieved without any loss of insulin secretion, even when the cells were challenged with high glucose concentrations. This proliferation was assumed to be due to the effects of STAT3 on CyclinD2 although this was not directly investigated in this study.

Deleting STAT3 in the ß-cell does not affect islet mass. However these mice show disordered islet architecture, with α- cells frequently seen within islets (Gorogawa, 2004).

1.9.2.9 Leptin

The effects of leptin in the CNS are well characterised but leptin has also been shown to act directly on β-cells to suppress insulin secretion (Kulkarni *et al.*, 1997). When applied

to isolated islets leptin was found to reduce both insulin secretion and also expression of insulin mRNA (Kulkarni *et al.*, 1997; Yildiz *et al.*, 2005). Leptin also inhibits glucose stimulated insulin secretion in both rodent and human islets (Yildiz *et al.*, 2005). It should be noted though, that many of the *in vitro* studies have used leptin at high doses, and it is not clear whether physiological levels of leptin would influence insulin secretion. However leptin administered, at physiological concentrations, to the leptin-deficient *ob/ob* mouse it resulted in a reduction in blood insulin levels and a marked increase in blood glucose (Kulkarni *et al.*, 1997).

Recently it was shown that disrupting leptin signalling in the β-cells and hypothalamus of mice using the *RIPCre* transgene resulted in mice which developed obesity, hyperinsulinaemia, impaired glucose stimulated insulin secretion and glucose intolerance. However, these mice did not show any differences in food intake or in response to leptin (Covey *et al.*, 2006), suggesting that leptin can regulate glucose homeostasis in the β-cell independently of leptin pathways which control food intake.

1.10 Defects in β-cell mass in humans

Type 2 diabetes is characterised by insulin resistance and a decline in β-cell function. Although obesity is the major risk factor for its development, the majority of obese subjects do not develop type 2 diabetes. It has been shown in rodents that there is a compensatory increase in β-cell mass, which overcomes the insulin resistance. Diabetic

rodents have also been shown to have a relatively reduced islet mass compared to non diabetic controls.

Due to the difficulties in obtaining autopsy samples (the pancreas has to be harvested soon after death before it begins to autolyse), relatively few studies have looked at β-cell mass in human diabetic subjects although it has been demonstrated that β-cell mass in patients with type 2 diabetes is reduced by 40-60% (Kloppel, 1989). In addition to this, it was found that β-cell mass was increased in obese nondiabetic subjects in comparison to normal subjects. In a study on Korean non-obese type 2 diabetic patients, it was seen that patients with type 2 diabetes had over a 50% reduction in β-cell mass compared to BMI matched nondiabetic control subjects (Yoon *et al.*, 2003). The same study showed that the ratio of α-cells to β-cells in the pancreas was increased in diabetic patients, suggesting a selective loss in β-cells.

A 60% reduction in β-cell mass in patients with type 2 diabetes has also been reported and suggests that this reduction is due to an increase in apoptosis (Butler *et al.*, 2003a), which implies that human β-cell mass is dynamic.

1.11 Insulin receptor substrate (IRS) proteins

Irs proteins (Fig 5) act as molecular adaptors, recruiting various downstream pathways. Irs proteins also transduce signals from other activated tyrosine kinase receptors including insulin-like growth factor 1 (Withers, 2001). The physiological roles of the four major Irs proteins have been revealed by murine gene targeting strategies. *Irs3* and *Irs4* knockout mice have mild metabolic, endocrine and growth phenotypes (Withers, 2001).

1.12 Insulin receptor substrate knockouts

1.12.1 Irs1knockout mice

Mice lacking *Irs1* display profound growth retardation and insulin resistance but do not develop overt diabetes due to hyperinsulinaemia associated with increased β-cell mass (Araki *et al.*, 1994).

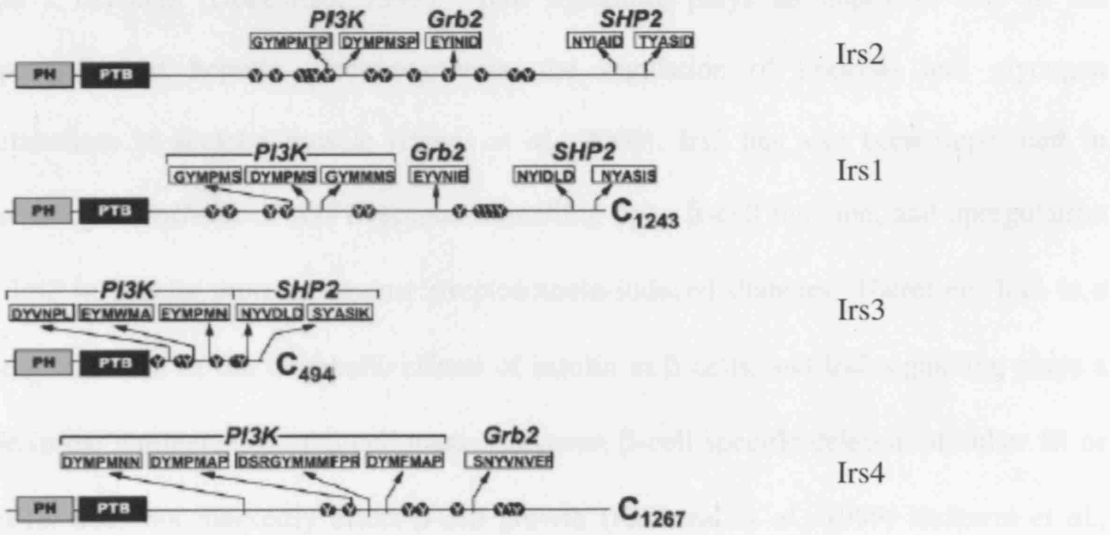

Figure 5. Structure of Irs proteins.

All four Irs proteins have evolutionarily conserved PH and PTB domains. They also all have intracellular domains containing many tyrosine residues and binding sites for PI3K, Grb2 (except Irs3) and SHP2 (except Irs4) allowing recruitment of several different signalling pathways. From White, 2001.

1.12.2 Irs2 knockout mice

A murine model that results in the development of a β-cell failure phenotype is the insulin receptor substrate 2 knockout mouse (Withers *et al.*, 1998). These mice were generated by standard murine gene targeting strategies and lack expression of *Irs2* in all tissues. *Irs2* null mice exhibit mild peripheral insulin resistance and β-cell deficiency at birth, but have adequate compensatory insulin secretion for several weeks. However, subsequent β-cell failure in the face of continued peripheral insulin resistance causes overt fasting hyperglycaemia without ketoacidosis, a common characteristic of human type 2 diabetes (DeFronzo, 1997). Irs2 signalling plays an important role in the suppression of hepatic gluconeogenesis, the regulation of lipolysis and glycogen metabolism in skeletal muscle (Previs *et al.*, 2000). Irs2 has also been implicated in mediating the effects of IGF1 receptor signalling upon β-cell function, and upregulation of Irs2 in β-cells protects against streptozotocin-induced diabetes. Therefore, Irs2 is a major mediator of the metabolic effects of insulin in β-cells, and Irs2 signalling plays a role in the maintenance of β-cell mass. However, β-cell specific deletion of either IR or IGF1R does not markedly affect β-cell growth (Kulkarni *et al.*, 1999; Kulkarni *et al.*, 2002), implying that β-cell autonomous pathways may not be important for β-cell mass.

1.13 Central nervous system regulation of energy homeostasis

In addition to the mechanisms described previoulsy, insulin acts acutely to reduce circulating plasma glucose levels by inhibiting gluconeogenesis in the liver. Insulin also acts in skeletal muscle to promote glycogen synthesis and storage, and in adipose tissue to promote trigylyceride synthesis.

In addition to these acute effects, it is well established that insulin may control longer-term aspects of energy homeostasis such as the maintenance of body fat stores (Porte *et al.*, 2002). The impressive stability of body adiposity over long periods of time, despite often marked variations in daily food intake and energy expenditure, led Kennedy to propose that a signal generated in proportion to body fat stores acts on the brain to regulate energy homeostasis (Kennedy, 1953)

1.14 Hypothalamic circuits regulating food intake and adiposity

The hypothalamus is one of the major regions of the CNS regulating food intake and energy homeostasis. Areas of the hypothalamus involved in control of food intake were initially identified in lesioning experiments. Ablation of the lateral hypothalamus (LHA), results in hypophagia, weight loss and eventual death, and lesions of the ARC, VMH, dorsomedial hypothalamus (DMH) and paraventricular nucleus (PVN) result in hyperphagia and weight gain (Hetherington, 1983). It has also been shown that central administration of leptin is more effective than peripheral administration (Campfield *et al.*, 1995), suggesting that the major site of leptin action is the hypothalamus. It has now become apparent that the hypothalamic nuclei form a complex neural network involved in the regulation food intake and energy expenditure. It has also become evident that there is a complex interplay between these circuits and peripheral signals (Porte *et al.*, 2002).

1.14.1 Arcuate nucleus (ARC)

The arcuate nucleus is located at the base of the hypothalamus on either side of the third ventricle. The ARC effectively lies outside the blood brain barrier and thus, ARC

neurones are accessible to circulating hormones and nutrients. Two groups of neurons in the ARC, the Agouti-related protein (AgRP)/Neuropeptide Y (NPY) neurons (orexigenic) and the proopiomelanocortin (POMC)/ Cocaine-amphetamine-regulated transcript (CART) neurones (anorexigenic), act as the site in the brain for integrating the humoral signals that reflect body energy status. Projections between ARC AgRP/NPY and POMC/CART allow cross talk between neurones and hence a co-ordinated response (Fig.6). These neuronal populations are often referred to as first order neurones, because of their direct contact with peripheral signals. From the ARC, neurons project to second order neurons in the PVN, VMH, DMH, and LHA (Schwartz *et al.*, 2000). Second order neurons project to target sites, including the nucleus of the solitary tract (NTS) in the brainstem and the dorso-motor nucleus of the vagus (DMV). The communication between hypothalamic pathways and the caudal brainstem in response to peripheral satiety signals, is essential for the long-term regulation of energy homeostasis.

Selective ablation of AgRP-expressing neurones in mice rapidly reduces food intake and body weight (Gropp *et al.*, 2005), confirming the role of AgRP neurones as orexigenic. In contrast to this, selective ablation of POMC neurones resulted in a gradual increase in food intake and body weight (Gropp *et al.*, 2005).

1.15 Peripheral signals of long-term energy balance

The neuronal and molecular hypothalamic circuits described above are now known to represent a major component of the brain centres that Kennedy proposed as responding to humoral adiposity signals. However, in contrast to the complexity and significant numbers of factors involved in hypothalamic function, the search for peripherally

produced adiposity signals have, to date, revealed only a few key molecules. Insulin enters the brain from the circulation and acts there to reduce energy intake, and was one of the first hormonal signals implicated in the control of body weight by the CNS (Woods *et al.*, 1979). However, it was the subsequent identification of the adipocyte hormone leptin (Halaas *et al.*, 1995) and the delineation of its role in the CNS regulation of energy homeostasis that provided the impetus for many of the recent advances in our understanding of the mechanisms controlling food intake and energy homeostasis. These are summarised in Figure 6.

1.16 Leptin: an adiposity signal acting in the CNS

The adipocyte-derived hormone leptin is the best-characterised peripheral adiposity signal. Its expression and circulating concentration reflect fat stores (Frederich *et al.*, 1995; Zhang *et al.*, 1994). Leptin synthesis and release in proportion to fat mass is also regulated in the short term by food intake (Ahima *et al.*, 1996). In both rodents and humans, leptin deficiency or defects in the leptin receptor result in hyperphagia (uncontrolled food intake), obesity, reduced energy expenditure and infertility (Zhang *et al.*, 1994). These abnormalities are also seen in the obese, leptin deficient *ob/ob* mouse. In both leptin deficient humans and mice, obesity can be reversed by peripheral administration of leptin (Barash *et al.*, 1996; Farooqi *et al.*, 1999). The long isoform of the leptin receptor is expressed in both NPY/AgRP and POMC/CART neurones (Fig.7) (Kaji *et al.*, 1998) with leptin known to regulate the expression of these peptides. Fasting increases expression of NPY and AgRP, whilst CART and POMC expression are reduced, and these changes in expression can be reversed by administration of leptin (Mizuno *et al.*, 1999a; Mizuno *et al.*, 1999b). In addition to this, it has been demonstrated

that POMC neurones express K_{ATP} channels, which are activated by leptin. Electrophysiological recordings have demonstrated that leptin also acutely modulates the activity of both NPY and POMC neurones, hyperpolarizing the NPY neurones and depolarising the POMC neurones (Cowley *et al.*, 2001).

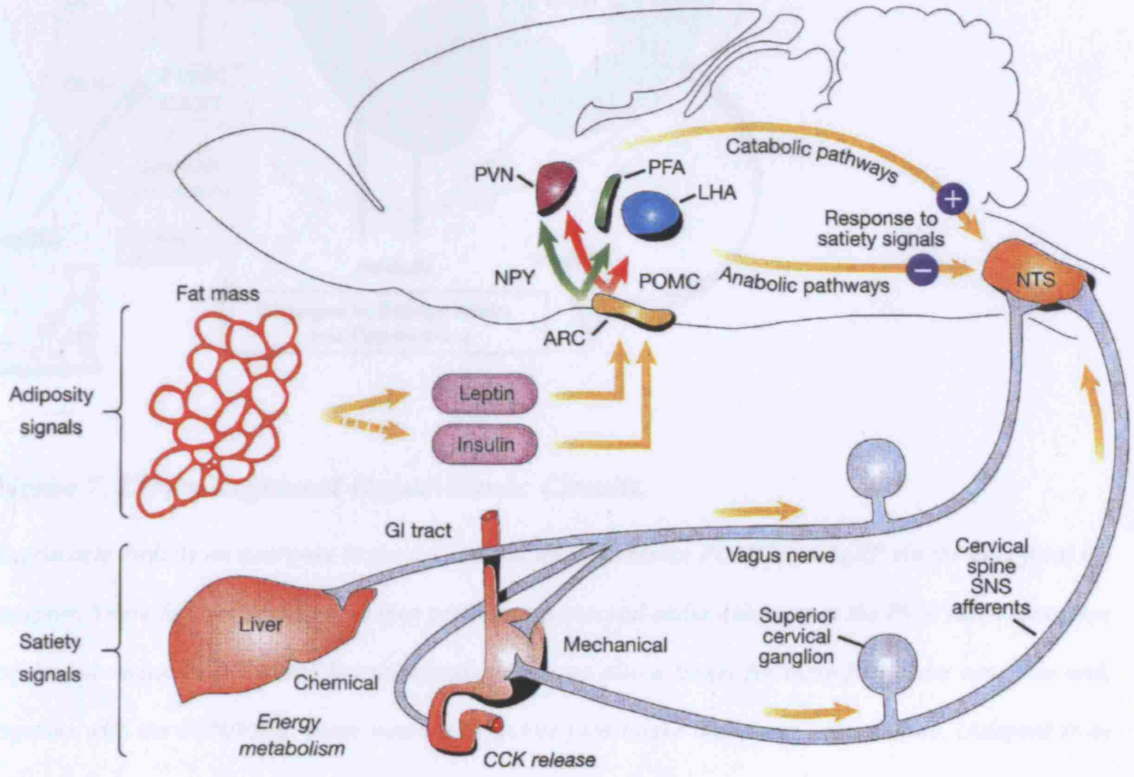

Figure 6: Representation of how insulin and leptin act as adiposity signals to the CNS and regulate energy homeostasis.

Both insulin and leptin act upon the first order neurons, stimulating the anorectic POMC/CART neurones and inhibiting the orexigenic AgRP/NPY neurones. Projections from ARC AgRP/NPY and POMC/CART expressing neurones signal to second order neurones, which then relay signals to the caudal brainstem integrating a response to energy expenditure. Adapted from (Schwartz et al., 2000).

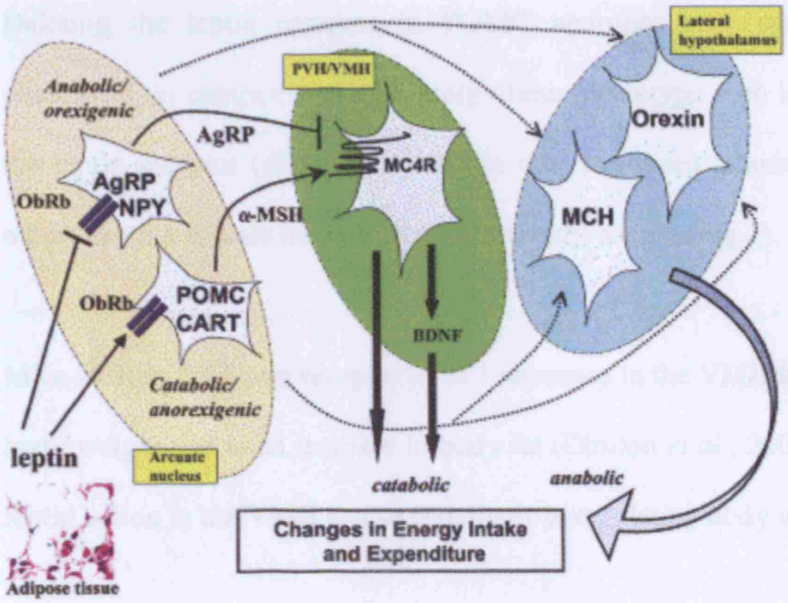

Figure 7. Leptin-Regulated Hypothalamic Circuits.

Leptin acts directly on neurones in the arcuate nucleus expressing POMC and AgRP via the long-form Ob receptor. These first order neurones then project to the second-order neurones in the PVN/VMH. Neurones expressing melanocortin in the lateral hypothalamus are also a target for these first order neurones and, together with the PVN/VMH, these neurones regulate food intake and energy expenditure. (Adapted from (Flier, 2004).

1.16.1 Sites of leptin action in the CNS

Mice lacking the leptin receptor in POMC neurones are mildly obese and hyperleptinaemic. The obesity was shown to be due to an increase in fat pad mass with corresponding hyperleptinaemia (Balthasar *et al.*, 2004). These mice also show changes

in hypothalamic gene expression: POMC, AgRP and NPY are all decreased. The decrease in NPY/AGRP is not seen until the onset of obesity and is possibly due to hyperleptinaemia (Balthasar *et al.*, 2004).

Deleting the leptin receptor in POMC neurones only resulted in a mildly obese phenotype, in contrast to the severely obese phenotype seen in mice completely lacking the leptin receptor (*db/db* mice). It has therefore been assumed that leptin acts in sites other then the arcuate nucleus to regulate body weight (Fig.7).

Mice lacking the leptin receptor in SF1 neurones in the VMH have significantly increased body weight due to an increase in body fat (Dhillon *et al.*, 2006). This study showed that leptin action in the VMH is also important in regulating body weight.

1.17 Effects of leptin on insulin secretion

Leptin receptors are expressed in β-cells (Kieffer *et al.*, 2000), and leptin signalling is involved in many pathways in the β-cell including Jak/STAT signalling, PI3K pathways. Leptin also activates K_{ATP} channels (Fruhbeck, 2006; Yildiz *et al.*, 2005). Therefore, there is evidence that leptin, which is increased in obesity, may contribute to the impaired glucose homeostasis seen in type 2 diabetes.

1.18 Melanocortin knockout mice

The *MC4*$^{-/-}$ mouse displays adult onset obesity, with hyperphagia, hyperinsulinaemia and hyperglycaemia (Huszar *et al.*, 1997). In addition to this *MC4*$^{-/-}$ mice also show increased

linear growth. MC4 receptors are expressed in a number of hypothalamic sites including the VMH, PVN and lateral and ventricular hypothalamus, which regulate food intake. The endogenous ligands for the MC4 receptor are derived from POMC and include adrenocortocotrophin (ACTH) and α-melanocyte stimulating hormone (α-MSH). It has therefore been proposed that MC4 receptor ligands play an inhibitory role in energy balance and homeostasis.

This is supported by studies using the melanocortin analogue, melanotan II (MTII). MTII was administered centrally in four different models of hyperphagia, and in each case caused a dose-dependent reduction in food intake (Fan *et al.*, 1997).

1.19 Insulin: actions in the CNS

Chronic intracerebroventricular (ICV) administration of insulin causes a dose-dependent reduction in food intake, coupled with a moderate decrease in body mass (Woods *et al.*, 1979). Insulin receptors are expressed in many regions of the hypothalamus particularly, in the arcuate nucleus (ARC) and para-ventricular nucleus (PVN) (Unger *et al.*, 1998). It has also been shown that insulin binds at high levels in the arcuate nucleus. It has therefore been suggested that insulin and leptin target the same neurones in the hypothalamus, i.e. NPY/AgRP and POMC/CART neurones.

Conditional gene targeting in the mouse has shown that deletion of the brain insulin receptors causes mild hyperphagia and increased adiposity in females, and diet-sensitive obesity in both males and females (Bruning *et al.*, 2000). In addition to reducing food intake, hypothalamic administration of insulin further suppresses mRNA expression of the orexigenic NPY (Schwartz *et al.*, 2000).

1.20 Potential roles of central leptin and insulin upon peripheral glucose metabolism

In addition to their role as peripheral signals acting in the hypothalamus to regulate long-term energy homeostasis, there is recent evidence that both insulin and leptin act in the CNS to acutely regulate peripheral glucose homeostasis. For example, icv administration of leptin has been shown to modulate hepatic glucose fluxes (Liu *et al.*, 1998). Likewise inhibition of hypothalamic insulin receptor expression using antisense strategies also impairs hepatic glucose homeostasis (Obici *et al.*, 2002a).

1.21 Leptin receptor signalling cascade

The leptin receptor was first isolated from the mouse choroid plexus using an expression cloning strategy (Tartaglia *et al.*, 1995). It belongs to the type 1 cytokine family and consists of a single membrane-spanning domain. There are at least six leptin receptor isoforms, Ob-Ra, OB-Rb, Ob-Rc, Ob-Rd, Ob-Re and Ob-Rf (Fig 8). Each has an identical extracellular ligand-binding domain at the amino terminus but they all differ at the carboxy terminus. Only the Ob-Rb (the long receptor isoform) contains intracellular motifs required for signal transduction and is highly expressed in the hypothalamus. Upon leptin binding the receptor recruits and activates a member of the janus kinase (Jak) family, primarily Jak2 (Banks *et al.*, 2000). Once activated, JAK2 phosphorylates the intracellular domain of the leptin receptor, creating a binding site for the signal transducers and activators of transcription 3 (STAT3). In response to leptin stimulation, activated STAT-3 translocates to the nucleus where it functions as a transcription factor (Banks *et al.*, 2000). Intracellular negative feedback to this signalling system is provided

by a family of suppressor of cytokine signalling (SOCS) molecules that are synthesized in response to STAT-3 activation following leptin stimulation. Leptin receptor activation is also known to activate ERK-regulated pathways (Banks *et al.*, 2000).

1.22 RIPCreSTAT3KO mice

As the global *STAT3* null mouse is not viable, mouse models with tissue specific deletions have been used to further investigate the role of STAT3.

Mice harbouring a floxed allele of *STAT3* were crossed into mice expressing *Cre recombinase* inder the control of the rat insulin 2 promoter (RIPCre) to generate mice lacking STAT3 in the beta cell and hypothalamus (Cui *et al.*, 2004). At weaning *RIPCreSTAT3* mice were hyperglycaemic and hyperinsulinaemic. Analysis of pancreatic islets in these mice showed that while the number of islets was similar to that seen in wild type littermates, the size of the islets of *RIPCreSTAT3* mice appeared to be increased, with a corresponding increase in insulin release. Glucose tolerance tests demonstrated impaired glucose clearance in the *RIPCreSTAT3* mice suggesting an insulin resistant phenotype.

Analysis of the hypothalamic phenotype in these mice shows that, while body weight was not significantly different at weaning, the *RIPCreSTAT3KO* mice showed an increase in adiposity at this age. After weaning these mice were shown to be hyperphagic. This hyperphagia persisted into adulthood and was accompanied by an increase in body weight and increased adiposity.

At 4 weeks of age these mice showed an increase in plasma leptin with this hyperleptinaemia becoming more pronounced with age, reflecting the increased adiposity of these mice. These mice also displayed partial resistance to leptin: central administration of leptin failed to replicate the total loss of body fat seen when leptin is centrally administered to the ob mouse.

1.23 Role of Irs2 in hypothalamic function

Irs2 signalling also plays complex roles in neuroendocrine function. *Irs2* null mice are hyperphagic and develop obesity despite having elevated plasma leptin levels. These findings not only suggest the presence of CNS leptin resistance but also that CNS insulin action or components of the insulin signalling pathways are also necessary for intact neuronal responsiveness to leptin. Indeed, STAT3 phosphorylation in response to leptin is defective in *Irs2* null mice, suggesting some signalling convergence between leptin and insulin (Burks *et al.*, 2000). Such findings support the notion that Irs2 may act as a convergence point for insulin and leptin signalling in the CNS.

The CNS phenotype is complicated by the observation that *Irs2* null mice display a 30% reduction in brain size (Schubert *et al.*, 2003), suggesting that Irs2 pathways are important in CNS growth and development.

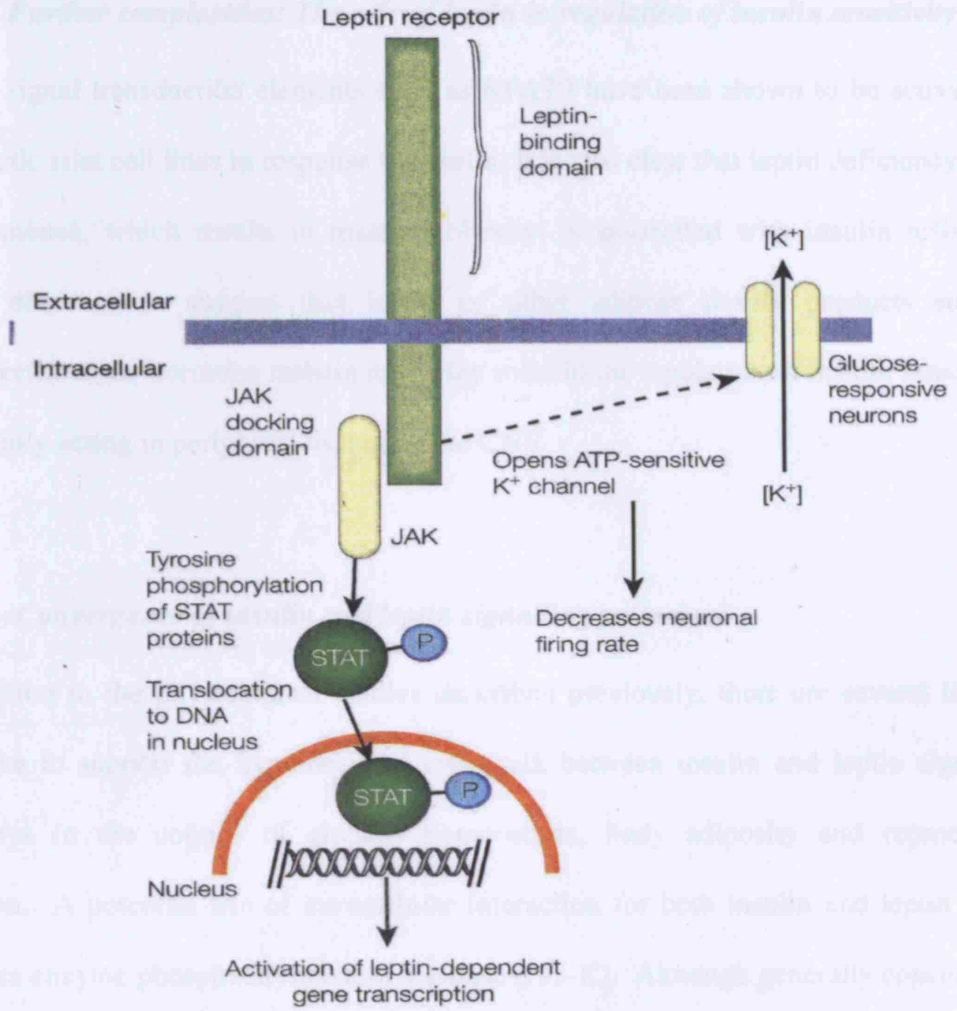

Figure 8: Leptin signalling pathways:

There are at least six leptin receptor isoforms, Ob-Ra, OB-Rb, Ob-Rc, Ob-Rd, Ob-Re and Ob-Rf. The long form the Ob-Rb receptor contains intracellular motifs required for signal transduction. Upon leptin binding the receptor recruits and activates a member of the janus kinase (Jak) family, Jak-2 (Banks et al., 2000) Activated, Jak-2 phosphorylates the intracellular domain of the leptin receptor, creating a binding site for the signal transducers and activators of transcription (STAT) molecules. In response to leptin stimulation, activated STAT-3 translocates to the nucleus where it activates leptin-dependent gene transcription (Banks et al., 2000).

1.24 Further complexities: The role of leptin in regulation of insulin sensitivity

Leptin signal transduction elements such as STAT3 have been shown to be activated in pancreatic islet cell lines in response to insulin. It is also clear that leptin deficiency in the *ob/ob* mouse, which results in massive obesity, is associated with insulin resistance. These observations suggest that leptin or other adipose tissues products such as adiponectin or the hormone resistin may play roles in the regulation of insulin sensitivity, potentially acting in peripheral tissues or the CNS.

1.25 Convergence of insulin and leptin signalling pathways

In addition to the physiological studies described previously, there are several lines of evidence to support the hypothesis of cross-talk between insulin and leptin signalling pathways in the control of glucose homeostasis, body adiposity and reproductive function. A potential site of intracellular interaction for both insulin and leptin action involves enzyme phosphatidylinositol 3 kinase (PI3-K). Although generally considered a downstream effector of Irs1 and Irs2 signalling, studies in hepatocyte cell lines have demonstrated that leptin enhanced insulin-induced association of Irs1 with PI3-K and increased PI3-K activity *per se* (Cohen *et al.*, 1996). Subsequent studies in hepatocytes demonstrated that leptin activates PI3-K, via tyrosine phosphorylation of Irs1 and Irs2, leading to activation of downstream targets such as PKB and phosphodiesterase 3B (PDE3B) (Zhao *et al.*, 2000). However, it was subsequently shown that Irs2 signalling in hepatocytes is not required for maintenance of glucose homeostasis (Simmgen, 2005).

The actions of leptin in the CNS may also be mediated through PI3-K signalling. Electrophysiological experiments, investigating the effects of leptin on hypothalamic

neurons in rat brain slice cultures, showed that leptin caused a population of hypothalamic neurons in the arcuate and ventromedial nuclei to hyperpolarize through the activation of ATP-sensitive K+ channels (Spanswick *et al.*, 2000). The same population of neurons were also hyperpolarized by insulin, indicating that the acute cellular effects of insulin and leptin might converge. Hence, an intracellular signalling pathway might exist, in which activation of PI3K is the target not only of insulin signalling, but also of leptin signalling. In support of this model, the ability of insulin to regulate the firing of certain arcuate nucleus neurons is blocked by inhibitors of PI-3 kinase (Niswender *et al.*, 2001). Blocking of neuronal PI- 3 kinase signalling *in vivo* using a specific PI-3 kinase inhibitor, resulted in complete prevention of leptin-induced anorexia, as compared with control animals given a vehicle injection (Niswender *et al.*, 2001).

A further potential site of convergence of leptin and insulin signalling in the regulation of glucose and energy homeostasis is the AMP-activated protein kinase (AMPK). This family of heterotrimeric enzymes are allosterically activated by cellular 5' AMP levels as well as by a currently unidentified upstream kinase. Physiological stimuli that activate AMPK include skeletal muscle contraction and the peptide hormones leptin (see above) and adiponectin. The findings that the system is activated by exercise, and by adipocytokines involved in the control of appetite, body weight and insulin sensitivity also point to its potential importance in energy homeostasis and implicate it as a point of convergence of insulin and leptin action.

1.26 RIPCre Irs2KO mice.

While the studies documented here were being completed, two groups attempted to address the importance of β-cell autonomous Irs2 dependent signalling by generating mice lacking *Irs2* in β-cells. These groups crossed mice expressing a floxed allele of *Irs2* into mice expressing a rat insulin 2 promoter (RIP) Cre recombinase transgene, which is expressed in pancreatic β-cells and in population of hypothalamic neurones in the ARC. In both of these studies (Kubota *et al.*, 2004; Lin *et al.*, 2004) deletion of *Irs2* was demonstrated in the pancreatic β-cell and in an, as yet unidentified, hypothalamic neuronal population.

These conditional knockout mice displayed increased body weight, accompanied by hyperphagia. Further analysis showed that the conditional knockout mice had disproportionately increased fat mass with hyperleptinaemia. The mice also developed mild diabetes with a decrease in β-cell mass. However the diabetes did not progress due to a recovery in β-cell mass, but the mechanism of this recovery is unknown. These mice were also resistant to leptin but again the mechanism for this is unclear.

While these studies highlighted an important role of Irs2 in the β-cell and hypothalamus, there are still some unanswered questions: These mice displayed leptin resistance which was not explained by their obesity, as leptin resistance was seen before obesity developed. Thus the mechanism by which reduced Irs2 in the hypothalamus reduces leptin sensitivity is unclear. In addition to this, the precise location and identity of these neurones is unknown.

In addition to this, neither the mechanism of the β-cell recovery or the source of the new β-cells were investigated.

AIMS:

To investigate the role of Irs2 in the β-cell and the hypothalamus, and in particular to address the identity of RIPCre expressing neurones and the mechanism of β-cell recovery I have generated mice lacking Irs2 in the β-cell and the hypothalamus. This was achieved by crossing mice expressing a floxed allele of *Irs2* with mice expressing Cre recombinase under the control of the rat insulin II promoter (*RIPCre*). Once generated I have studied these mice, and their littermate controls for:

- Glucose metabolism
- Pancreatic β-cell function and morphology
- Body weight and food intake
- Leptin sensitivity
- Characterisation of the neuronal population expressing RIPCre

I have also generated mice lacking STAT3 in the same tissues in order to investigate the role of leptin signalling in the β-cell and hypothalamus. Mice were generated by crossing mice expressing a floxed allele of *STAT3* with *RIPCre* mice. Once generated I have studied these mice for:

- Glucose metabolism
- Pancreatic β-cell function and morphology
- Body weight and food intake
- Body fat composition
- Feeding behaviour
- Leptin sensitivity

2. MATERIALS & METHODS

2.1 Animals

All animal procedures were approved under the British Home Office Animals Scientific Procedures Act 1986 (Project Licence No. 70/5179 and 70/9195).

Animals were housed in specific pathogen-free barrier facilities and maintained in a controlled environment (temperature 21-23°C, 12-hour light/dark cycle, lights on at 07:00h) with *ad libitum* access to water and food. Standard rodent chow (9607 TRM diet, Harlan, UK) consisted of 4.3g fat, 44.3g carbohydrate and 19g protein per 100g, providing 13.25MJ/kg of metabolic energy.

2.1.1 Irs2lox strain

Mice harbouring alleles of the *Irs2* gene flanked by loxP-target sites for the Cre recombinase (*Irs2lox*+/+) were generated in Prof. Withers' laboratory. Using gene-targeting strategies, a mouse was made in which the *Irs2* gene was flanked by loxP sites (floxed) (Figure2.1). This allowed conditional knockout mice to be generated by crossing the *Irs2* floxed mouse into mice expressing Cre recombinase under the control of tissue-specific promoters. These animals were indistinguishable from their wild type littermates.

2.1.2 RIPCre strain

Animals expressing Cre recombinase under the control of the rat insulin II promoter *(B6.Cg-tg(Ins2-cre)25Mgn/J)* were obtained from Jackson Laboratories, USA. These mice were maintained on a C57/Black 6 genetic background.

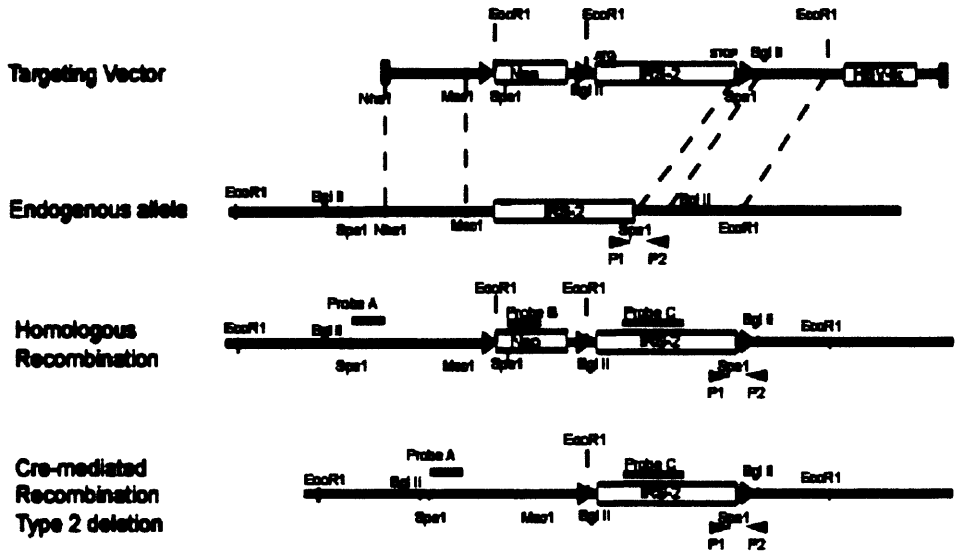

Figure 2.1 Targeting strategy for Irs2lox mouse.

A targeting vector was designed in which the Irs2 gene was flanked by loxP sites. The vector then underwent homologous recombination into the endogenous allele, with the neomycin cassette acting as a selectable marker. In vitro Cre-mediated recombination removed the neomycin cassette leaving the Irs2 floxed allele.

2.1.3 STAT3lox strain

Mice harbouring alleles of the *STAT3* gene flanked by loxP target sites for the Cre recombinase (*STAT3 lox/lox*) on a mixed genetic background were obtained from V. Poli (Alonzi *et al.*, 2001).

2.1.4 Z/EG mice

Z/eg mice, which express green fluorescent protein under the control of cre recombinase (figure 2.2) were obtained from Corrine Lobe (Novak *et al.*, 2000), these mice were maintained on a C57/Black 6 background.

2.2 Mouse identification and tail tissue sampling

Animals were earmarked and tail tipped (< 5mm of tail) at the age of 14 days. Ethyl chloride spray was applied to the tails for local anaesthesia. The tissue was subsequently used for DNA extraction and PCR based genotyping.

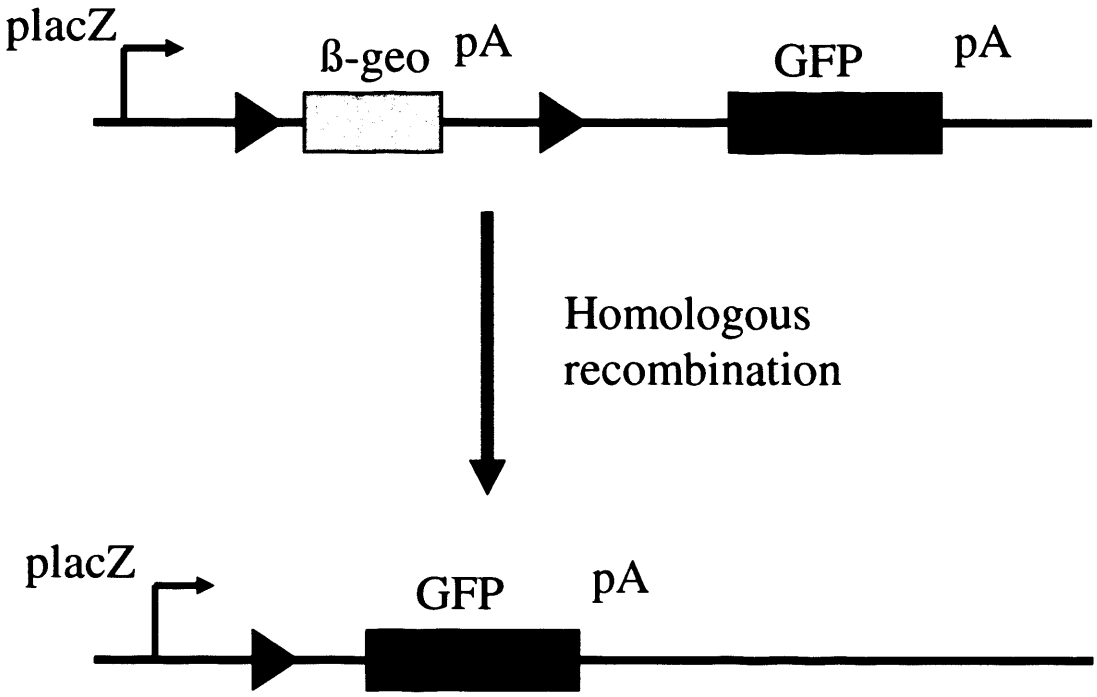

Figure 2.2 LacZ/GFP mice.

Z/eg mice express a floxed ß-geo fusion cassette under the control of the lacZ promoter. Under normal conditions transcription stops after the ß-geo cassette due to a polyA sequence. In cells expressing Cre recombinase homologous recombination occurs between the loxP sites deleting the ß-geo/polyA sequence and allowing transcription of the GFP gene.

2.3 DNA extraction from tissues

For DNA extraction from tail tissue the proteinase K method was used. DNA was obtained from hypothalamus and the pancreas using the chloroform: isoamyl alcohol method.

2.3.1 Proteinase K method

The tail biopsy was placed in a 1.5mL reaction tube, 100µL of tail lysis buffer added [6.7mM Tris pH 8.8, 1.66mM $(NH_4)_2SO_4$, 0.67mM $MgCl_2$, 0.5% Triton X-100, 1% β-mercaptoethanol (supplemented freshly)], and the sample heated to 95°C for 10 minutes in a heat block. Following cooling to room temperature, proteinase K was added to a final concentration of 1mg/mL and the tissue incubated at 55°C for at least 6 hours, or overnight. Heating to 95°C for 10 minutes subsequently inactivated proteinase K. The digested tissue was centrifuged at 15,600 x g for 5 minutes and the supernatant used as template for PCR amplification.

2.3.2 Chloroform-isoamyl alcohol method

Approximately 100mg of snap frozen tissue was placed in a 1.5mL reaction tube, 525µL of extraction buffer [50mM Tris pH 8.0, 100mM EDTA, 100mM NaCl, 1% SDS, proteinase K 0.65mg/mL] was added and the sample incubated at 55°C for 12 hours. To disperse the tissue the specimen was briefly vortexed, 2µL of RNAse A (0.2mg/mL) added, and at 37°C incubated for 1 hour. 200µL of 5M NaCl was added and the sample gently mixed by inversion. 700µL of chloroform-isoamyl alcohol (24:1 vol/vol) was added and the specimen incubated at room temperature for 2 hours on a rocking platform. Following centrifugation at 15,600 x g for 10 minutes, 500µL of the upper aqueous layer was transferred into a new reaction tube, 500µL of isopropanol added, and gently mixed by inversion. Following centrifugation with 15,600 x g for 10 minutes, the supernatant was discarded, 300µL of 70% ethanol was added, and the sample incubated at 4°C for 1

hour. The supernatant was discarded, the pellet resuspended in 20μL of TE buffer [10mM Tris pH 8.0, 1mM EDTA], and used as template for PCR amplification.

2.4 PCR amplification

PCR amplification of genomic DNA extracted from tissue was performed to determine the genotypic status of the animals and also to confirm the Cre-mediated IRS2 deletion event in the liver. 1μL of the DNA extracts was used as template, the final primer concentrations were 0.4μM in a commercial PCR reagent mixture (ReddyMix®, ABgene, UK), and the reactions were carried out in a 12μL volume in a thermocycler (MJ Research, USA). The PCR products were separated by electrophoresis in a 2% agarose gel prepared with TAE buffer [40mM Tris acetate pH 8.3, 1mM EDTA] and 0.02% ethidium bromide, and were subsequently photographed under ultraviolet light.

2.4.1 PCR strategy for Irs2lox detection

Primers flanking the 3' loxP site, loxP-F and loxP-R (table 2.1) were used to detect the presence of a floxed allele of *Irs2*. PCR amplification from a wild-type allele yielded a 200bp product, whilst the presence of the loxP region and an adjacent short linker sequence increased this size to 250bp (Figure 2.3). Cycling conditions were 94°C for 1min, followed by 30 cycles of 94°C for 30sec, 65°C for 30sec, and 72°C for 1:30min, and finally 72°C for 10min.

2.4.2 PCR strategy for Irs2 deletion

To confirm deletion of *Irs2*, a primer binding 1.1kb upstream of the 5' loxP site loxP-Del-F (table 2.1) was used instead of the loxP-F primer. Thus, if Cre-mediated recombination had occurred, a 1.3kb fragment was amplified (Figure 2.3). The length of the intervening *Irs2* gene prohibited a successful PCR reaction otherwise. Cycling conditions were 95°C for 3min, followed by 30 cycles of 95°C for 1min, 52°C for 1min, and 72°C for 1min, and finally 72°C for 7min.

2.4.3 PCR strategy for RIPCre transgene presence

The presence of the RIPCre transgene was confirmed by amplification of a 100bp fragment from within the Cre transgene primers Cre1084 and Cre1085 (Table 2.1). As this PCR strategy only demonstrates the presence or absence of Cre, control primers for an interleukin gene, ILF and ILR (Table 2.1) served as internal control and resulted in a 324bp fragment (Figure 2.3). Cycling conditions were 94°C for 2 mins followed by 30 cycles of: 94°C for 20s, 56°C for 30s, and 72°C for 1 min 10s followed by a final extension of 72°C for 3 minutes.

2.4.4 PCR strategy for STAT3 lox detection

The presence of the *STAT3* floxed allele was confirmed using primers APRF11-up APRF11-down and APRF14-down (Table 2.1). PCR amplification of a wild type allele gave a band of 210 bp while a floxed allele gave a band of 370bp. This PCR was also used to comfirm deletion of *STAT3* as a deleted allele resulted in a band of 310bp (Figure 2.3).

Cycling conditions were: 94°C for 4 minutes, followed by 30 cycles of 94°C for 1 minute, 60°C for 2 minutes and 72°C for 3 minutes, and finally 72°C for 10 minutes.

2.4.5 Z/eg genotyping

Genotyping for the *Z/eg* allele was performed using primers: Z/eg forward and Z/eg reverse (Table 2.1). PCR conditions were: 94°C for 1min, followed by 30 cycles of 94°C for 30s, 55°C for 30s and 72°C for 1min 30s and a final extension step of 72°C for 10 min resulting in a 650 b.p. band (Figure 2.3).

Irs2lox detection	
loxPF	*ACT TGA AGG AAG CCA CAG TCG*
loxPR	*AGT CCA CTT TCC TGA CAA GC*
Irs2 deletion	
LoxP-DelF	*GGG AAC CTG ACA AGT GAA TG*
RIPCre	
Cre1084	*GCG GTC TGG CAG AGT GAA TG*
Cre1085	*GTG AAA CAG CAT TGC TGT CAC TT*
ILF	*CTA GGC CAC AGA ATT GAA AGA TCT*
ILR	*GTA GGT GGA AAT TCT AGC ATC ATC C*
STAT3	
APRF11-up	*CAC CAA CAC ATG CTA ATT GTA GG*
APRF11-down	*CCT GTC TCT GAC AGG CCA TC*
APRF14-down	*GCA GCA GAA TAC TCT ACA GCT*
Z/eg	
Z/egF	*CCT CTG CCA AAA ATT GGG*
Z/egR	*ACT ATG GTT GCT GAC TAA TTG*

Table 2.1 Primer sequences.

Sequences are given for primers used for PCR genotyping. All sequences read in 5' – 3' direction.

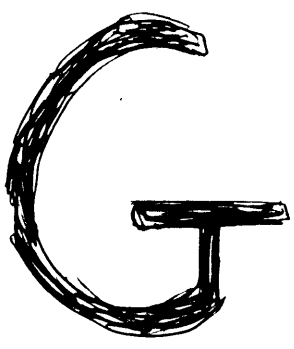

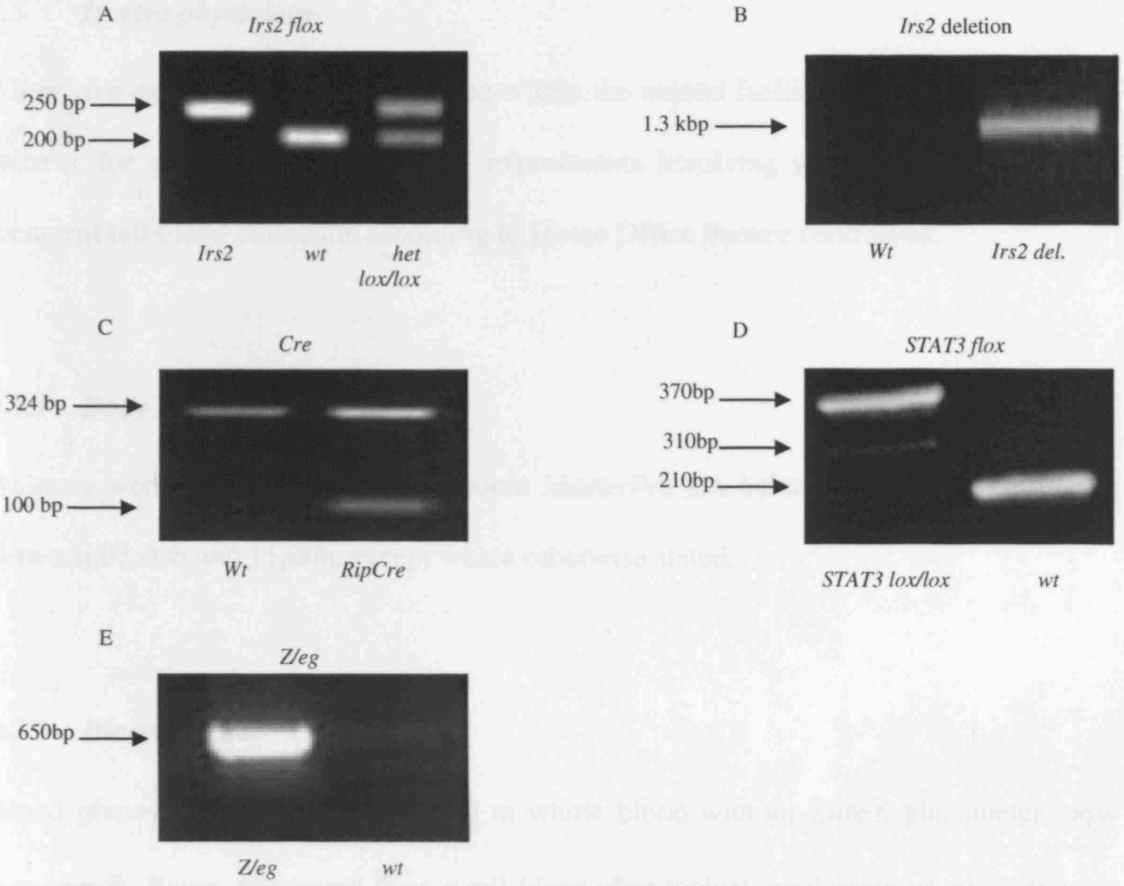

Figure 2.3. PCR genotyping

Gel images illustrating the results of PCR genotyping are shown. (A) Irs2lox genotyping showing, in the first lane a mouse carrying 2 floxed alleles of Irs2, in the second lane a wild-type mouse and in the third lane a mouse carrying one wild-type and one floxed allele of Irs2. (B) Irs2 deletion PCR, no band is visible in the wild type mouse while deletion of Irs2 results in a 1.3kbp band. (C) Cre genotyping, from the wild-type mouse only the internal control band is seen, while presence of the Cre transgene results in a 100bp band. (D) STAT3 lox PCR. Presence of a floxed allele of STAT3 results in a 370bp band, the band seen at 310bp results from deletion of STAT3. The wild-type allele gives a band of 210bp. (E)Z/eg genotyping. Presence of the Z/eg transgene results in a 650bp band which is not seen in mice lacking the transgene.

2.5 In vivo physiology

All *in vivo* experiments were performed within the animal facility. Mice were allowed to recover for at least 5 days between experiments involving an overnight fast and/or recurrent tail blood collection according to Home Office licence conditions.

2.5.1 Body weight

Animals were weighed with an electronic MasterPro LA balance (Sartorius, Germany) between 08:00h and 11:00h, except where otherwise stated.

2.5.2 Blood glucose

Blood glucose levels were determined in whole blood with an Elite® glucometer (now Ascensia®, Bayer, Germany) from a tail bleed after topical application of ethyl chloride as a local anaesthetic with a sample volume of 1µl per bleed.

Fasted blood glucose (FBG) levels were obtained after an overnight fast of 14 hours during the early light phase between 08:00h and 10:00h.

2.5.3 Intraperitoneal glucose tolerance test (ipGTT)

Animals were weighed, fasted for 14 hours overnight, and FBG levels obtained as above. Subsequently an intraperitoneal injection of 20% glucose at a dose of 1.5g kg^{-1} body weight was administered. Tail vein whole blood glucose levels were measured 15, 30, 60, and 120 minutes post-injection.

2.6 Terminal procedures

Animals were terminally anaesthetised by intraperitoneal injection to allow open cardiac puncture or intravenous insulin stimulation. Sodium pentobarbitone (Euthatal®, Rhone Mérieux, UK) was used for anaesthesia at a dose of 500mg kg^{-1} body weight for gene expression studies requiring rapid dissection.

Following each procedure the insulin-responsive tissues were collected (in the sequence of liver, quadriceps muscle, and epididymal adipose tissue), snap frozen in liquid nitrogen, and stored at –70°C until analysis. Tissues were obtained immediately after cardiac puncture.

For studies in which anaesthetic could not be used animals were sacrificed by cervical dislocation.

2.6.1 Cardiac puncture

Mice were anaesthetised as above. A midline and a central transverse abdominal incision were made, carefully avoiding the infracostal vessels to reduce blood loss from the wound. A 1ml insulin syringe with a 12mm fixed 30G needle (Becton Dickinson, UK) was gently inserted into the right ventricle through the diaphragm. Blood was slowly aspirated and expelled into a 1.5ml reaction tube to reduce haemolysis. The sample was allowed to clot and placed on ice until centrifugation at 4°C with 15,600 x g for 10 minutes. Serum was immediately separated and stored at -70°C until analysis. Where plasma was required blood was collected as above and expelled into a 1.5ml reaction tube containing 10µl heparin to prevent coagulation. Blood was then centrifuged as above.

2.6.2 Paraffin embedded tissue

Pancreata were fixed in aqueous Bouin's solution [saturated picric acid, 40% aqueous formaldehyde, glacial acetic acid; 15:5:1 vol/vol/vol] for 4 hours, rinsed twice in 70% ethanol and stored in 70% ethanol for a further 20 hours. All tissues samples were subsequently dehydrated and brought to paraffin in a Hypercenter XP tissue processor (Thermo Shandon, UK) following a standard 22-hour protocol. Following embedding in paraffin, 5μm tissue sections were cut on a Finesse 325 microtome (Thermo Shandon, UK), mounted and stored. Dewaxing and hydration of slides was performed immediately prior to staining by sequential immersion in Xylene twice for 5min each, and for 2min each in 100% Ethanol, 90% Ethanol, 70% Ethanol, and dH_2O.

2.6.3 Isolation of pancreatic islets

Mice were killed by cervical dislocation and a midline abdominal incision was made. The pancreatic duct was cannulated, and the junction of the pancreatic duct with the duodenum was clamped. The pancreas was then inflated with 1.5ml liberase solution (highly purified collagenase enzyme blend) and removed into a falcon tube containing 2ml liberase solution. The pancreas was then incubated at 37°C for 20 minutes. After incubation quenching buffer (HBSS + 1% penicillin/streptomycin + 0.5%BSA) was added up to a volume of 10ml and shaken vigorously for 10sec. The suspension was then passed through a net well (400-500μm) into a 50ml falcon tube. The 15ml falcon was then rinsed with a further 10ml quenching buffer and passed through the net well into the 50ml falcon.

The 50 ml falcon was centrifuged at 1000RPM for 1 minute at 4°C. The supernatant was discarded and the pellet resuspended in 20ml quenching buffer. This washing step was repeated and the final pellet resuspended in 10ml quenching buffer.

The islet suspension was then split into 2x90mm petri dishes and islets were hand-picked under a light microscope into a 30mm petri dish using a 200µl pipette. All petri dishes were kept on ice throughout the picking process. A second and third round of picking were carried out to ensure purity of the islet preparation. Islets were then picked into a 1.5ml eppendorf and centrifuged at 9000RPM for 1 min to pellet islets. The supernatant was discarded and the pellet resuspended in 1ml HBSS and centrifuged as above. The supernatant was discarded and the pellet stored at -80°C.

2.6 Assays

Serum specimens were collected by open cardiac puncture as described above or from a prolonged tail bleed obtained with the aid of a pipette. The latter samples were transferred into 0.5mL reaction tubes, allowed to clot and placed on ice until centrifugation at 4°C with 15,600 x g for 10 min. Serum was immediately separated and stored at -70°C until analysis.

2.6.1 Insulin

Insulin levels were measured according to the manufacturer's instructions with a commercially available rat insulin ELISA kit (CrystalChem, Illinois, USA). In brief,

guinea pig anti-rat insulin antibody coated onto a microtitre well was incubated with 100µL of diluted mouse serum for 2 hours. Following a series of washes 100µL of HPO-conjugated anti-insulin antibody was added and incubated for 30min. After further washes, 100µL of TMB substrate solution was added, incubated for 40min, the reaction terminated with 100µL of 0.5M sulphuric acid, and the absorbance at 450nm measured. The lyophilised standard was reconstituted to concentrations of 0.0, 0.1, 0.2, 0.4, 0.8, 1.6, 3.2, and 6.4ng/mL. All samples were assayed in duplicate and in one assay to avoid inter-assay variation.

2.6.2 Leptin

Leptin levels were measured in a similar way, but both a rabbit-anti mouse leptin antibody bound to the microtitre plate and a soluble guinea pig anti-mouse leptin IgG were used in the first reaction step. The secondary antibody consisted of an anti-guinea pig IgG antibody conjugated to HPO. Otherwise the protocol as described for insulin was followed.

2.7 Feeding studies

Mice were singly housed in individually ventilated cages at weaning and allowed to acclimatise for 1 week prior to any studies.

2.7.1 Fast-refeed

Mice were weighed in the evening (5:00PM) and their food removed. The next morning mice were re-weighed and ~75g chow was weighed out and given to each mice. Food intake was then measured after 1hr, 2hr, 4hr, 8hr and 24hrs.

2.7.2 Response to peripheral leptin

Prior to leptin treatment each mouse was sham injected with 100µl of 0.9% saline for 3 days. Mice were randomised into a treatment group and a control group and on the morning of the first day of treatment were weighed to establish the dose of leptin they would receive. One hour before the start of the dark phase food and body weight for each mouse was measured. Mice were then injected intra-peritoneally with either recombinant mouse Leptin (R&D systems) at a dose of 5g/kg in ~100µl or vehicle. Food intake was monitored for a 5-day washout period after treatment and the study then crossed over.

2.7.3 Response to melanocortin agonist (melanotan II)

Prior to treatment mice were sham fasted and injected with saline, and allowed to recover for 3 days. Mice were weighed and food and bedding removed. They were fasted for 16 hours overnight and in the early light phase were injected with either MTII (50µg per mouse) or phosphate buffered saline in a volume of 100µl. Approximately 50g of food was then weighed out and given to each mouse. The food was reweighed at 1h, 2h, 4h and 8h.

2.8 Hypothalamic immunocytochemistry and in-situ hybridisation

Mice were terminally anaesthetised and brains harvested following transcardiac perfusion with RNAse-free phosphate-buffered saline and 4% paraformaldehdye using a Marlow Watson peristaltic pump. Brains were post-fixed overnight in 4% paraformaldehyde, transferred to RNAse-free 30% sucrose and subsequently frozen after 48 h.

For studies on floating sections, 30 µm sections were cut from frozen brains using a sliding microtome and samples processed immediately or stored at -20°C in cryoprotectant before use. Alternatively, 20 µm sections were cut using a cryostat and thaw mounted on polylysine coated microscope slides (Sigma-Aldrich) and stored at -80°C before use.

For immunocytochemistry on floating sections samples were washed 3 times in potassium phosphate buffered saline (KPBS) pH 7.4, blocked with 2% serum (appropriate to the species of the secondary antibodies used) in KPBS/0.4% Triton X-100 for 1 h at room temperature and then incubated with primary antibodies in KPBS/0.4% Triton X-100 for 48 h at 4°C. Slices were then washed 4 x 10 min at room temperature with KPBS and then incubated with appropriate secondary antibodies (either fluorescently or biotin labelled) for 1h in KPBS/0.4% Triton X-100 at room temperature before being washed 4 x 10 min in KPBS at room temperature.

For chromagenic detection, slices were incubated for 60 min in avidin-DH/biotinylated horse-radish peroxidase (ABC Elite, Vector Laboratories) in KPBS/0.4% Triton X-100, washed 2 x 10 min in KPBS, 2 x 10 min in 150mM sodium acetate and then nickel-

enhanced detection performed with a 3, 3'-diaminobenzidine substrate kit for peroxidase (Vector Laboratories). In this case an additional fluorescent BLAST protocol was used with a biotinylated tyramide amplification stage and fluorescent detection with streptavidin-conjugated Alexa Fluor 594 being employed.

Slices were mounted on polylysine-coated microscope slides and cover-slipped with buffered glycerol. GFP neurons were visualised directly. Primary antibodies used were rabbit anti-IRS2 antibody from Upstate Group Inc. (1 in 200) with batches of this antibody being tested for specificity of IRS2 detection in immunocytochemistry using tissues from mice with global deletion of IRS2 as negative controls, and mouse monoclonal anti-GFP (Chemicon Inc: 1 in 500). Fluorescently labelled secondary antibodies were from Molecular Probes (Eugene, Oregon) and included chicken anti-rabbit IgG conjugated to Alexa Fluor 488 (green) or Alexa Fluor 594 (red), chicken anti-mouse IgG conjugated to Alexa Fluor 488 (green), donkey anti-sheep IgG conjugated to Alexa-Fluor 594 (red). Biotin labelled secondary antibodies were from Abcam and included biotinylated chicken anti-rabbit and chicken anti-mouse antibodies both used at 1 in 600 dilution.

2.9 In situ hybridisation

For combined *in situ* hybridisation and immunocytochemistry, ISH was performed first under RNAse free conditions.

In brief, sections were fixed in formaldehyde solution (0.8ml of 36% formaldehyde in 400ml 0.01M PBS) for 20 min on ice. Section were then washed twice in PBS for 5 min

and acetylated at RT for 10 min in 400 ml 0.1M triethanolamine (pH 8.0) containing 1 ml acetic acid anhydride.

After washing two times with PBS, sections were then dehydrated in graded alcohol and air-dried for 30 min. Probes were labelled with digoxigenin (DIG) (Roche Diagnostics Ltd) with DIG-UTP. Hybridization buffer (0.1M NaCl, 30% deionized formamide, 0.3×Denhardts 12.5mM Tris-HCl pH8.0, 12.5mM EDTA, 12.5% dextran sulphate, 10mM DTT, and 0.25 mg/ml tRNA) containing 2ng/µl DIG-labelled probe was applied to each section and the section covered with glass cover-slip. The sections were hybridized overnight at 60 °C in a humidified chamber.

The sections were then placed in 4× SSC to remove coverslips and RNase A treated (20µg/ml in 0.5M NaCl, 10mM Tris-HCl, 1mM EDTA) for 30 min at 37 °C. Following RNase treatment sections were washed in 2x SSC at 60 °C for 10 min, 1x SSC at 60 °C for 10 min, 0.5× SSC at 60 °C twice for 10 min and 0.1× SSC at 60 °C for 30 min. Sections were then cooled to RT in 0.1× SSC and immuno-histochemical detection of bound DIG-labeled probe was carried out using alkaline phosphatase-conjugated anti-DIG antibody (Roche Diagnostics Ltd).

Sections were first blocked for 1 h with blocking solution containing 0.1M Tris-HCl (pH7.5), 0.15M NaCl, 5% Fetal Bovine Serum and 0.05% Tween-20 and then incubated for 2 hours with anti-DIG antibody (1:2000 in blocking solution). Following two washes of 5 min each in wash buffer (0.1M Tris-HCl pH 9.5, 0.15M NaCl, 0.05% Treen-20), chromogenic detection was performed at RT for 3-16 hours in the dark using nitro-blue

tetrazolium and 5-bromo-4-chloro-3-indolylphosphate as substrates. *In situ* ribo-probes were generated using mouse sequences (POMC: accession number NM_008895 and NPY: NM_023456).

Subsequent immunocytochemical detection of GFP was performed essentially as described above except that it was performed on slide-mounted sections rather than floating sections. Imaging was performed with an Olympus BX51 microscope with either a Hamamatsu 95 black and white camera or a Jenoptik PrgRsC14 color camera combined with SimplePCI capture and deconvolution software. Confocal microscopy was performed on a Biorad MRC1000 microscope.
This work was carried out with Dr Choudhury (Centre for Diabetes and Endocrinology, UCL).

2.10 Pancreatic immunocytochemistry and measurement of islet mass and number

Animals were killed by terminal anaesthesia. The pancreas removed, cleared of fat and lymph nodes and fixed in Bouin's solution, embedded in paraffin and cut into 5 μm sections. For detection of IRS2, the pancreas was harvested from mice that had been perfused with 4% paraformaldehyde as above.

For islet hormone staining for morphometric analysis, sections were treated with 0.01M citrate buffer for 10 min at 95°C and incubated with blocking solution containing PBS buffer with 5% normal chicken serum and 2% BSA for 30 min. Then a cocktail of primary antibodies in blocking buffer containing mouse anti-insulin antibody (clone

K36aC10, Sigma-Aldrich) and rabbit anti-glucagon (Abcam Ltd) was applied for 2 h at RT or overnight at 4°C.

The sections were then incubated with chicken anti-mouse IgG-AlexaFluor 594 and 488 conjugates (Molecular Probes) for 2 h at RT. Transmitted light and fluorescent images were captured with Metamorph software using a Zeiss Axiophot 2 microscope or with SimplePCI software using an Olympus BX51 microscope equipped with Hamamatsu 95 black and white camera.

For quantification of beta cell area and islet number, five pancreata were analysed per genotype at each time point. For each pancreas four sections, which were at least 150 um apart, were analysed. For each section the total area occupied by insulin-positive cells was scored using Simple PCI software, together with the number of islets on the section. Results are expressed as the percentage of the total islet area and the mean islet density for each pancreatic section.

2.11 Magnetic resonance imaging (MRI) and spectroscopy (MRS)

Mice were scanned using a 4.7T Varian system (Palo Alto, USA). Anaesthesia was induced and maintained by inhalation of 1-2% isoflurane/oxygen mix. Whole body images (between 50-60 slices; 2 mm thick) were obtained for each mouse using a spin-echo sequence (TR4500/TE20). Following a 16h fast, localised proton spectra of liver were obtained from a 3x3x3 mm voxel using a PRESS sequence (TR10000/TE14). Semi-automatic image segmentation software (sliceOmatic v4.2, Tomovision, Canada) was used to separate and quantify respective tissue volumes (Ross et al., 1991).

Briefly, structures (eg adipose tissue, liver, kidney, brain, intestines, skeletal muscle, lungs and other organs) were assigned colour tags using differences in signal intensity and anatomical location. Once the pixels were assigned, tissue volumes for each organ were calculated. For adipose tissue the volume was multiplied by a correction factor of 0.9 in order to account for hydration (Tang et al., 2002).

This work was done by Jimmy Bell at Hammersmith

2.12 DEXA Scanning

Mice were terminally anaesthetised and their body composition analysed using a DEXA scanner. Dual-energy x-ray absorptiometry (DEXA) scanning is widely used both clinically and experimentally to determine bone density.

This study employed the PIXImus DEXA scanner (Lunar, GE Healthcare, USA) specifically designed to study the skeleton of small rodents. DEXA scanning works on the principle that x-rays reflect from bone in a density dependent manner. The PIXImus system exposes the entire animal to a cone shaped beam of high energy (80 kV) and low energy (55 kV) x-rays. A CCD (charged couple device) camera detects the radiation hitting a luminescent panel below the test subject. The varied compositions of bone mineral, fat and lean tissue means they differentially absorb or reflect the dual energy x-rays; thus by digitally processing the detected radiation, the PIXImus can calculate the relative quantities of bone, fat and lean tissue along the x-ray path.

During each scan, the dual x-ray exposure is performed four times and on completion, the data is collated to produce a 'summary' image, the density of which is compared to a standard object (mouse phantom) used to calibrate the instrument. All data was analysed using the PIXImus software (version 1.8, Lunar, GE Healthcare, USA).

2.13 Gene expression

Gene expression studies were performed at Astra Zeneca, Alderley Park site under the supervision of Dr. Dave Smith.

2.13.1 RNA extraction

Throughout handling of tissue and the extraction process, standard precautions were taken to reduce the risk of RNAse contamination. Bench surfaces, tools, and pipettes were treated with RNAse inhibitor spray (RNAaseZap, Ambion, UK), filtered pipette tips used, and gloves frequently changed.

100mg of tissue, or the whole hypothalamus, was homogenised on ice in a 5mL flat-bottom universal container at 12,000rpm with a rotor-stator dispersing tool (Turrax T25, IKA, Germany) in 1mL of a phenol/guanidine isothiocyanate solution according to the manufacturer's instructions (Trizol reagent, Invitrogen, UK). The precipitated RNA was resuspended in 100µL of nuclease-free H_2O (Promega, UK). RNA was then DNase treated to remove any contaminating genomic DNA (Ambion TurboDNase kit). RNA content and purity were determined by measuring absorbance at 260nm and the 260/280 ratio using a nanodrop (ND-1000 NanoDrop Technologies).

2.13.2 Real time PCR of target genes

Quantitative PCR was performed with the TaqMan® system (Roche Molecular Systems, California, USA). All target gene probes (Sigma Genosys, UK) were 5'-labelled with FAM as reporter dye and 3'-labelled with TAMRA as quencher dye.

2μL of the generated cDNA was used as template and final primer concentrations were 0.3μM and those of the probes were 0.15μM in the supplied TaqMan® reaction mix. PCR was performed in duplicate in a 10μL sample volume in a 384-well plate in an ABI Prism 7900 HT thermocycler (Applied Biosystems, UK). A standard curve was prepared by pooling aliquots from each cDNA specimen and a subsequent serial dilution of 1:2:2:2:2:2, which were included in each PCR run. The standard curve method of quantification was employed to test the quality of the cDNA prior to running gene cards. Standard curves were generated for hprt and IRS-2 using products from both the +RT and –RT reverse transcription reactions. The manufacturer's recommended cycling conditions were employed, consisting of 50°C for 2min and subsequent 95°C for 10min, followed by 40 cycles of 95°C for 15sec and 60°C for 1min. All temperature changes occurred at maximum ramp speed. The integrated 488nm Argon laser excitation/detection system used SDS 2.1 software (Applied Biosystems, UK).

2.13.3 AB Gene Cards

Gene cards were custom made to allow screening of 48 different genes. Of these, 3 were housekeeping genes (18S, hprt and α-tubulin). The cards were a modified 384 well plate, where the probes and primers for each gene were spotted onto the wells.

2.13.4 Data analysis

The target gene C_t values were read off the generated standard curve and converted to arbitrary units by inverse logarithm. The same mathematical procedure was applied to the hprt C_t values and the target gene/hprt ratio calculated. The corrected values were expressed as relative difference in gene expression.

2.13.5 Gene card analysis

To analyse the data generated by the gene cards, the ΔΔCT method was used. Using SDS software, a study group was created combining multiple plates. Once the plates had been added to the study group a calibrator sample was chosen and an endogenous control gene selected. The first set of data was analysed separately using each of the control genes and hprt subsequently selected as the control for further studies. An experimental report was then exported into excel for further analysis.

For each sample a delta CT value was calculated, giving the Ct of the target gene – Ct of the endogenous control. Delta delta CT was then calculated by subtracting the delta CT of the calibrator from the delta Ct of the sample. The ΔΔCT value was used to calculate fold change (RQ), which is $2^{-\Delta\Delta CT}$.

2.14 Data analysis and presentation

Data was initially collected using Microsoft Excel spreadsheets. Subsequent calculations, statistical analyses, and graph generation were carried out with GraphPad Prism Version 4 (GraphPad Software, California, USA). Differences between groups were compared by an unpaired, two-tailed Student's t-test except where stated. A p-value <0.05 was considered significant and is indicated by one asterisk (*), a p-value <0.01 is indicated by two asterisks (**). Results are representative of at least five animals per group, unless stated otherwise, and are expressed as an average ± standard error of the mean (SEM).

2.15 Suppliers

Chemicals were purchased from Sigma-Aldrich, UK, except where otherwise stated.

3. Analysis of Irs2 deletion in mice derived from *RIPCreIrs2lox/lox* and *RIPCreZ/eg* intercrosses.

3.1 Generation and genotypic frequencies of RIPCre Irs2 flox offspring

To obtain all genetic combinations of *RIPCre* and *IRS-2flox* genes, *Irs2flox/flox* and *RIPCre* positive mice were crossed to obtain double heterozygotes. These double heterozygotes were then intercrossed. Double heterozygotes were fertile and produced litters comparable in size to wild-type mice.

This cross produced all of the expected genotypes which were seen at frequencies close to their expected Mendelian ratios. With 18.5% offspring having the *RIPCreIrs2lox/lox* (*RIPCreIrs2KO*) genotype (Table 3.1).

Genotype	Number	Percentage	Expected percentage
Irs2 lox	221	15.8	12.5
Irs2 lox/lox	113	8.1	6.3
Wild-type	147	10.5	6.3
RIPCreIrs2 lox	359	25.7	37.5
RIPCreIrs2 lox/lox	**258**	**18.5**	**18.8**
RIPCre	297	21.3	18.8
TOTAL	**1395**		

Table 3.1 Genotypic frequencies of offspring from RIPCreIrs2lox/lox mice.

Mice were PCR genotyped at 14 days of age.

3.2 Generation of Fluorescent indicator mice

Both *RIPCre* mice and *RIPCreIrs2KO* mice were intercrossed with *lacZ/GFP* (*Z/eg*) mice (Novak *et al.*, 2000) to obtain mice in which cells expressing the *Cre* transgene also expressed GFP

3.3 Proof of IRS-2 deletion

To demonstrate deletion of *Irs2* three techniques were used; initially deletion of *Irs2* was confirmed by PCR techniques, this deletion was then further investigated by immunocytochemistry.

Deletion of the *Irs2* gene from the islets of *RIPCreIrs2KO* mice was demonstrated by PCR on DNA from isolated islets. The presence of a 1.3kb PCR product indicates recombination and deletion of *Irs2*. No product was amplified in the control mice. The 0.32kb band is an internal control PCR product (Figure 3.1A) Analysis of *RIPCreZEG* mice demonstrated that cells expressing *GFP* also express α insulin, indicating that RIPCre causes recombination in, at least some β-cells within the islets (Fig 3.1B), though it is not clear what proportion of β-cells the recombination occurs in.

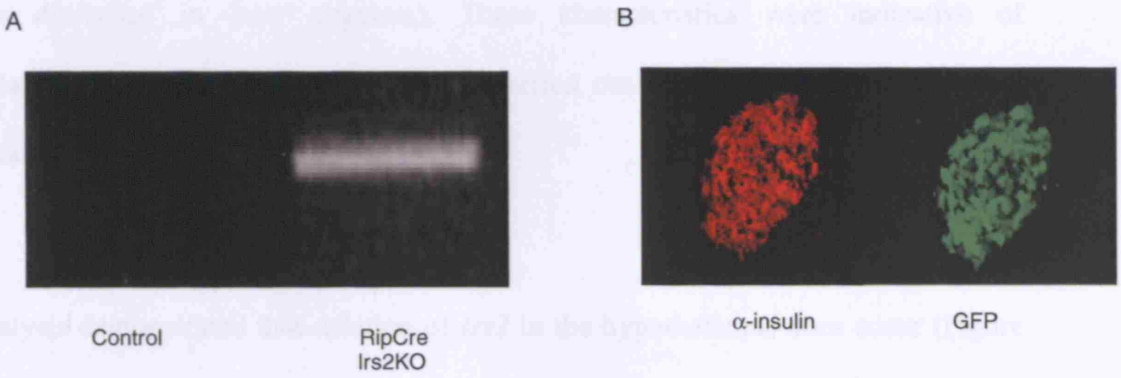

Figure 3.1. Analysis of Irs2 deletion in islets.

(A) PCR analysis was performed to detect recombination of the loxP sites flanking the Irs2 locus in genomic DNA isolated from islets of 6 week old RIPCreIrs2KO and control mice. (B) Staining of islets for α insulin and GFP form RIPCreZEG mice. Results presented are typical of those obtained from 4 animals of each genotype.

As the studies on *RIPCreIrs2KO* mice progressed it became clear that they displayed some phenotypic characteristics that could not be explained by β-cell specific deletion of *Irs2* (as discussed in later chapters). These characteristics were indicative of hypothalamic disruption and so studies were carried out to assess *Irs2* deletion in the hypothalamus of *RIPCreIrs2KO* mice.

PCR analysis demonstrated that deletion of *Irs2* in the hypothalamus does occur (Figure 3.2A). This was further investigated using immunohistochemical analysis which showed co-localisation of Irs2 with GFP in a significant number of neurones in *RIPCreZEG* mice. However *RIPCreIrs2KOZ*/eg mice showed no co-localisation of Irs2 and GFP confirming Irs2 deletion in the neurons that expressed Cre recombinase (Figure 3.2C). It is interesting to note that there are still cells within the hypothalamus which express Irs2 but do not express Cre, and therefore there will be no recombination event in these cells. For this reason western blot analysis was not performed on hypothalami, as the proportion of cells expressing Cre recombinase is very small and the resulting reduction in Irs2 expression would be too small to be detected using western blotting.

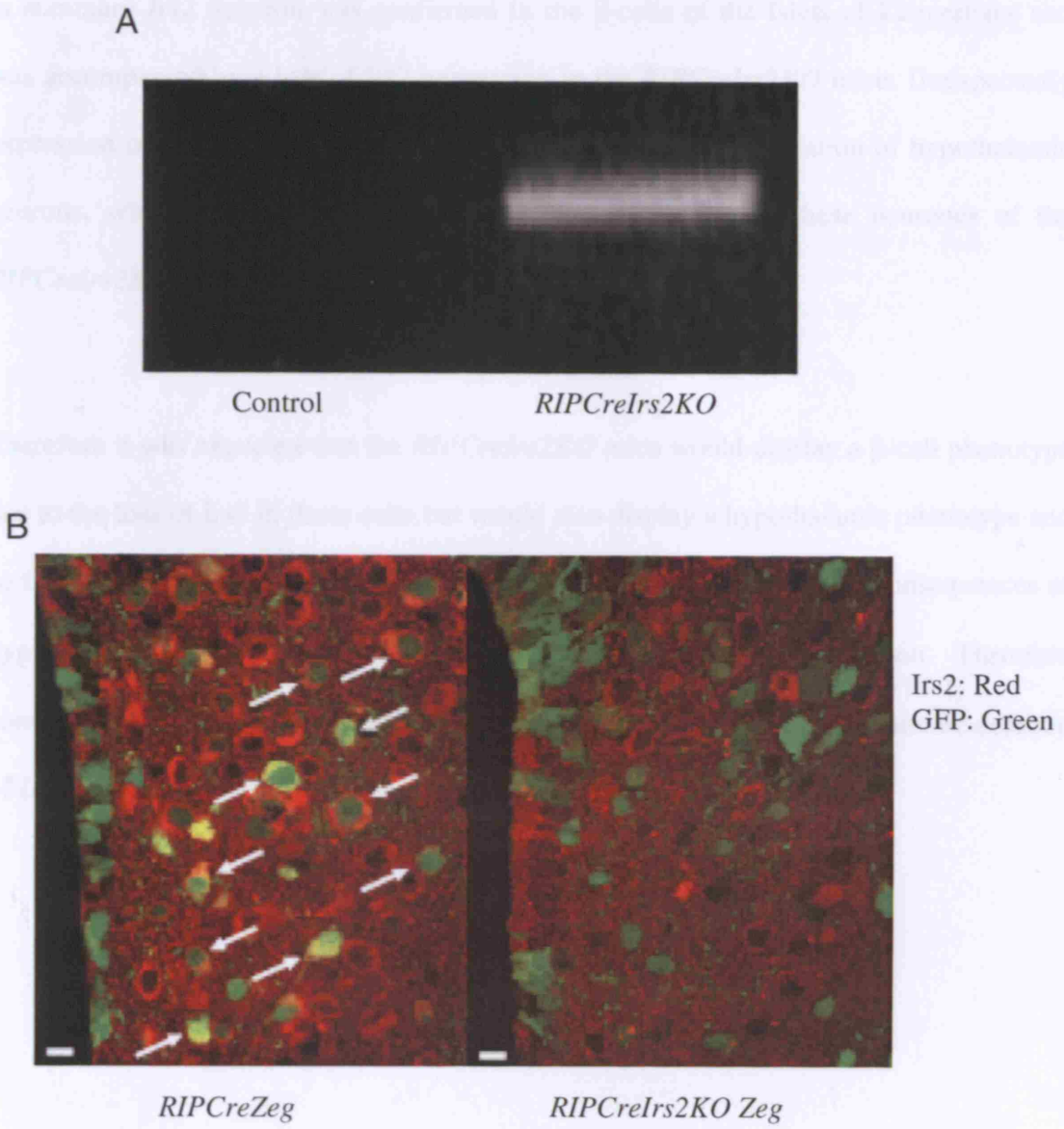

Figure 3.2. Verification of Irs2 deletion in the hypothalamus of RIPCreIrs2KO mice.

(A) PCR analysis was performed to detect recombination in the hypothalamus of RIPCreIrs2KO and control mice. (B) Fluorescence immunohistochemical analysis of Irs2 expression in the hypothalamus in RIPCreIrs2KO and control mice. Results presented are typical of those obtained from 4 animals of each genotype.

In summary *Irs2* deletion was confirmed in the β-cells of the Islets of Langerhans and was accompanied by a loss of Irs2 expression in the *RIPCreIrs2KO* mice. Unexpectedly expression of Cre recombinase was also detected in a small population of hypothalamic neurons, which would result in a loss of *Irs2* expression in these neurones of the *RIPCreIrs2KO* mouse.

Therefore it was expected that the *RIPCreIrs2KO* mice would display a β-cell phenotype due to the loss of Irs2 in these cells but would also display a hypothalamic phenotype and so these two phenotypes were investigated independently. However, the consequences of hypothalamic deletion, such as obesity, can influence β-cell function. Therefore components of the ß-cell phenotype may also be as a result of the hypothalamic deletion of *Irs2*.

4. Analysis of glucose homeostasis in *RIPCreIrs2KO* mice.

The *Irs2* global knockout mouse develops insulin resistance and, eventually, overt type 2 diabetes. This complex phenotype was a result of deleting *Irs2* in all tissues and further investigation is necessary to determine the function of Irs2 in specific tissues, in particular the pancreas as, in the global knockout mouse the glucose homeostasis phenotype seen may be partly due to *Irs2* deletion in the other insulin target tissues such as the liver and white adipose tissue. The *RIPCreIrs2KO* mouse should therefore allow us to determine the effect of Irs2 in the β-cell in maintaining glucose homeostasis. In order to assess the effect of deleting *Irs2* in the β-cell, metabolic studies were carried out post-weaning and at later time points as indicated.

4.1 Fasting blood glucose

Fasting blood glucose in *RIPCreIrs2KO* mice at 4 weeks old was indistinguishable from that of control animals (Fig 4.1A). By 12 weeks old *RIPCreIrs2KO* mice showed a significant hyperglycaemia, in both males and females (figure 4.1. B and C). This hyperglycaemia was even more pronounced at 6 months of age (Fig 4.1D). Although blood glucose is increased it did not reach the levels required for diagnosis of diabetes.

As there were no significant differences between any of the control groups (*RIPCre, RIPCreIrs2lox, Irs2lox, wt*) this data was grouped with equal representation of each genotype.

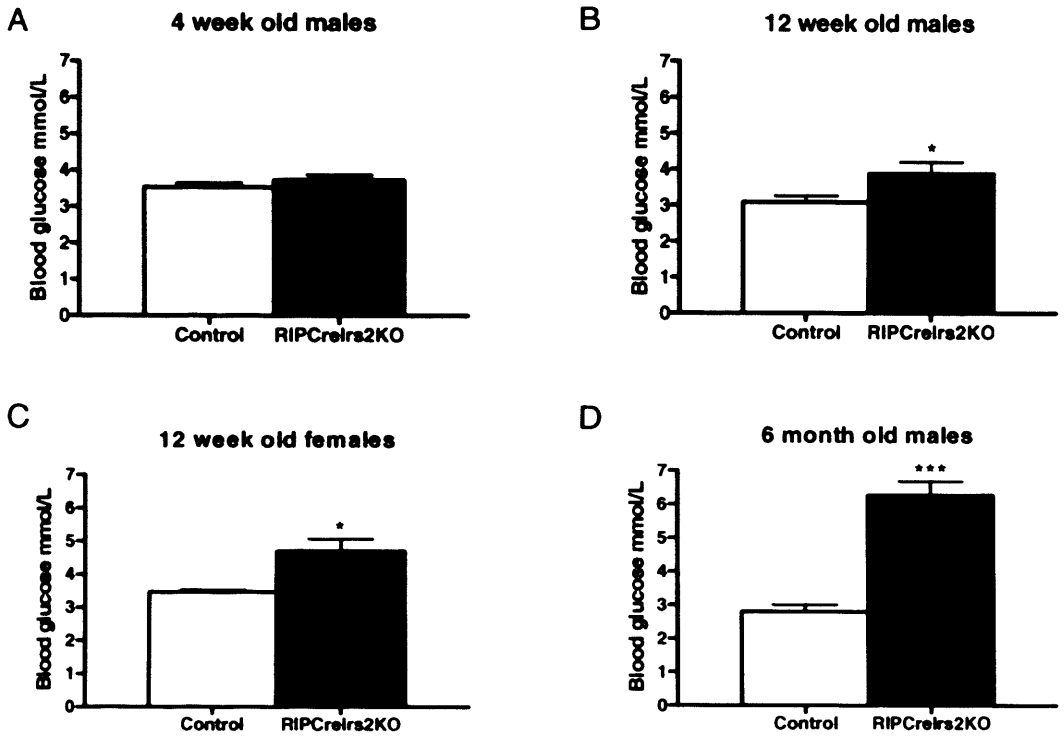

Figure 4.1. Fasting blood glucose in RIPCreIrs2KO and control mice.

Fasting blood glucose levels were measured in male RIPCreIrs2KO mice and control mice at 4 wks (A), 12 wks (B) and 6 m (D) of age, and in female mice at 12 weeks of age (C). Following a 16 h overnight fast, fasting blood glucose was measured. Data represent the mean ± SEM for 8-10 animals of each genotype.

** $P < 0.05$, ** $P < 0.01$ and *** $P < 0.001$*

Therefore deletion of *Irs2* in islets did not recapitulate the progressive onset of type 2 diabetes seen in the global *Irs2* knockout mouse. Although the *RIPCreIrs2KO* mice did display increased fasting blood glucose compared to control mice which worsened with age, this was not as pronounced as expected.

Glucose tolerance tests were performed on male *RIPCreIrs2KO* and control mice at 4 wks (Fig 4.2A), 12 wks (Fig 4.2B) and 6 months (Fig 4.2C) of age after a 16 h overnight fast. Following an intraperitoneal injection of D-glucose (1.5g/kg body weight) blood glucose was measured at the indicated time-points. At 4 and 12 weeks of age *RIPCreIrs2KO* mice were mildly glucose intolerant but did not display signs of diabetes (Fig4.2. A, and B). Females at 12 weeks were also glucose intolerant (Fig 4.3). By 6 months old male *RIPCreIrs2KO* mice were significantly glucose intolerant (Fig4.2.E and F). Again, the *RIPCreIrs2KO* mice did not display the progressive glucose intolerance seen in the global *Irs2KO* mouse. *RIPCreIrs2KO* mice were glucose intolerant compared with control mice, but this did not progress to type 2 diabetes, even at 6 months of age.

Glucose tolerance tests on female *RIPCreIrs2KO* mice at 12 weeks of age reflect the results seen in male mice (Fig 4.3). The *RIPCreIrs2KO* females are significantly glucose intolerant compared to control mice, but as with male mice, this does not meet the diagnostic criteria for type 2 diabetes.

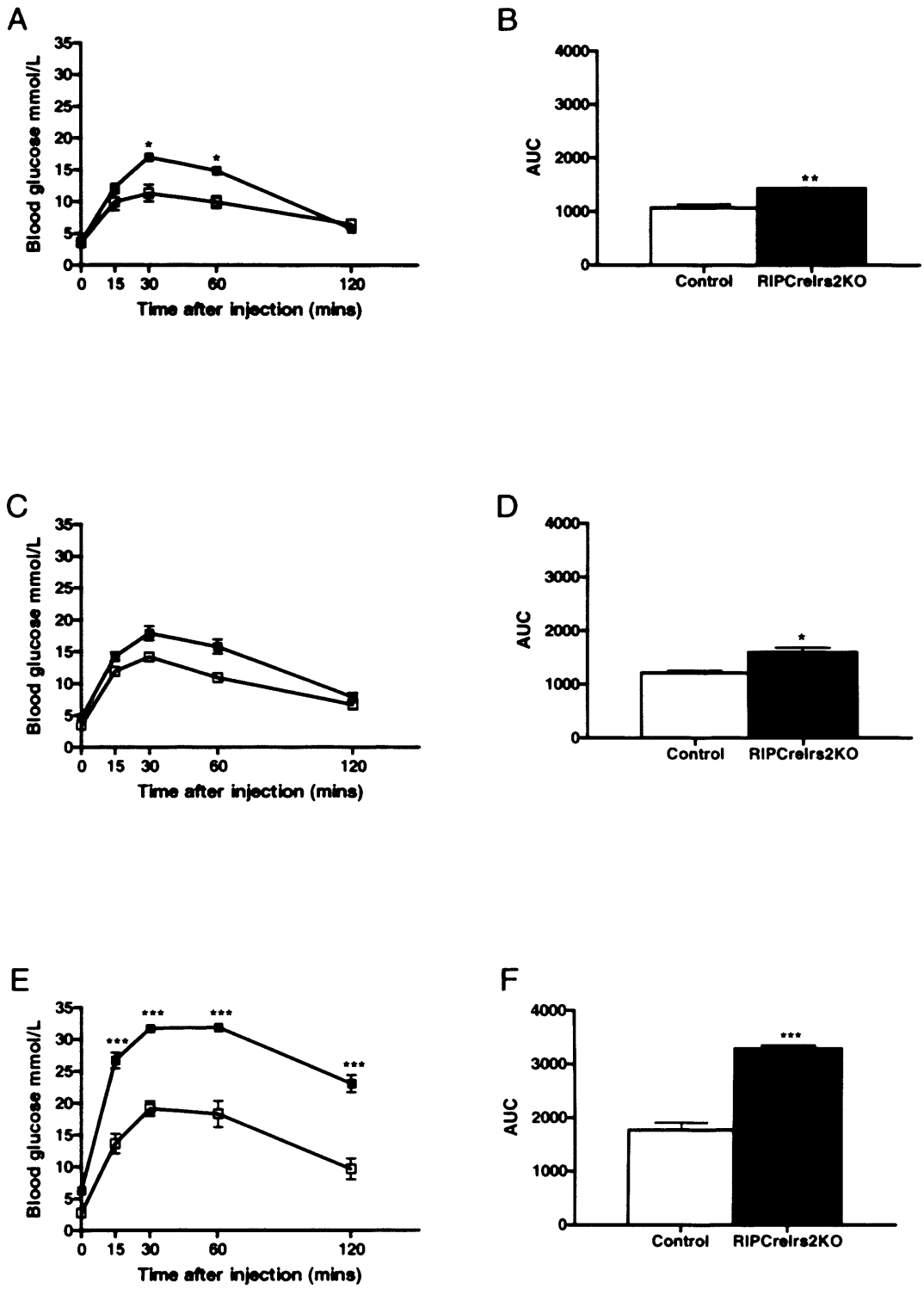

Figure 4.2. Glucose Tolerance Test.

*Intraperitoneal Glucose tolerance testes were performed on male RIPCreIrs2KO (closed squares) and control (open squares) mice at 4 weeks (A&B), 12 weeks(C&D) and 6 months(E&F) of age and the area under the curve calculated(inset). Data represent the mean ± SEM for 8-10 animals of each genotype. * P < 0.05, ** P < 0.01 and *** P < 0.001*

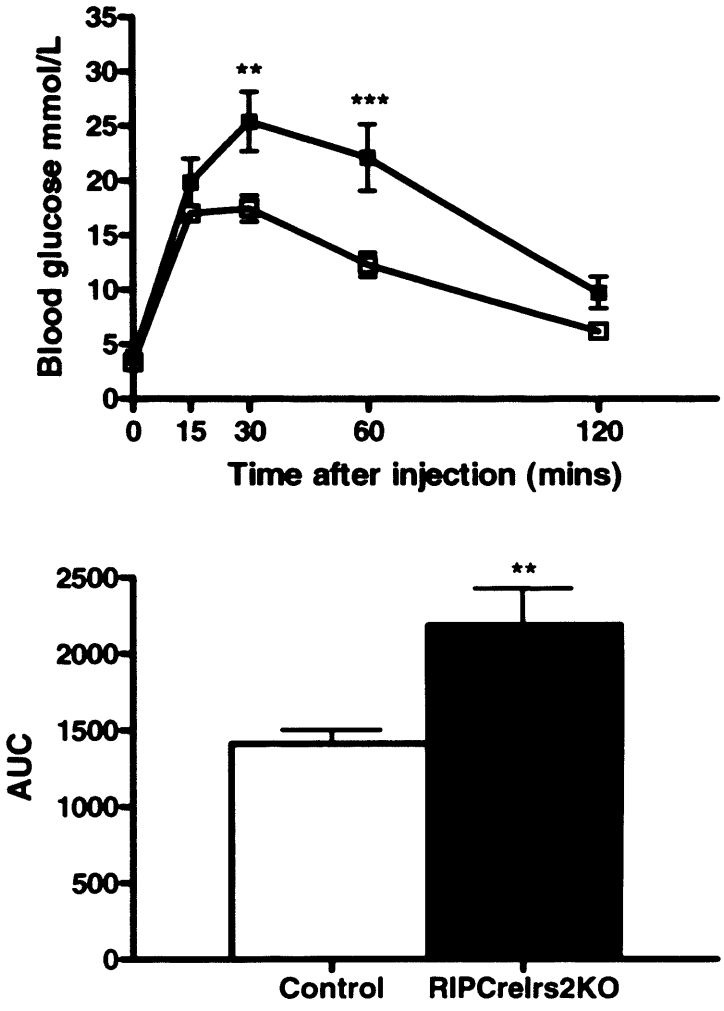

Figure 4.3 Glucose tolerance test.

*Intraperitoneal glucose tolerance tests were performed on female RIPCreIrs2KO (closed square) and control (open square) female mice at 12 weeks of age. Data represent the mean ± SEM for 8 mice of each genotype. ** $P < 0.01$*

4.2 Fasting blood insulin levels

Deletion of *Irs2* in the β-cells should prevent β-cells from increasing insulin production as is demonstrated in the global *Irs2KO* mouse which is unable to mount a hypoglycaemia response to peripheral insulin resistance.

Analysis of fasting blood insulin levels in the *RIPCreIrs2KO* mice was therefore carried out using a mouse insulin ELISA. Male mice at 4 weeks old showed significant hyperinsulinaemia, after a 16h overnight fast, which persisted at 12 weeks and 6 months of age (Fig 4.4).

Deletion of *Irs2* in the β-cell causing an increase in insulin production is unexpected and it is likely that this may be secondary to the obesity phenotype described later.

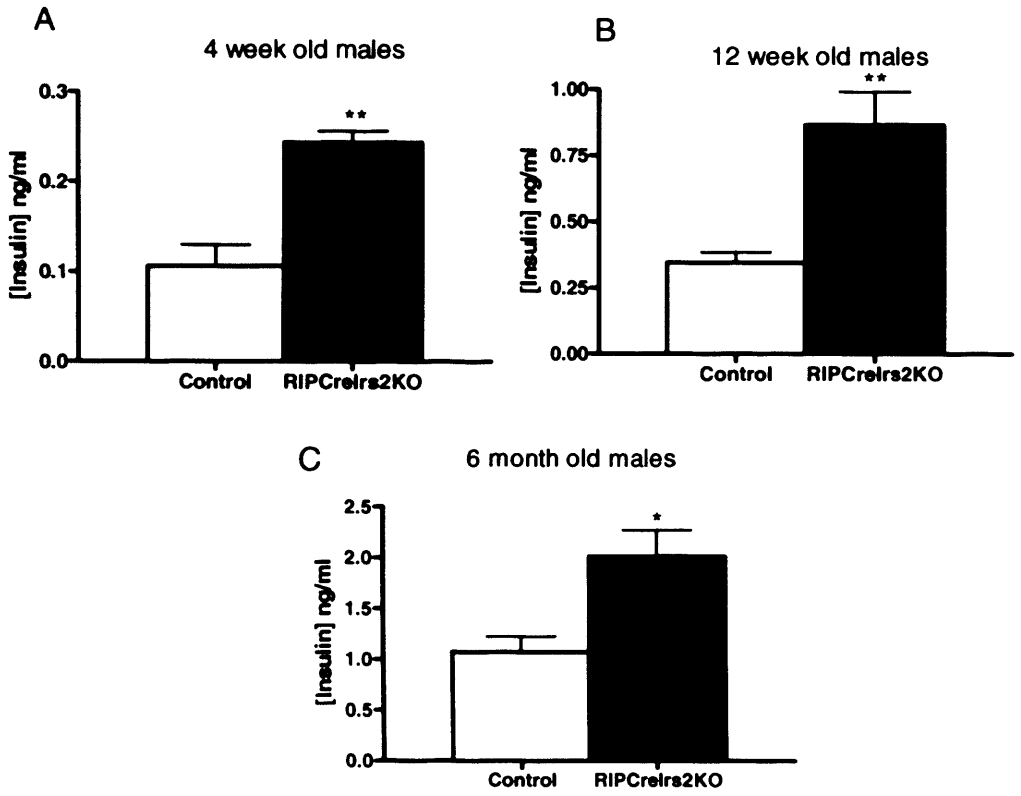

Figure 4.4. Fasting serum insulin.

*Fasting insulin levels were measured by ELISA from male RIPCreIrs2KO and control mice. Mice at 4 weeks (A), 12 weeks (B) and six months (C) were fasted for 16h overnight prior to blood collection. Data represent the mean ± SEM for 8 mice of each genotype. * $P < 0.05$, ** $P < 0.01$*

4.3 Pancreatic islet mass and density

The global *Irs2* knockout mouse develops progressive diabetes due to a failure of the ß-cells to mount a hyperinsulinaemia response to peripheral insulin resistance. This failure is largely due to a significant reduction in islet mass in these mice. As discussed in the previous chapther the *RIPCreIrs2KO* mouse does not develop the diabetic phenotype seen in the global knockout and shows an increase in circulating insulin. Therefore, islet mass and density in the *RIPCreIrs2KO* mouse was investigated.

Analysis of islet size and density in male mice shows that at 4 weeks old there is no significant difference in islet size or density (Fig 4.5 A and C). At 12 weeks old, however, a 40% reduction in islet area was seen, as well as a significant decrease in islet density (Fig 4.5 B and D). In control mice the islet density did not change over time, indicating a static number of islets in the pancreas.

By 9 months of age the islet area in *RIPCreIrs2KO* males was still significantly lower than that of control mice (Fig 4.6). However, the islet mass of the *RIPCreIrs2KO* mice had increased significantly at 9 months of age compared with the area at 12 weeks of age. However, the persistent reduction in islet mass in the *RIPCreIrs2KO* mouse shows a defect in β-cells that worsens with age as indicated by the Glucose tolerance test at 6 months of age. The small increase in islet mass seen at later ages suggests that the defect is not present in all β-cells, and that the unaffected cells are still able to mount a small hyperinsulinaemic response preventing the development of overt diabetes

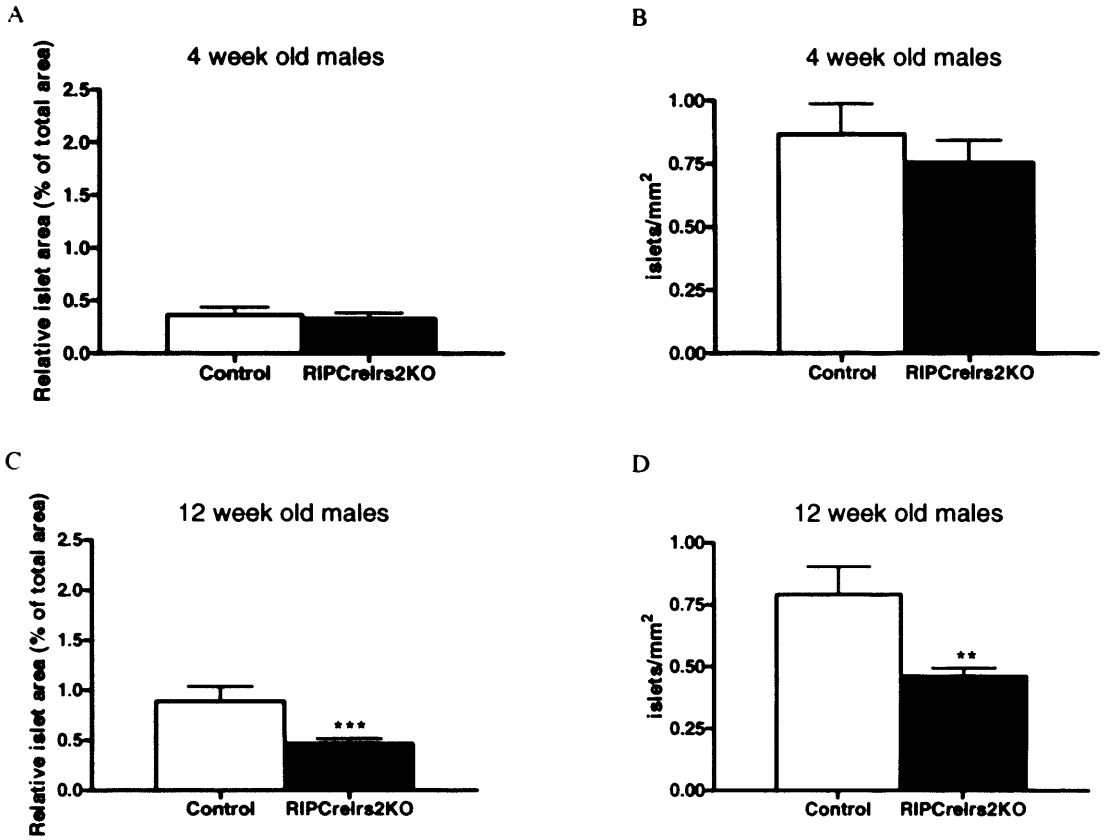

Figure 4.5 Pancreatic islet mass and density in male RIPCreIrs2KO and control mice.

*The percentage of the total pancreatic area occupied by beta cells at 4 wks of age (A) and 12 wks of age (C) for male RIPCreIrs2KO mice and control mice. The data presented are mean ± SEM for five mice of each genotype. Islet density at 4 wks of age (B) and 12 wks of age (D) for male RIPCreIrs2KO and control mice was calculated. The data presented are mean ± SEM for five mice of each genotype. * $P < 0.05$ and ** $P < 0.01$.*

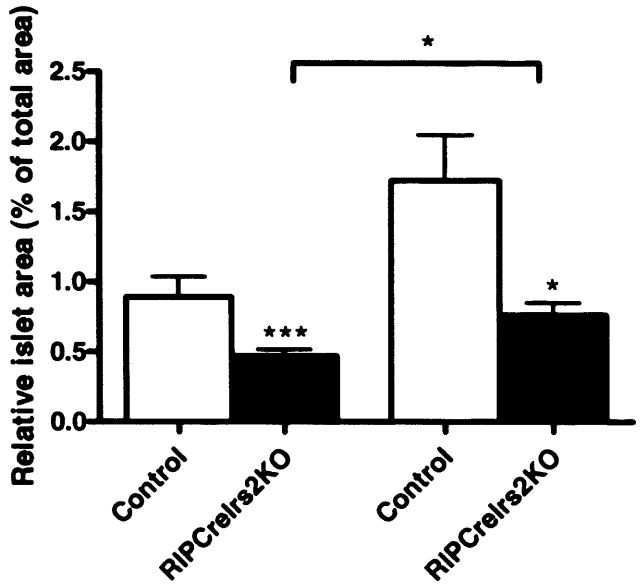

Figure 4.6 Islet area in male RIPCreIrs2KO and wild type males.

*The percentage of the total pancreatic area occupied by islets at 12 wks of age (left-hand side) and 9 months of age (right-hand side) for male RIPCreIrs2KO mice and control mice. The data presented are mean ± SEM for five mice of each genotype. * $P < 0.05$ and *** $P < 0.001$.*

The global *Irs2KO* mouse displays hyperglycaemia and glucose intolerance which rapidly progresses to type 2 diabetes and, if untreated, leads to death. It was expected that the *RIPCreIrs2KO* mouse would have a similar phenotype however this was not the case. *RIPCreIrs2KO* mice were hyperglycaemic and glucose intolerant compared to wild-type controls, but this was not as severe as the phenotype seen in the *Irs2KO* mouse and did not progress to diabetes, even at 9 months of age.

Interestingly, despite lacking Irs2 in β-cells the *RIPCreIrs2KO* mice displayed an increase in fasting insulin levels suggesting they are still able to partially mount a hyperinsulinaemia, which was lacking in the global *Irs2KO*.

Analysis of pancreatic morphology in male *RIPCreIrs2KO* mice shows that, as expected these mice have a significantly reduced β-cell mass compared with wild-type control mice. Interestingly, by 9 months *RIPCreIrs2KO* males showed some increase in islet area possibly as a result of increased pressure on β-cells due to an increase in peripheral insulin resistance. This may explain why these mice did not progress to overt diabetes as, if there is some recovery of islets with age, the mice may be able to slightly increase insulin production which would compensate for the peripheral insulin resistance.

5. Recovery of islets in *RIPCreIrs2KO* mice.

As discussed above the islets of *RIPCreIrs2KO* mice seem to show some recovery in β-cell mass over time. However, the mechanisms by which islets repopulate are controversial.

Islets mass can be increased by reducing the rate of apoptosis or increasing the rate of islet proliferation. New ß-cells can either be formed by replication of existing ß-cells or by neogenesis from ductal precursor cells. It was recently demonstrated using cre/loxP technology that pre-existing ß-cells are the major source of new ß-cells during adult life (Dor *et al*).

In order to investigate the mechanism of ß-cell recovery *RIPCreIrs2KO* and control mice were crossed into mice expressing GFP under the control of the lacZ promoter (Zeg mice). This cross produced offspring in which GFP was expressed in all RIPCre expressing cells.

5.1 RIPCre expression in islets of RIPCreIrs2KO mice

Immunofluorescence staining in *RIPCreIrs2KOZeg* mice showed that, at 4 weeks of age the majority of insulin expressing cells also expressed GFP and therefore recombination was occurring in most cells (Fig 5.1A and B). However there were a small number of cells expressing insulin that did not coexpress GFP and therefore will have escaped

recombination. It is likely that *Irs2* would not be deleted in these cells and they may therefore contribute to the recovery of β-cell mass.

By 9 months of age a significant proportion of insulin positive β-cells no longer expressed GFP (Fig 5.1 C and D) and therefore insulin signalling in these cells would be intact.

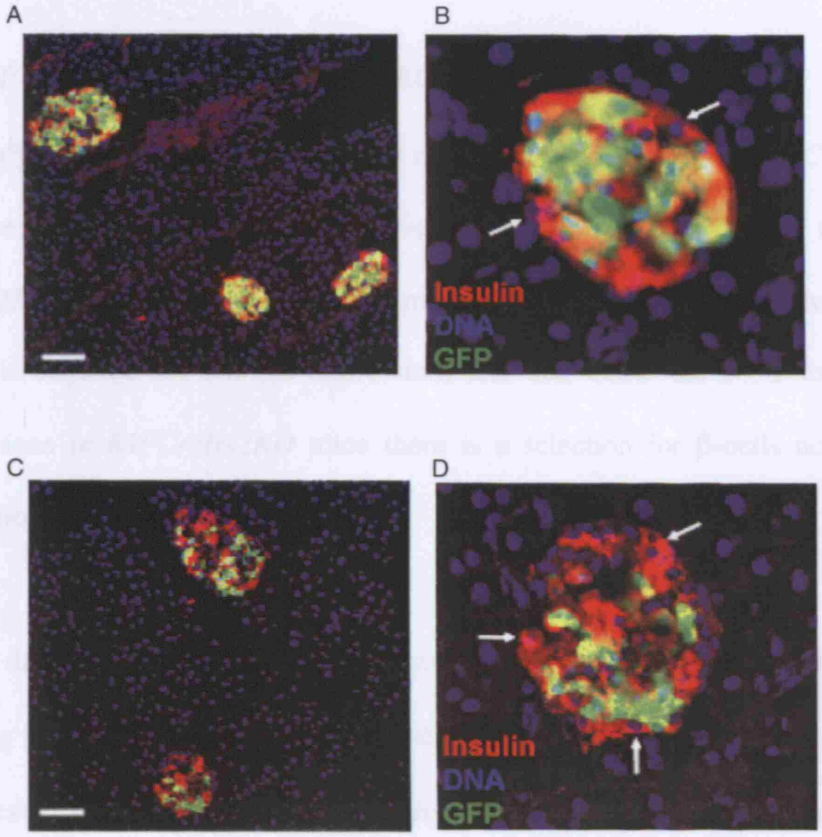

Figure 5.1. RIPCre expression.

Immunofluorescence staining for insulin (red) in islets from 4-week-old (A and B) and 9-month-old (C and D) RIPCreIrs2KOZeg mice stained for DNA (DAPI, blue). White arrows indicate β cells that do not express GFP and have not undergone recombination. Scale bars: 100μm.

5.2 GFP negative cells in RIPCreIrs2KO and control mice:

Further analysis of GFP negative cells in 9 month old *RIPCreZeg* and *RIPCreIrs2KOZeg* mice demonstrated that loss of GFP-positive β-cells occurred significantly more often in *RIPCreIrs2KOZeg* mice then in control mice (Fig5.2). This suggests that intact Irs2 signalling is required for RIPCre expression, and that under the conditions of insulin resistance seen in *RIPCreIrs2KO* mice there is a selection for β-cells not undergoing recombination to repopulate the islets.

The above data suggests that the partial recovery in β-cell mass is due to proliferation of pre-existing β-cells in which the Cre recombinase is not expressed. However it has also been suggested that ductal cells can give rise to new β-cells. To investigate this, duct epithelial cells were identified in *RIPCreIrs2KOZeg* mice using a duct-specific lectin (*Dolichos biflorus* agglutinin [DBA]). In 9-month-old *RIPCreIrs2KOZeg* mice, no GFP or insulin expression was seen in DBA positive cells and also no DBA positive cells were seen in islets (Fig 5.3). This suggests that, in *RIPCreIrs2KO* mice β-cells originating from ductal precursor cells do not significantly contribute to the β-cell repopulation.

Figure 5.2 GFP-negative cells in RIPCreIrs2KOZeg and RIPCreZeg mice at 9 months of age.

*Data shown from 2,062 β-cells sampled in 54 islets from 4 RIPCreIrs2KOZEG mice and 2,987 β-cells sampled in 45 islets from 3 RIPCreZEG mice. ***P<0.0001.*

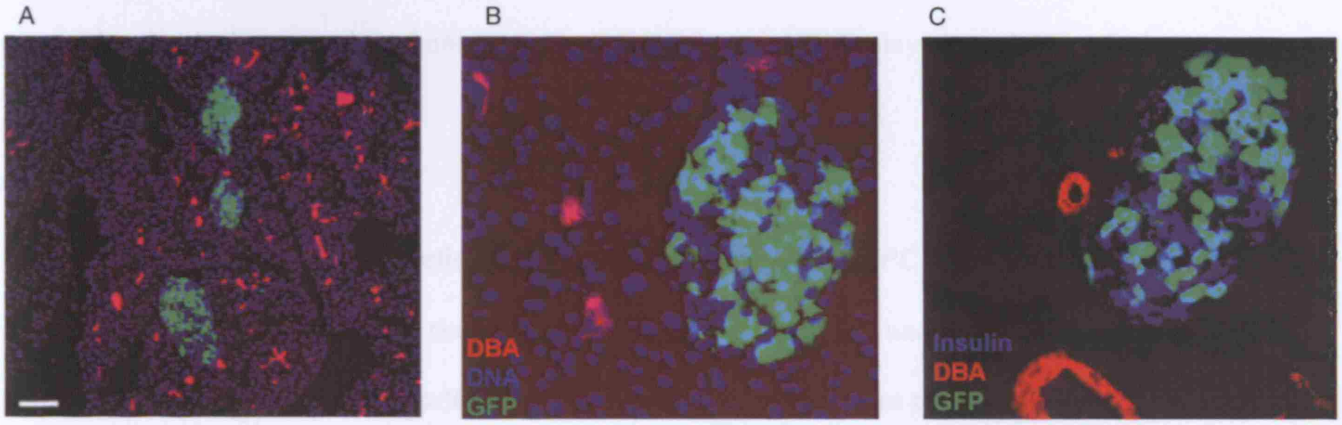

Figure 5.3 Duct cell marker labelling.

Labelling of ducts with DBA (red) in islets from 9-month-old RIPCreIrs2KOZEG mice stained blue for DNA and green for insulin. No duct marker is expressed in GFP-negative β cells. Scale bars: 100 μm.

Using the GFP indicator mouse, these studies have clearly shown that at 4 weeks of age small numbers of islet cells did not express Cre recombinase and therefore would not have undergone the recombination event. By 9 months of age significant numbers of β-cells in the *RIPCreIrs2KO* mouse did not express Cre, suggesting that the Cre negative cells had repopulated the islets. However many GFP positive cells remained in which recombination had occurred explaining why mice at this age still displayed a reduction in β-cell mass.

The reduction in GFP positive cells occurs predominantly in the *RIPCreIrs2KO* mouse suggesting that Irs2 signalling is needed for Cre expression and that under conditions of insulin resistance there may be selection for cells not expressing Cre to repopulate the islets.

The absence of GFP expression in ductal cells suggests that GFP negative β-cells could have arisen from ductal precursor cells. However, the lack of expression of the duct cell marker in islets of 9 month old mice suggests that the pre-existing β-cells which did not express Cre repopulated the islets.

The absence of Cre expression in ducts also suggests that the β-cell phenotype in *RIPCreIrs2KO* mice is the result of the loss of Irs2 in mature β-cells rather than precursor cells.

In summary, incomplete expression of Cre in the ß-cell population leaves a small proportion of cells which do not undergo recombination and are able to function

normally. Over time, these cells begin to repopulate the islets allowing recovery of ß-cell mass and function. In addition to this no ductal cell markers were seen in the islets, this supports the findings of Dor (Dor *et al.*, 2004), who proposed that existing ß-cells are the major source of new ß-cells in adults.

6. Hypothalamic function in *RIPCreIrs2KO* mice

As the β-cell phenotyping of the *RIPCreIrs2KO* mice progressed it became clear that they also displayed a hypothalamic phenotype. The demonstration of *RIPCre* expression in a population of neurons, and the subsequent deletion of Irs2 in these neurons led to a number of studies to determine the role of Irs2 in RIPCre neurones. Studies were carried out at post-weaning and at later ages

6.1 Body weight

Mice were weighed weekly from weaning to generate a growth curve. Male *RIPCreIrs2KO* mice were significantly heavier than all of the controls from 4 weeks of age and this increased weight persisted through life (fig 6.1 and 6.2) and female *RIPCreIrs2KO* mice were also significantly heavier from 12 weeks of age (figure 6.3.).

6.2 Analysis of length

It became apparent at weaning that *RIPCreIrs2KO* mice were longer then their wild-type littermates. This was therefore investigated by measuring naso-anal length.

Measurement of naso-anal body length at weaning showed a small, but insignificant increase of length of *RIPCreIrs2KO* male mice, by 12 weeks this increase was significant with *RIPCreIrs2KO* mice being approximately 10% longer than control mice (Fig 6.4.). Female *RIPCreIrs2KO* mice were also significantly longer then control mice from 4 weeks of age (Fig 6.5).

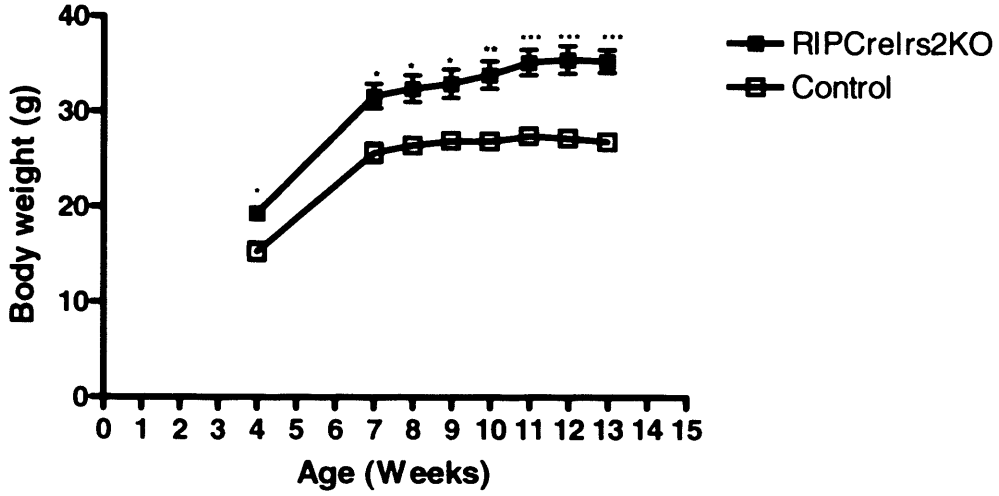

Figure 6.1 Serial body weight.

*Body weight in RIPCreIrs2KO (closed squares) and control (open squares) mice was measured weekly. Data represent the mean± SEM for 8-10 animals of each genotype. *P<0.05 **P<0.01 ***P<0.0001*

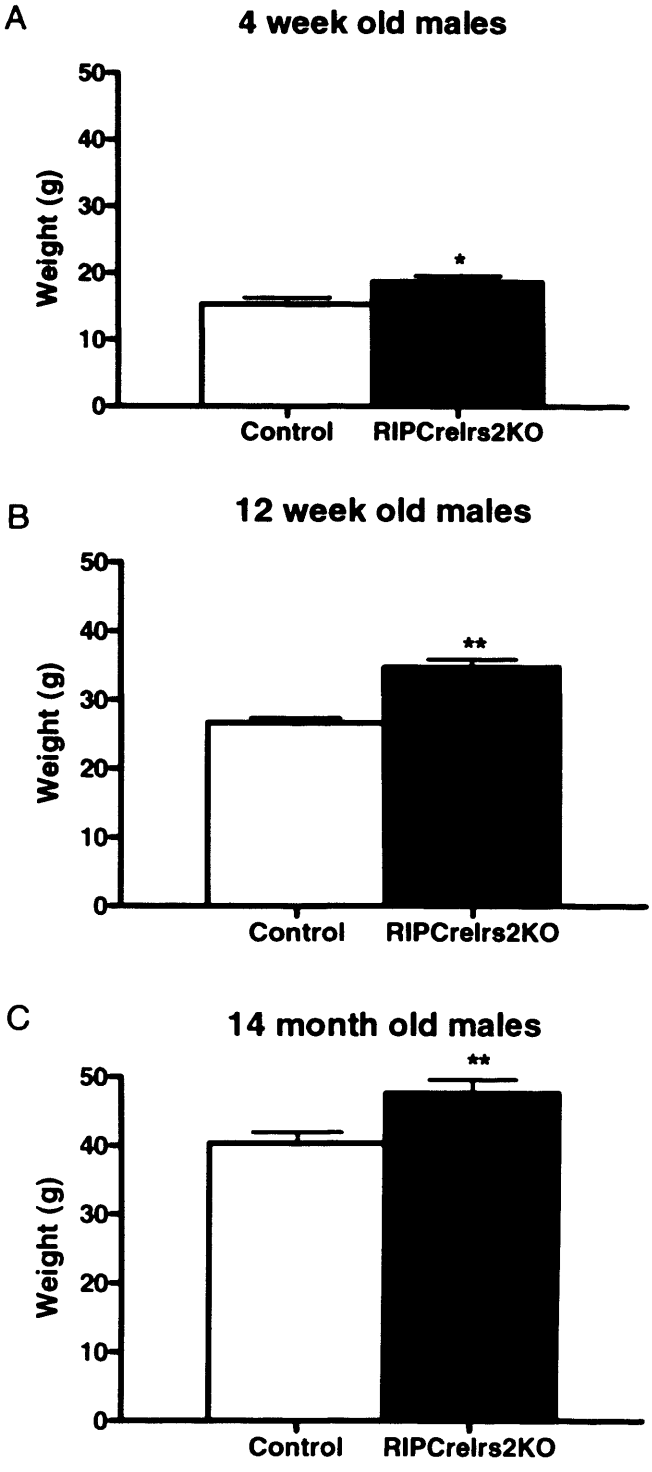

Figure 6.2. Analysis of body weight, in male RIPCreIrs2KO and control mice.

*Body weight was measured in RIPCreIrs2KO and control mice at 4 wks (A and B) 12 wks (C and D) and 14 months (E and F) of age. Data represent the mean ± SEM for 8-10 animals of each genotype. *P<0.05 **P<0.01*

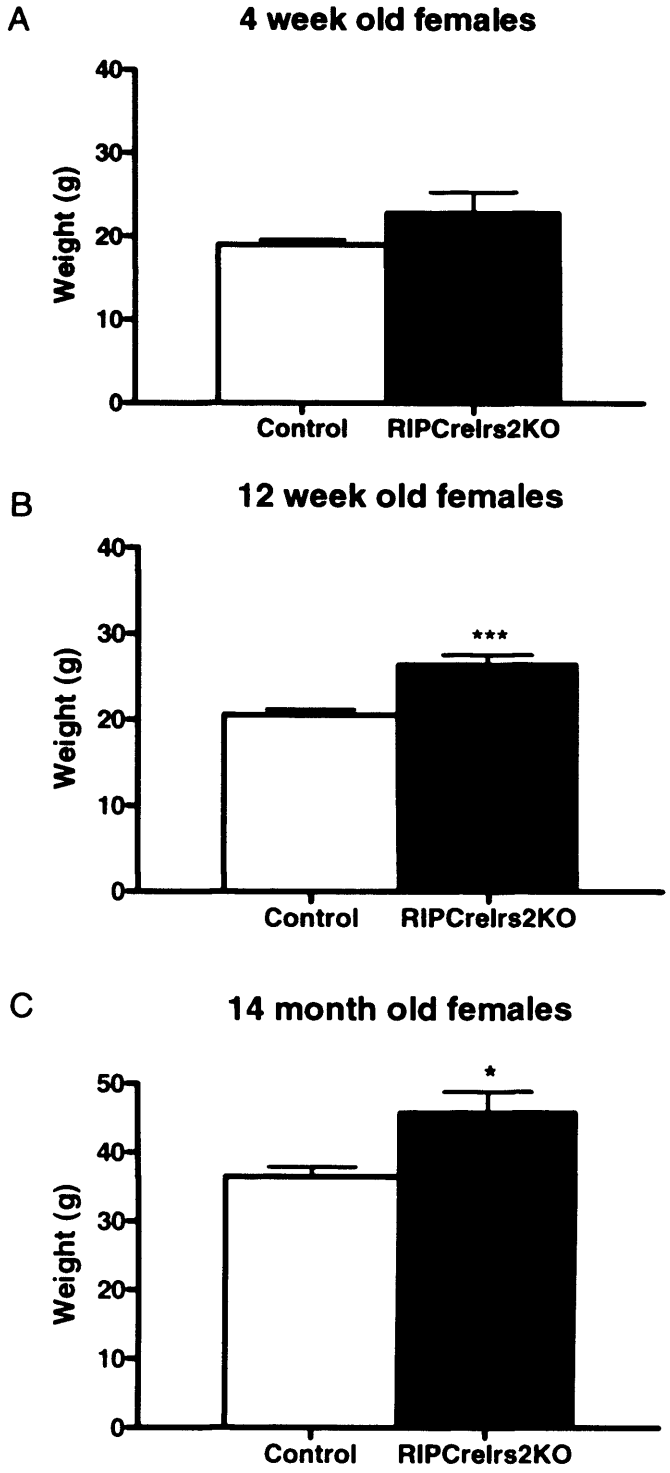

Figure 6.3. Analysis of body weight, in female RIPCreIrs2KO and control mice.

*Body weight was measured in RIPCreIrs2KO and control mice at 4 wks (A and B) 12 wks (C and D) and 14 months (E and F) of age. Data represent the mean ± SEM for 8-10 animals of each genotype. *P<0.05 ***P<0.0001*

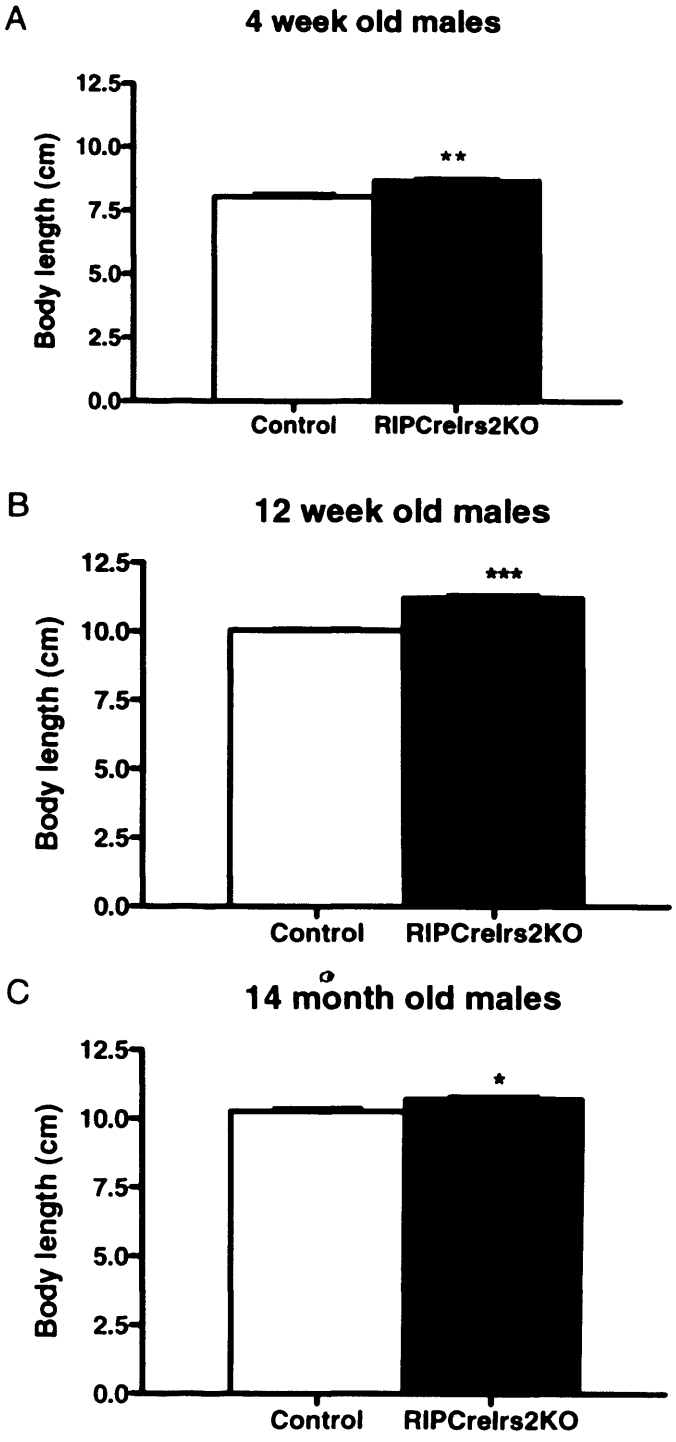

Figure 6.4. Body length.

*Naso-anal length was measured in male RIPCreIrs2KO and control mice at 4 wks (A), 12 wks (B) and 14 months (C) of age. Data represent the mean ± SEM for 8-10 animals of each genotype. *P<0.05 **P<0.01 ***P<0.0001*

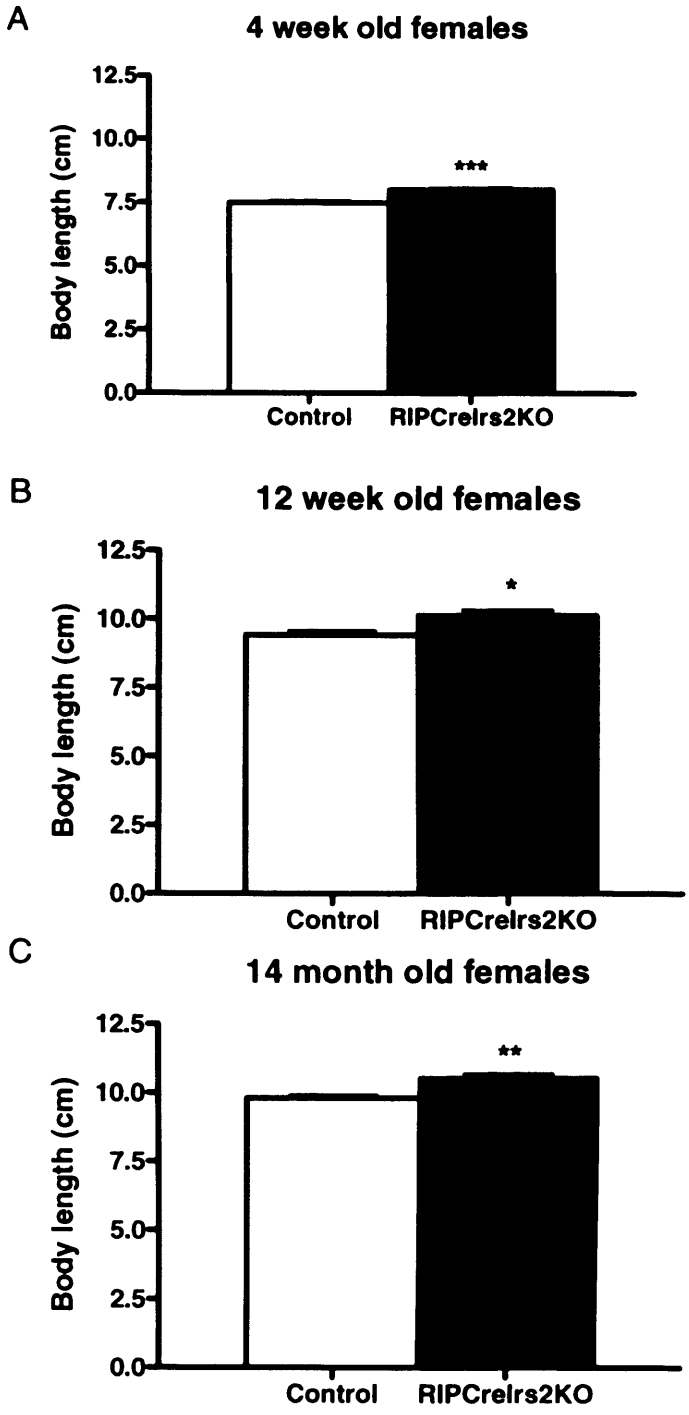

Figure 6.5. Body length.

*Naso-anal length was measured in female RIPCreIrs2KO and control mice at 4 wks (A), 12 wks (B) and 14 months (C) of age. Data represent the mean ± SEM for 8-10 animals of each genotype. *P<0.05 **P<0.01 ***P<0.0001*

6.3 Body composition

The increased body mass seen in *RIPCreIrs2KO* mice could be due to either an increase in fat mass or an increase in lean mass. In order to determine the predominant cause of this increase in body mass, body composition was investigated.

Body composition was investigated by comparing lean mass and fat mass in 12 week old *RIPCreIrs2KO* and control mice determined by DEXA scanning. Both lean mass and fat mass were significantly increased in *RIPCreIrs2KO* mice (Fig 6.6), with a significant increase in percentage body fat. However, this data suggests that the predominant cause of the increase in body mass is the increased adiposity of *RIPCreIrs2KO* mice.

6.4 Analysis of fat mass.

As the results of the DEXA scanning suggested that increased fat mass was the main reason for the increased body mass, fat content of *RIPCreIrs2KO* mice was more fully investigated by MRI imaging.

Dr Po Wah So carried out this work at Imperial College. MRI scanning of 6 month old mice showed an 80% increase in fat mass of RIPCreIrs2KO compared to control mice on a normal diet (4.3% fat) (Fig 6.7).

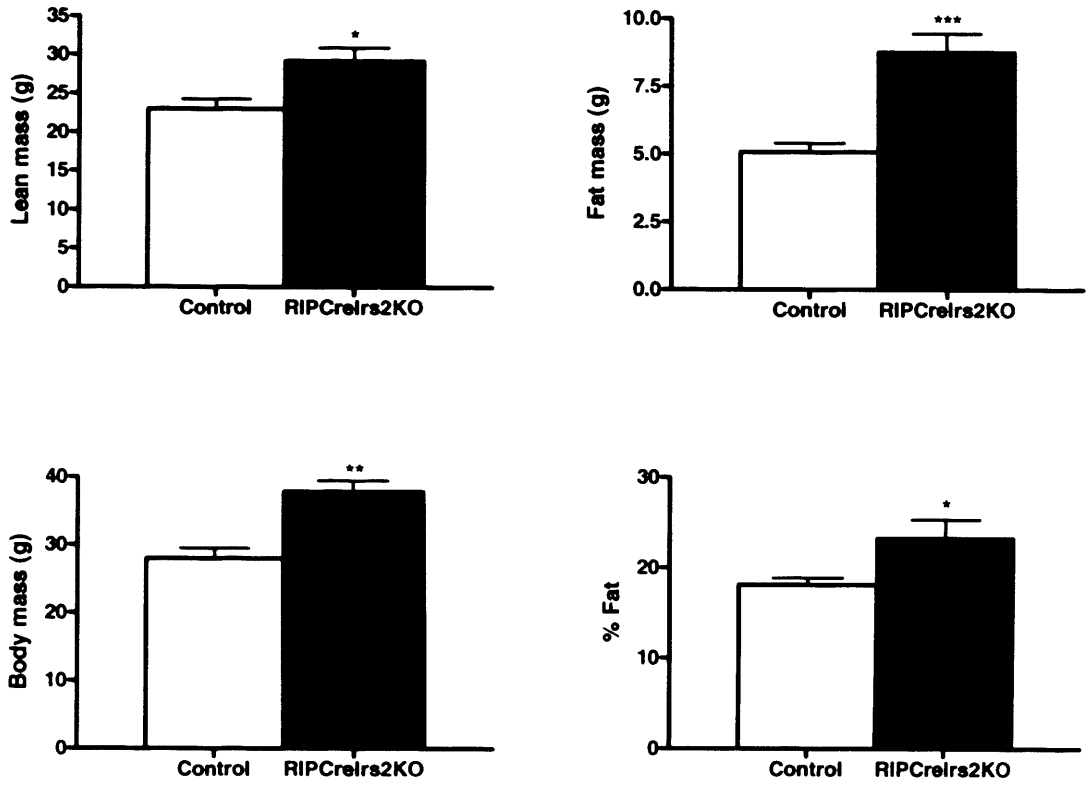

Figure 6.6 Body composition of RIPCreIrs2KO and control mice.

*Body composition was determined by DEXA scanning at 12 weeks of age. Data represent the mean ± SEM for 8 mice of each genotype. *P<0.05 **P<0.01 ***P<0.0001*

Figure 6.7. Body fat.

Analysis of body fat mass in male RIPCreIrs2KO and control mice. Percentage body fat was determined by MRI scanning in male RIPCreIrs2KO and control mice at 4 months of age. Data are presented as the percentage of body fat and are the mean ± SEM for 5-6 animals of each genotype.

6.5 Food intake

The body composition data above suggest disordered energy homeostasis in *RIPCreIrs2KO* mice. This could result in increased food intake or a change in metabolic rate.

Analysis of food intake at 4 weeks old showed that both male and female *RIPCreIrs2KO* mice were hyperphagic compared with their control littermates; eating ~30% more in a 24h period. This hyperphagia persists up to 12 weeks of age (Fig 6.8).

6.6. Response to fasting

The hyperphagia demonstrated by RIPCreIrs2KO mice could be due to dysregulation of either short-term or long-term food intake. To investigate feeding behaviour mice were fasted for 16 hours overnight and food intake was monitored. Up to 4 hours after refeeding *RIPCreIrs2KO* mice did not show any significant differences in food intake compared to control mice in both males and females. There was a trend for *RIPCreIrs2KO* mice to eat more than controls, which became significant after 8 and 24 hours (fig 6.9). This pattern was seen in both male and female mice.

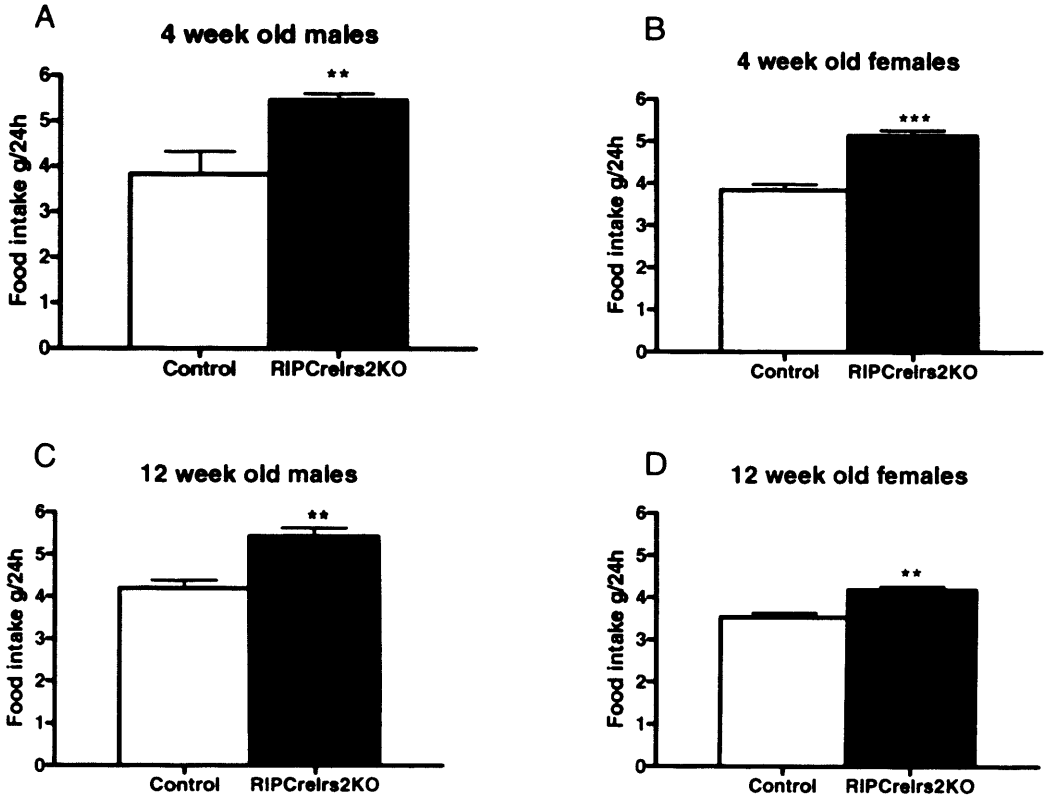

Figure 6.8. 24 h food intake.

*Food intake was measured in RIPCreIrs2KO and control mice at 4 wks (A and B) and 12 wks (C and D) of age. Data represent the mean ± SEM for 8-10 animals of each genotype. * P < 0.05, ** P < 0.01 and *** P < 0.001.*

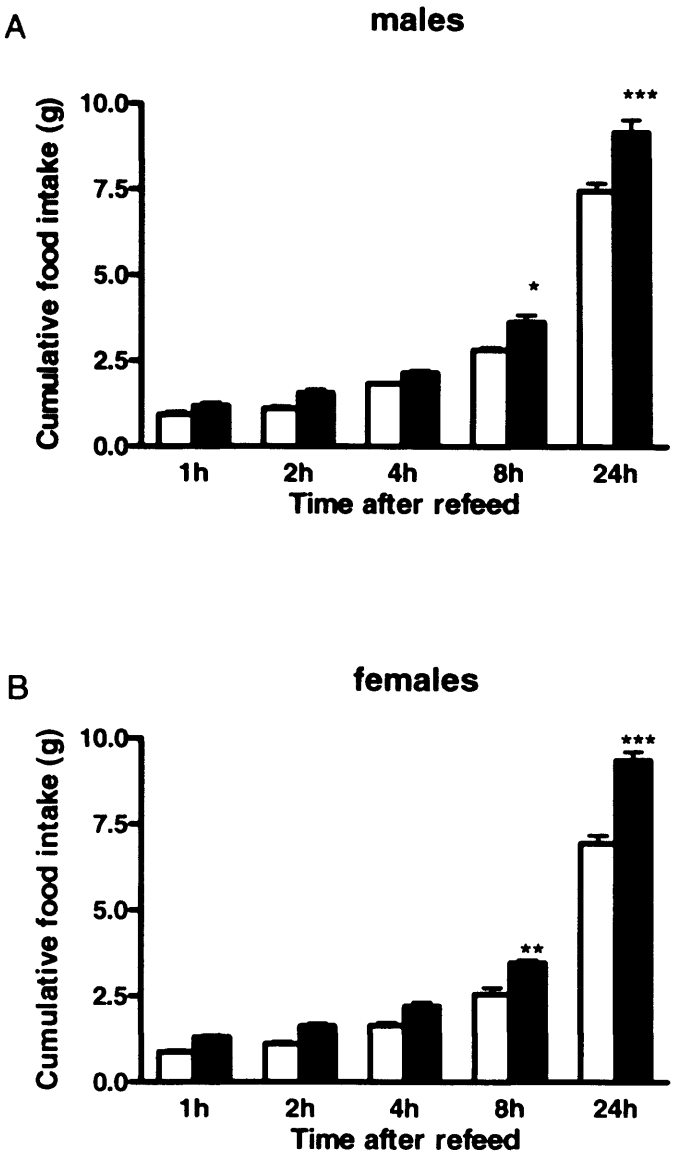

Figure 6.9. Response to fasting.

Following a 16 hour overnight fast, RIPCreIrs2KO (closed bars) and control (open bars) mice. mice were given ~50g food and cumulative food intake measured at the time points indicated, in males (A) and females (B). Data shown represent mean ± SEM for 8-10 mice of each genotype

6.7 Metabolic Rate.

The above data suggests that the increased adiposity in *RIPCreIrs2KO* mice is due to hyperphagia and long term disruption in food intake. However defects in metabolism could still be partly responsible for the increased fat mass in these mice.

Dr Colin Selman carried out this work at the University of Aberdeen. Metabolic rate was determined at 22± 0.1°C (housing temperature) by open-flow respirometry using a paramagnetic oxygen analyser. Data presented are mean ± SEM for 8 animals of each genotype. No significant difference in metabolic rate was seen between *RIPCreIrs2KO* mice compared to controls at 12 weeks old (Fig 6.10).

From the above results it is clear that the increase in body weight seen in RIPCreIrs2KO mice is due to hyperphagia rather then any defects in metabolic rate. In order to investigate this hyperphagia further studies were carried out.

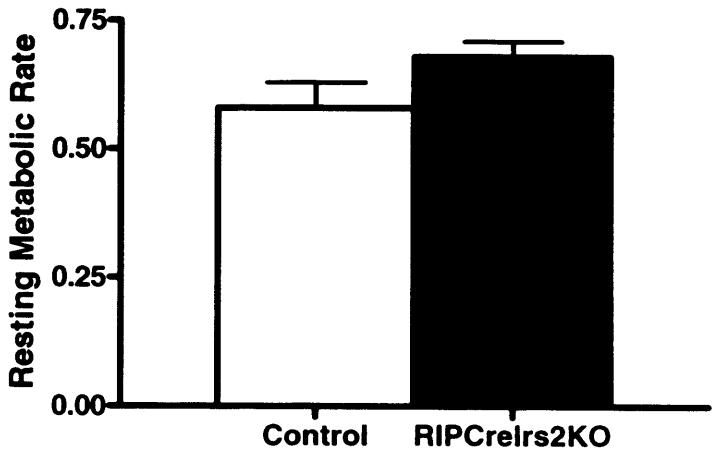

Figure 6.10. Metabolic rate.

Analysis of metabolic rate in male RIPCreIrs2KO and control mice. Resting metabolic rate (RMR) was estimated in 12 wk old male RIPCreIrs2KO and control mice n=8.

6.8 Serum Leptin Levels.

Analysis of fasting leptin levels in serum at 4 weeks old, when RIPCreIrs2KO show only a small increase in body weight, shows only a small increase in plasma leptin levels of *RIPCreIrs2KO* compared with control mice, demonstrating that these mice are leptin responsive. By 12 weeks of age, *RIPCreIrs2KO* mice show significant hyperleptinaemia consistent with the increased fat mass also seen at this age (Fig 6.12A).

6.9 Response to Leptin

To test whether the knockout mice were leptin resistant leptin was administered peripherally to 6-8 week old mice for 3 days and the cumulative food intake over this period was measured. The food intake over the period of treatment was compared with with food intake over the same period of time prior to treatment, and the reduction in food intake was calculated.

Leptin treatment (5mg/kg) inhibited food intake in control mice by 23% and RIPCreIrs2KO mice by 20% suggesting that young *RIPCreIrs2KO* mice are not resistant to the effects of leptin (Fig 6.11).

Following this period of leptin treatment, control mice displayed a 0.9g loss in body weight, compared with a 0.94g loss of weight in the *RIPCreIrs2KO* mice.

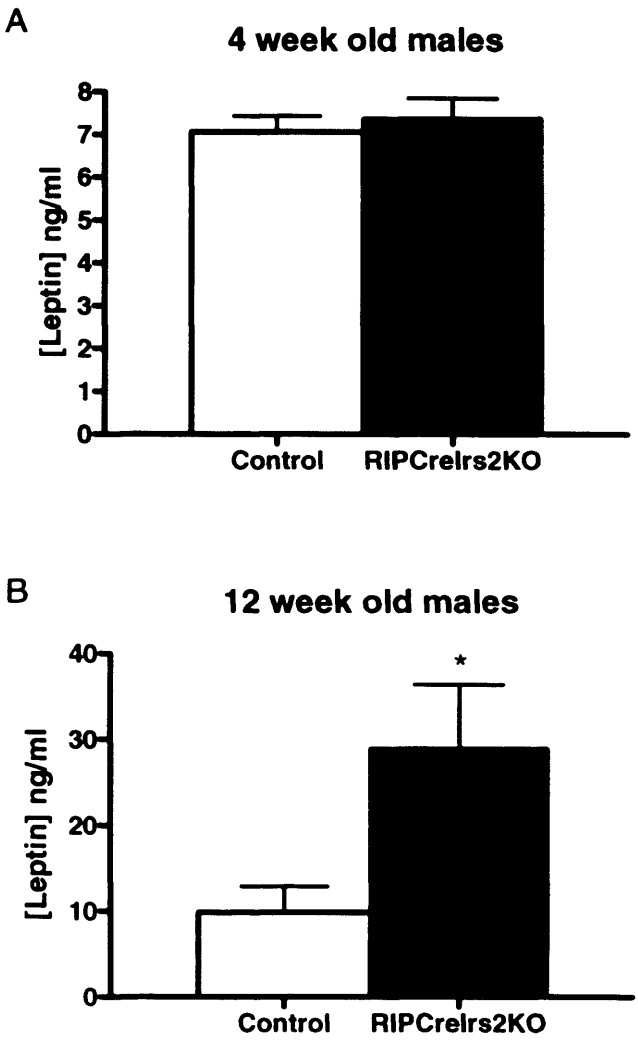

Figure 6.11 fasting blood leptin levels.

Leptin levels were measured in serum from male RIPCreIrs2KO and control mice at 4 wks (A) and 12 wks (B) of age after a 16 h overnight fast. Data represent the mean ± SEM for 8-10 animals of each genotype.

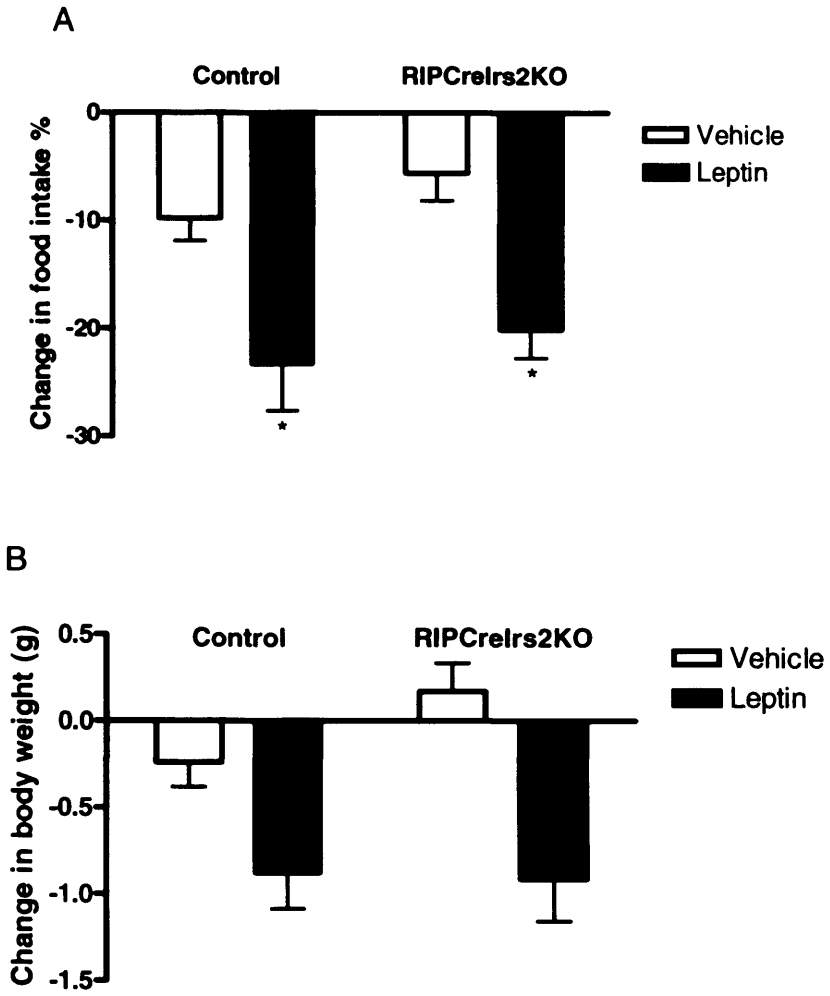

Figure 6.12 response to leptin.

*The response to 3 days of intraperitoneal leptin administration upon food intake was determined in acclimatized male control and RIPCreIrs2KO mice (A) at 8 weeks of age. The response to leptin treatment upon body weight in control and RIPCreIrs2KO mice (B) at 8 wks of age. Mice received either leptin (5 mg/kg) or vehicle for three days in a cross-over design study and accumulative food intake was recorded. Data represent the mean ± SEM for 6-8 animals of each genotype. * $P < 0.05$ and ** $P < 0.01$.*

6.10 Response to melanocortin receptor agonist

As the phenotype seen in the *RIPCreIrs2KO* mouse resemble that of the *MC4RKO* mouse, the sensitivity to melanocortins was examined. To test the response to melanocortin agonists, mice were fasted for 16 hours overnight and injected intraperitoneally with either the melanocortin receptor agonist, melanotan II or saline and then refed and cumulative food intake monitored. Both male and female *RIPCreIrs2KO* mice were more sensitive to MTII than control mice, showing a significant reduction in food intake when treated with MTII versus saline (figure 6.13)

6.11 Gene expression

Gene expression in *RIPCreIrs2KO* mice was analysed using microfluidic gene cards at AstraZeneca. This allowed fold changes in gene expression in the hypothalamus to be determined for a range of genes (Table 6.1). Due to the limitations of the gene cards only a fold change of 2 or more can be considered a significant change. This is because each sample was run only once rather then in duplicate and no negative control samples were run. In addition to this, the gene cards were custom made and therefore the primer and probe sequences are not known and therefore may only be designed to a single exon. The changes seen were below significance which could be, in part, due to the fact that Irs2 was deleted in only a small proportion of hypothalamic neurones and therefore changes in gene expression may be too subtle to be detected using this method.

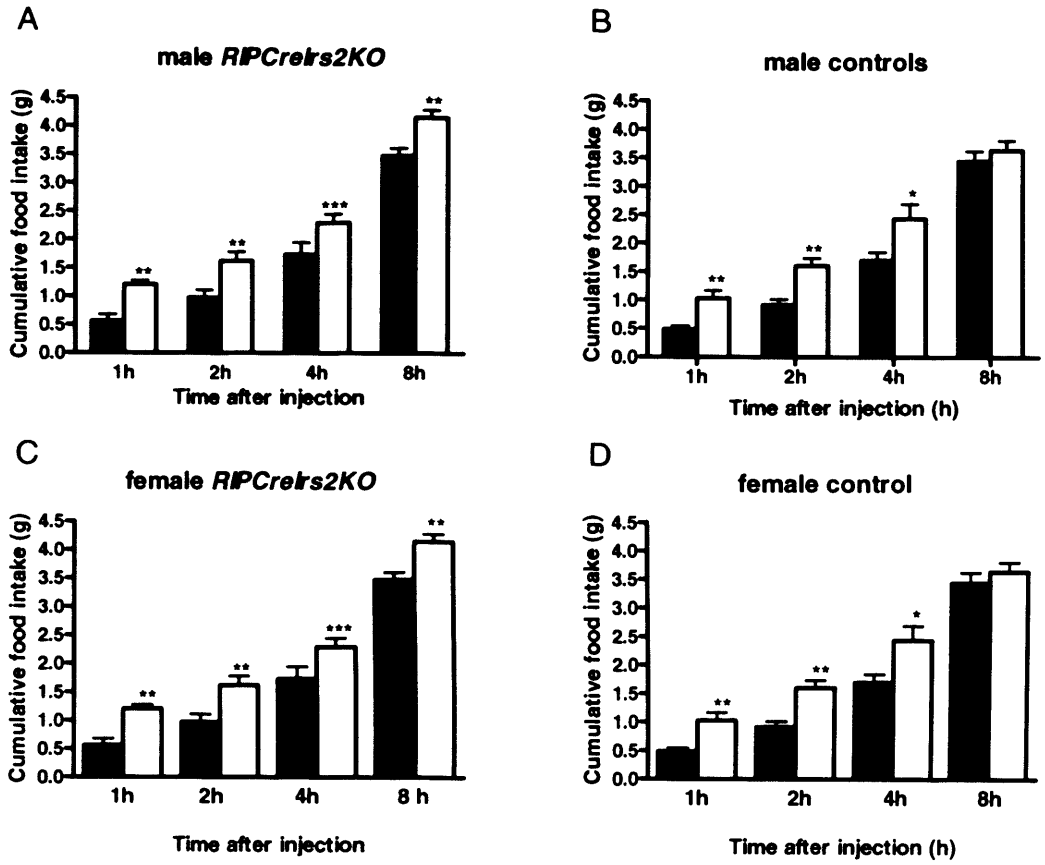

Figure 6.13. Response to MTII.

Following a 16 hour overnight fast, mice were injected with either MTII (black bars) or saline (white bars) and refed with ~ 50g food. Cumulative food intake was measured at the time points indicated.

Gene	Fold change
Abcc8	1.1043 ± 0.1704
Abcc9	1.31 ± 0.09958
Agrp	1.597 ± 0.1081
Akt1	1.6129 ± 0.1701
Cart	1.6087 ± 0.7122
Dpp4	1.0515 ± 01542
Gck	1.0515 ± 0.4066
Glp1R	1.229 ± 0.5221
Gpr119	**2.333 ± 0.708**
Gpr29	1.3781 ±0.2212
Hsd11b1	**2.9011 ± 1.318**
InsR	1.0449 ± 0.3326
Irs1	1.6624 ± 0.1391
Irs3	1.4836 ± 0.7694
Irs4	1.0036 ± 0.2546
Jak1	1.3187 ± 0.1790
Jak2	1.3536 ± 0.1849
Kcnj11	1.7107 ± 0.6236
Kcnj8	1.6963 ± 0.1133
LepR	1.7043 ± 0.8376
Mapk1	1.3197 ± 0.7057
Mc3R	1.1577 ± 0.2706
Mc4R	1.0507 ± 0.2162
Npy1R	1.2680 ± 0.3877
Npy2R	1.5869 ± 0.1778
Npy5R	1.1827 ± 0.2012
Npy	1.6873 ± 0.1525
Pcsk1	1.1323 ± 0.1525
Pcsk2	1.0484 ± 0.6179
Pik3R1	1.223 ± 0.3238
Pik3R2	1.1049 ± 0.1345
Pomc1	1.7895 ± 0.5848
Prkab1	1.1557 ± 0.1964
Prkag1	1.3652 ± 0.1730
Ptpn1	1.546 ± 0.1445
Slc2a4	1.3773 ± 0.1633
Stat3	1.2682 ± 0.1603
Wbsrc14	1.1098 ± 0.3503

Table 6.1 Fold change in gene expression of RIPCreIrs2KO mice.

Increases in gene expression are shown in black and decreases in gene expression are shown in red. Data shown represents mean ± SEM for 8 mice.

In addition to the β-cell phenotype described in previous chapters *RIPCreIrs2KO* mice also display a prominent hypothalamic phenotype. *RIPCreIrs2KO* mice are obese, with significant increases in both lean mass and fat mass, with a significant increase in percentage body fat. This was found to be due to hyperphagia rather then any disruption in metabolic rate.

Further investigation into the feeding behaviour of *RIPCreIrs2KO* mice showed that they respond normally to the anorexigenic peptide leptin and also respond to the melanocortin receptor agonist MTII. This suggests that RIPCre neurons are not POMC neurons. However further investigation is needed to fully characterise this population of neurons.

Analysis of gene expression was inconclusive, possibly due to the small number of neurons in which Irs2 was deleted.

7. Identification of RIPCre Neurons

The hypothalamic phenotype displayed by *RIPCreIrs2KO* mice is similar to that of the *Melanocortin receptor 4* knockout (*MC4RKO)* mouse. The *MC4RKO* mouse showed increased body weight due to an increase in fat mass and was hyperphagic but had no reduction in energy expenditure (Albarado *et al.*, 2004). *MC4RKO* mice also have an increase in body length (Butler *et al.*, 2002).

As described above the *RIPCreIrs2KO* mouse also displays increased body weight and hyperphagia, coupled with an increase in body fat. They also have an increase in body length. Therefore, it has been suggested that Irs2 is deleted in POMC neurones. Studies were therefore carried out to determine if POMC and Irs2 colocalise in RIPCre neurones.

7.1 Characterisation of RIPCre neurons

Dual in situ hybridization for POMC and immunocytochemistry for GFP was performed on hypothalamic sections from *RIPCreZEG* mice. These studies show no co-localisation between POMC and GFP neurones (Fig 7.1). Similar studies show the GFP neurones do not co-localise with NPY neurones.

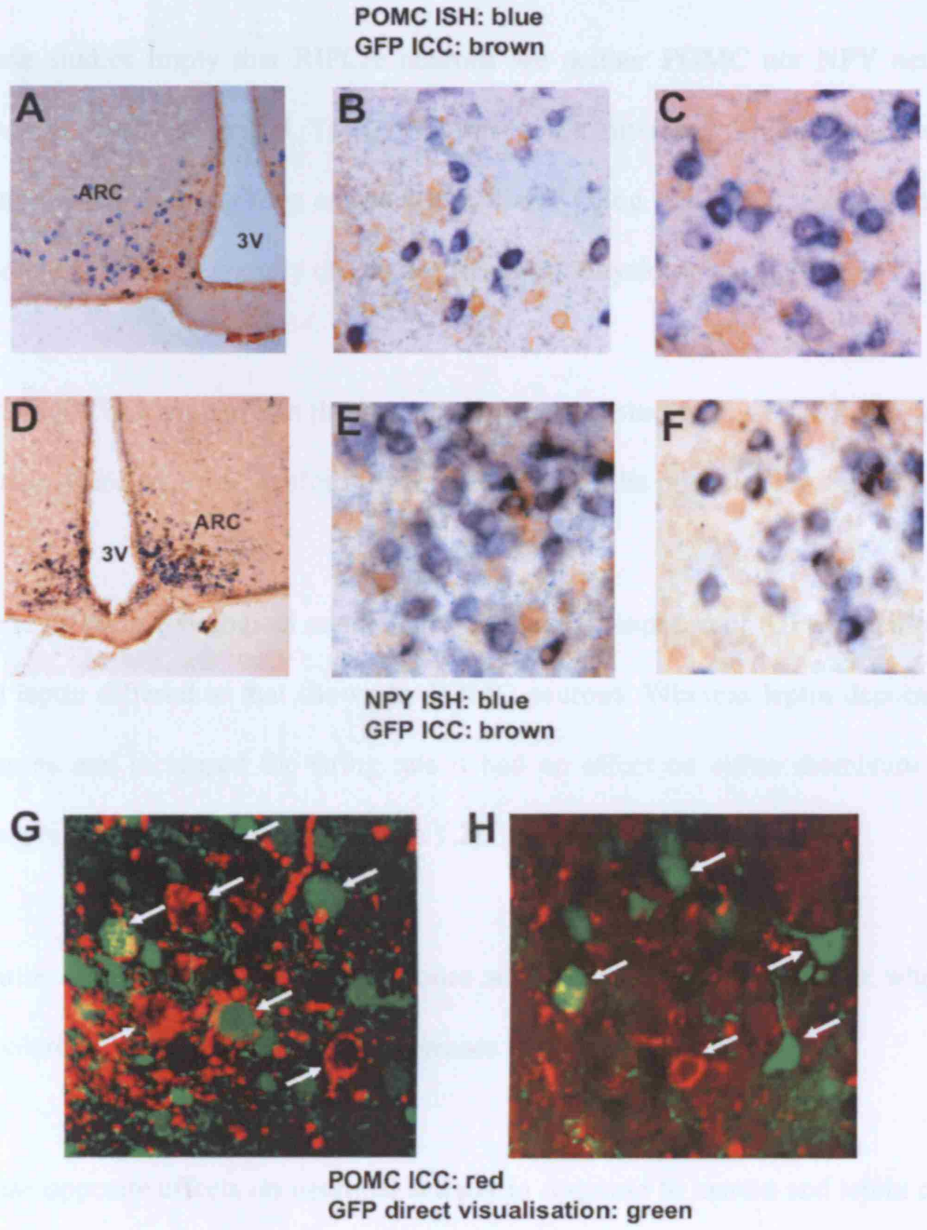

Figure 7.1. Characterisation of RIPCre neurons.

(A, B and C) Dual in situ hybridization for POMC and immunocytochemistry for GFP was performed on hypothalamic sections from RIPCreZEG mice. Neurons expressing POMC are blue and GFP are brown. Representative low (A) and high power (B and C) views are shown. (D, E and F) Dual in situ hybridization for NPY and immunocytochemistry for GFP was performed on hypothalamic sections from RIPCreZEG mice. Neurons expressing NPY are blue and GFP are brown. Representative low (D) and high power (E and F) views are shown. (G and H) Fluorescence immunocytochemistry for POMC was performed on hypothalamic sections from RIPCreZEG mice. Neurons expressing POMC are red and GFP are green. Arrows indicate non-colocalised neurons and GFP neurons which are abutted by POMC fibres. Representative high power views are shown.

These studies imply that RIPCre neurons are neither POMC nor NPY neurons as has been previously suggested. To confirm this, and to attempt to further characterise RIPCre neurones RIPCreIrsKOZeg and POMCCreIrs2KOZeg mice were sent to Prof. Ashford's laboratory at the University of Dundee for electrophysiological studies.

Although I did not perform the electrophysiological studies myself, I will now discuss the data provided by Prof. Ashford for completeness of the phenotyping studies.

These electrophysiological studies showed that the response of RIPCre neurons to insulin and leptin differed to that shown by POMC neurons. Whereas leptin depolarised POMC neurons and increased the firing rate it had no effect on either membrane potential or firing rate in RIPCre neurons (Figure 7.2).

Insulin hyperpolarises POMC neurones with a decrease in firing rate whereas insulin depolarises RIPCre neurones and increases the firing rate (Figure 7.3).

These opposite effects on neuronal activity in response to insulin and leptin confirms that RIPCre neurones are distinct from POMC neurones.

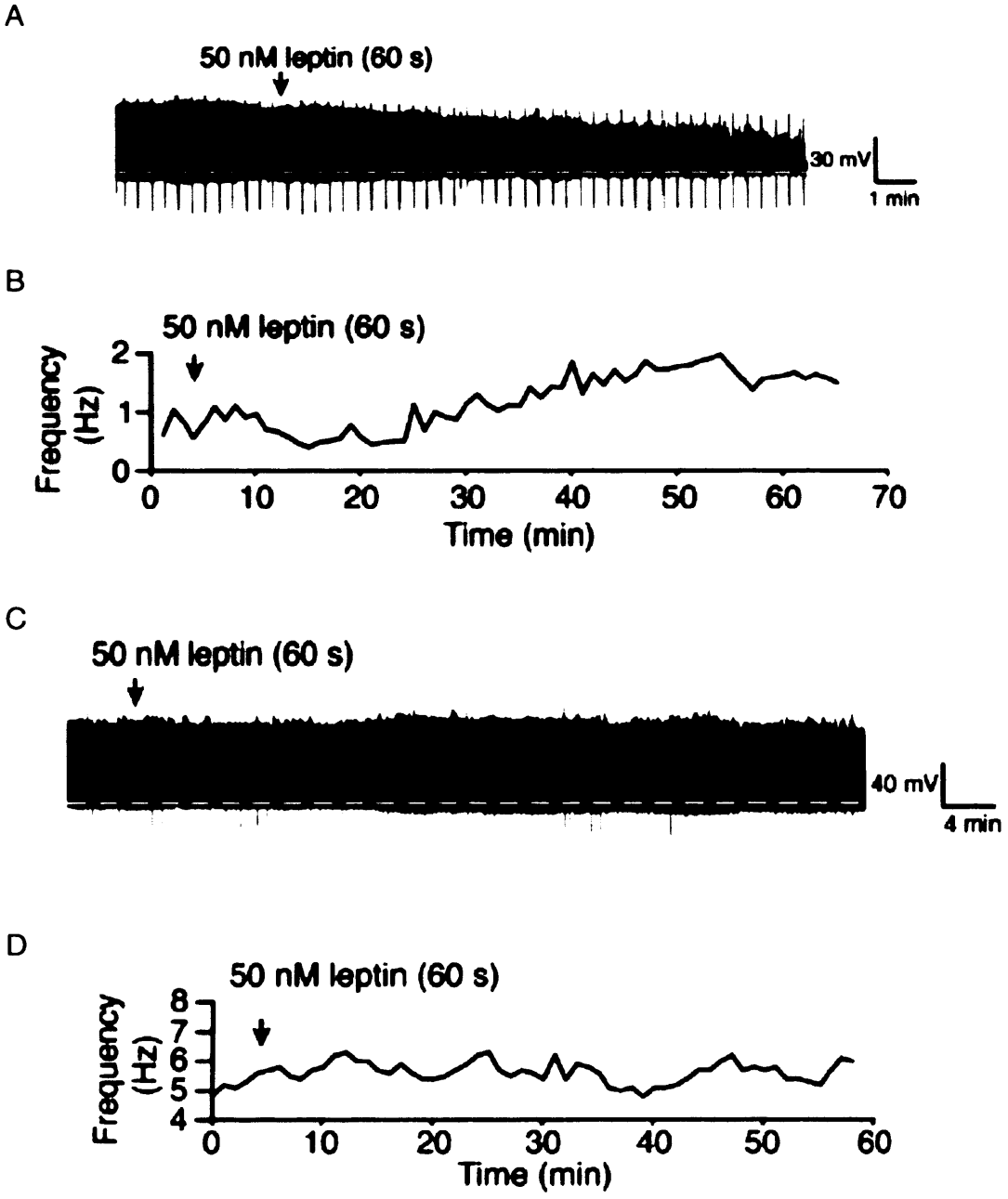

Figure 7.2 Response to Leptin.

The effects of leptin in POMCCreIrs2KOZeg (A and B) and RIPCreIrs2KOZeg (C and D) mice.

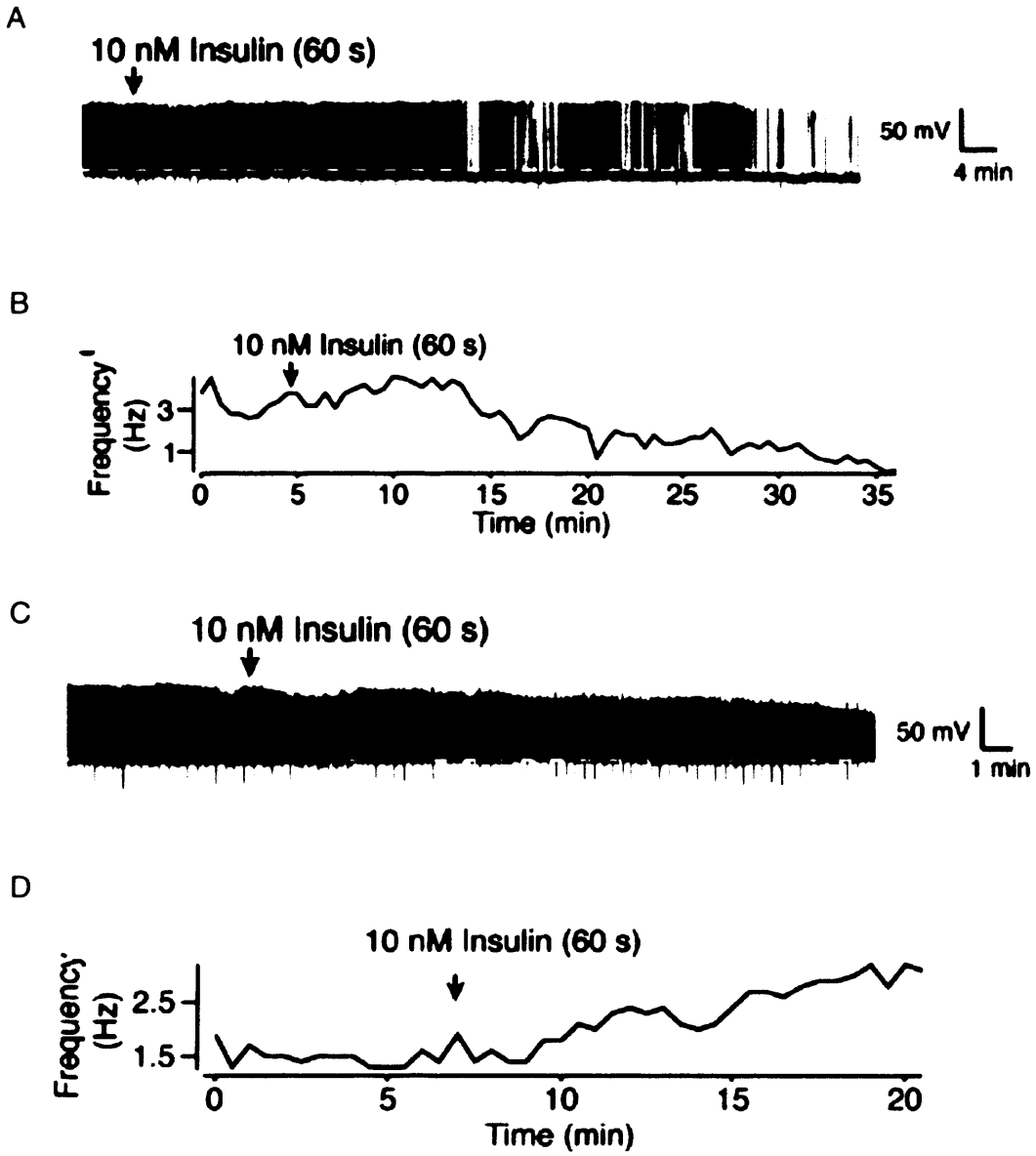

Figure 7.3. Response to Insulin.

The response to insulin on POMCCreIrs2KOZeg (A and B) and RIPCreIrs2KOZeg (C and D) mice.

8. *RIPCreSTAT3KO* mice

The loss of leptin signalling in the *ob/ob* mouse results in obesity and insulin resistance. It has, however proved difficult to study the role of STAT3 due to the embryonic lethality of the *STAT3* knockout. STAT3 has been shown to be activated in pancreatic cell lines in response to insulin. Therefore, in order to assess the importance of leptin signalling in the β-cell, and also the RIPCre neurones, mice lacking STAT3 in these tissues were generated.

8.1 Generation and genotypic frequencies of RIPCre STAT3 flox offspring

To obtain all genetic combinations of *RIPCre* and *STAT3 flox* genes, *STAT3 flox/flox* and *RIPCre* positive mice were crossed to obtain double heterozygotes. These double heterozygotes were then intercrossed. Double heterozygotes were fertile and produced litters comparable in size to wild-type mice. In addition there appeared to be no difference in maternal care of offspring.

This cross produced all of the expected genotypes which were seen at frequencies close to those predicted by Mendelian ratios. (Table 8.1).

	Number	Percantage	Predicted
STAT3lox	109	14.5	12.5
STAT3lox/lox	68	9	6.3
Wild-type	50	6.6	6.3
RIPCreSTAT3lox	246	32.7	37.5
RIPCreSTAT3lox/lox	190	25.2	18.8
RIPCre	90	12	18.8

Table 8.1 Genotypic frequencies of RIPCreSTAT3 offspring.

Mice were genotyped at 14 days of age.

8.2 Body Weight of RIPCreSTAT3KO mice

Body weight analysis at 4 weeks old showed no difference in weight between *RIPCreSTAT3KO* mice and control mice. However by 12 weeks old the *RIPCreSTAT3KO* mice were significantly heavier than controls (fig 8.1. A and B). This was also seen in female RIPCreSTAT3KO mice (Fig 8.2)

8.3 Body length of RIPCreSTAT3KO mice

Measurement of naso-anal length showed that at 4 weeks old *RIPCreSTAT3KO* mice were shorter then control mice but by 12 weeks old there was no difference in length (Fig 8.3). No significant differences in body length were seen in RIPCreSTAT3KO females (Fig 8.4)

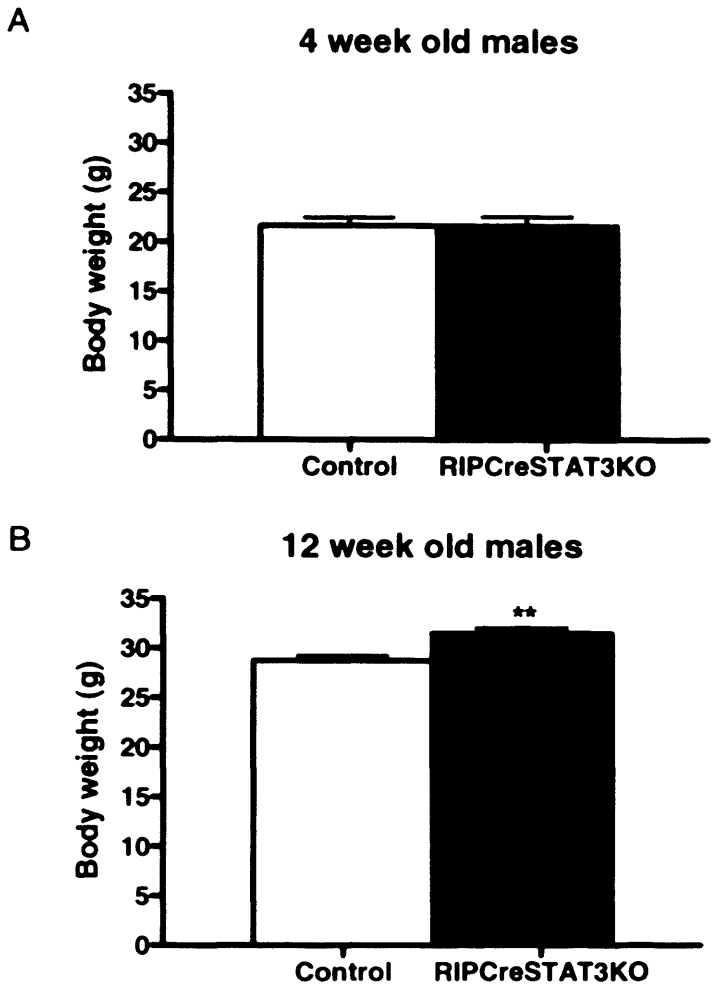

Figure 8.1. Analysis of body weight.

*(A and B) Body weight was measured in male RIPCreSTAT3KO and control mice at 4 wks (A) and 12 wks (B) of age. Data represent the mean ± SEM for 8-10 animals of each genotypeData represent the mean ± SEM for 8-10 animals of each genotype. ** P < 0.01*

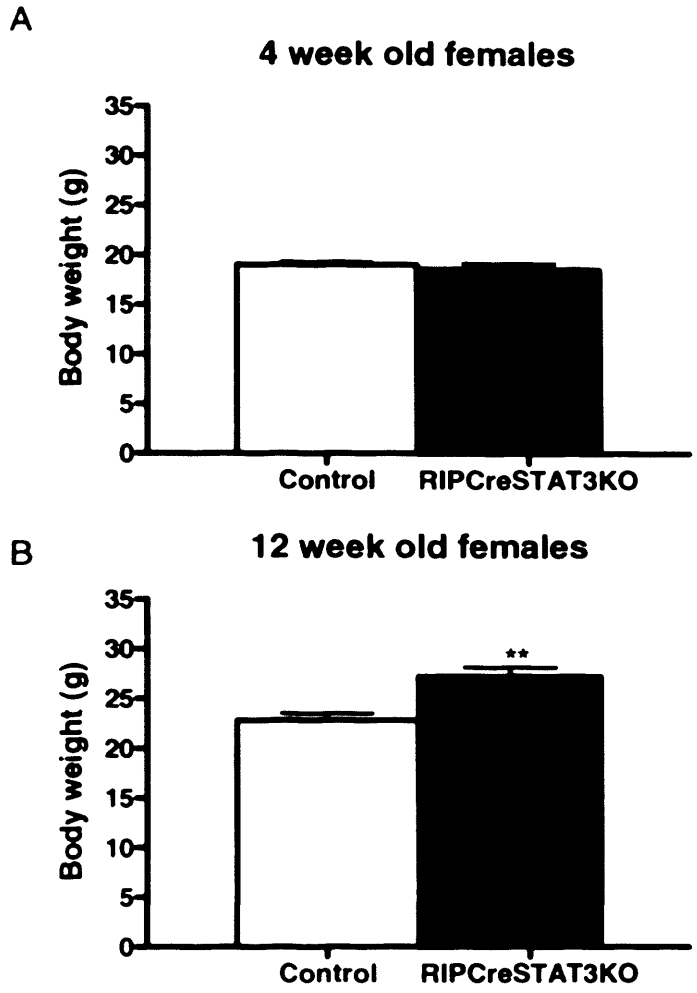

Figure 8.2. Analysis of body weight in female RIPCreSTAT3KO and control mice.

*(A and B) Body weight was measured in female RIPCreSTAT3KO and control mice at 4 wks (A) and 12 wks (B) of age. Data represent the mean ± SEM for 8-10 animals of each genotype. Data represent the mean ± SEM for 8-10 animals of each genotype. ** $P < 0.01$*

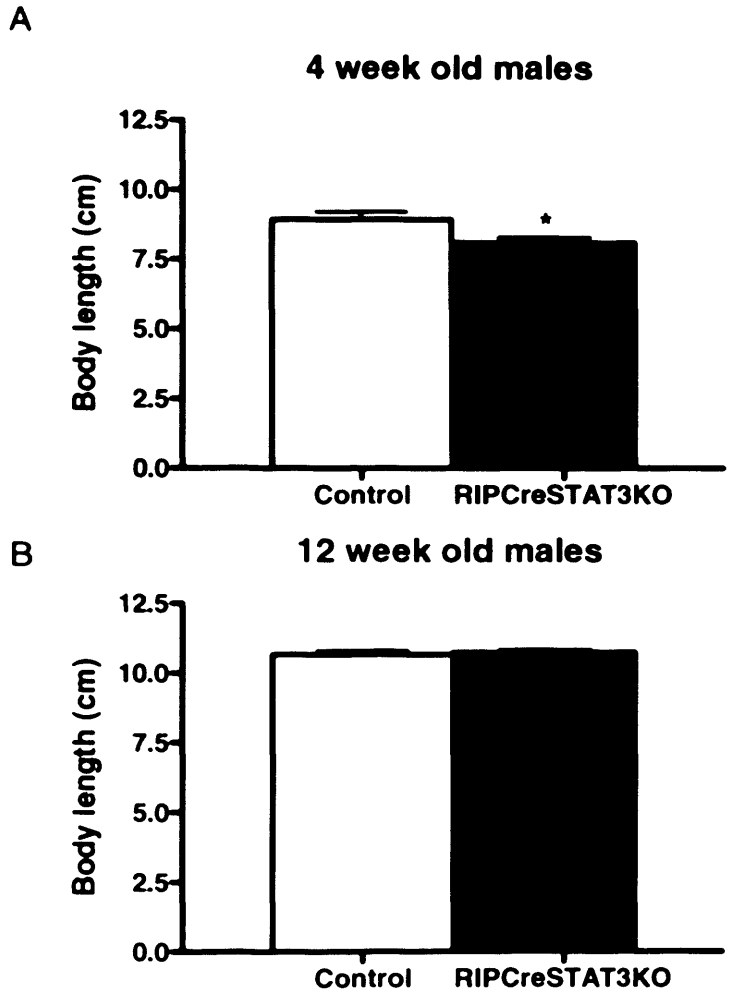

Figure 8.3. Analysis of body length in male RIPCreSTAT3KO and control mice.

*(A and B) naso-anal length was measured in male RIPCreSTAT3KO and control mice at 4 wks (A) and 12 wks (B) of age. Data represent the mean ± SEM for 8-10 animals of each genotype. Data represent the mean ± SEM for 8-10 animals of each genotype. * $P < 0.05$*

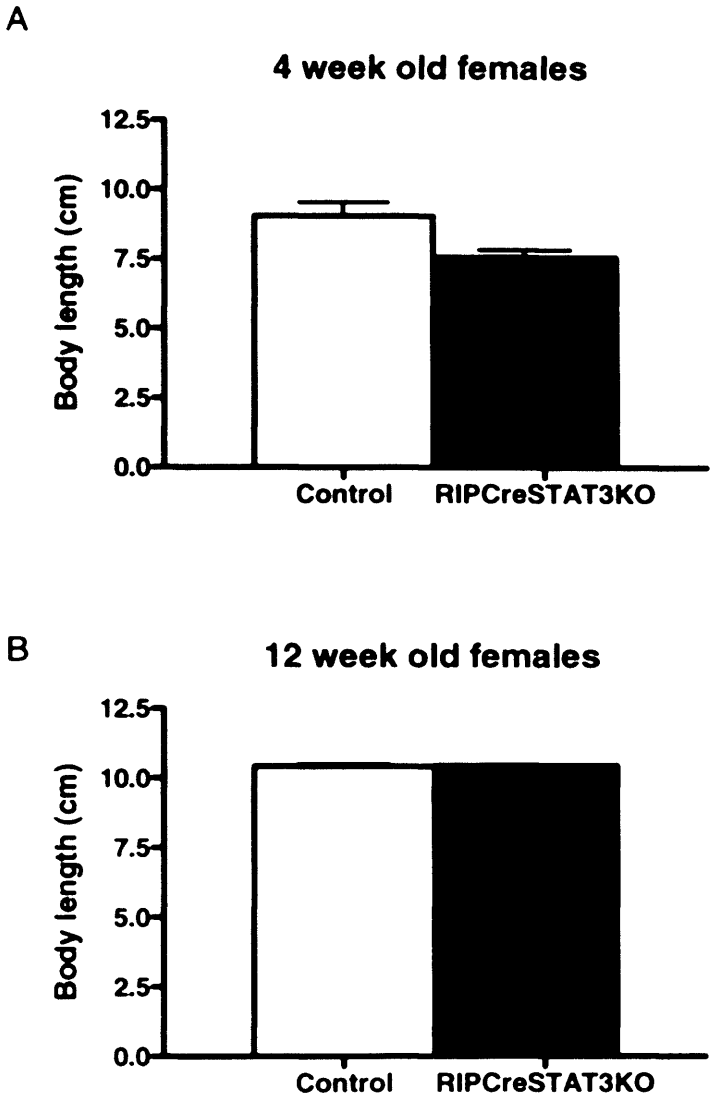

Figure 8.4. Analysis of body length in female RIPCreSTAT3KO and control mice.

(A and B) naso-anal length was measured in female RIPCreSTAT3KO and control mice at 4 wks (A) and 12 wks (B) of age. Data represent the mean ± SEM for 8-10 animals of each genotype. Data represent the mean ± SEM for 8-10 animals of each genotype.

8.4 Body composition in RIPCreSTAT3KO mice

DEXA scanning of RIPCreSTAT3KO mice at 12 weeks of age showed that they have a significant increase in body fat but no change in lean mass. Therefore the increase in total body mass is due to an increase in fat (Fig 8.5)

8.5 Food intake in RIPCreSTAT3KO mice.

Food intake studies showed that *RIPCreSTAT3KO* do not eat more then control mice at any age (Fig 8.6) suggesting that the increase in body weight is not due to hyperphagia. This was also seen in RIPCreSTAT3KO female mice (Fig 8.7).

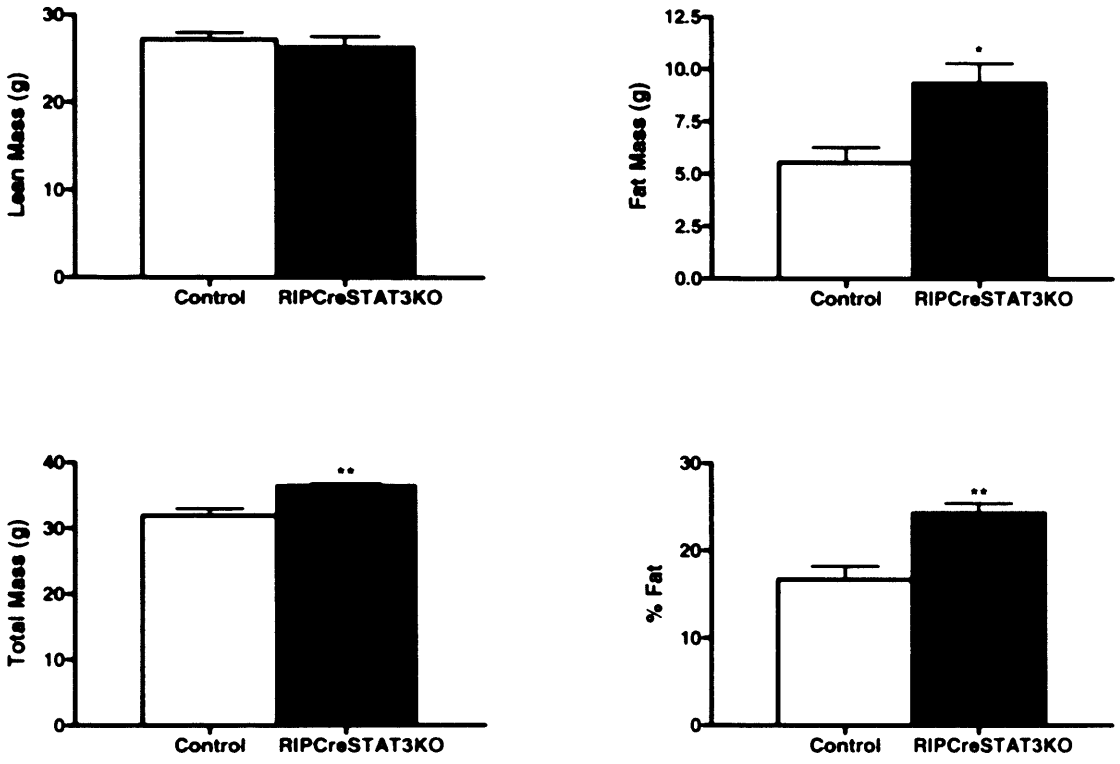

Figure 8.5 Body composition of RIPCreSTAT3KO mice determined by DEXA scanning.

*RIPCreIrs2KO and control mice had body composition analysed be DEXA scanning to show lean mass, fat mass, total body mass and percentage body fat. Data represent mean ± SEM for 8 mice of each genotype. *P<0.05, **P<0.01.*

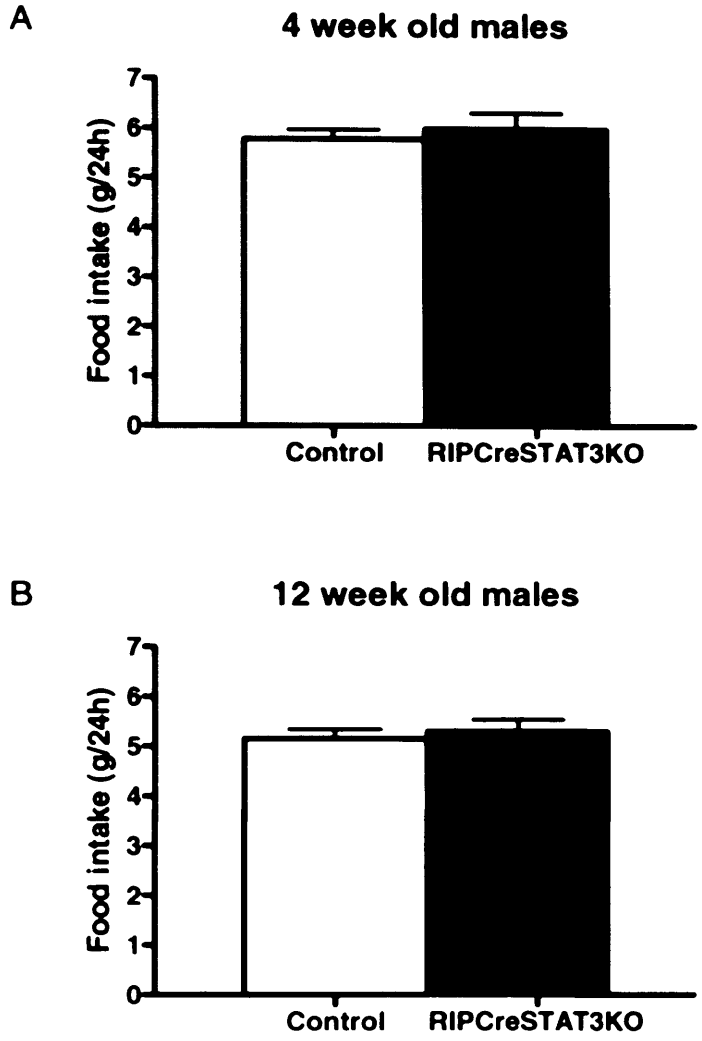

Figure 8.6. Analysis of food intake in male RIPCreSTAT3KO and control mice.

(A and B) Food intake was measured in male RIPCreSTAT3KO and control mice at 4 wks (A) and 12 wks (B) of age. Data represent the mean ± SEM for 8-10 animals of each genotype. Data represent the mean ± SEM for 8-10 animals of each genotype.

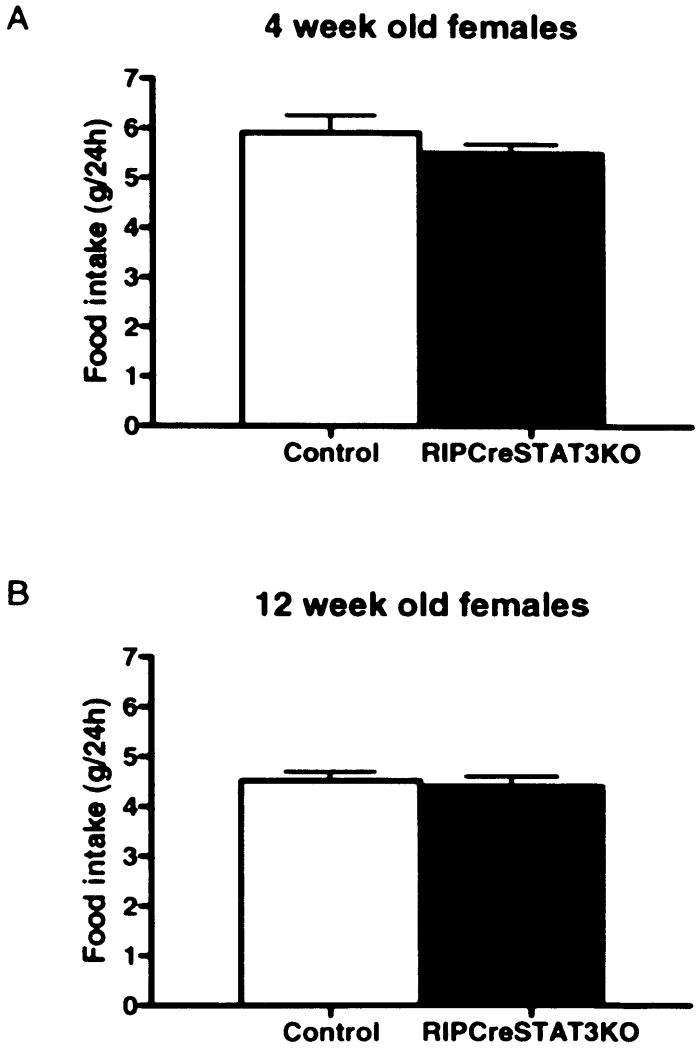

Figure 8.7. Analysis of food intake in female RIPCreSTAT3KO and control mice.

(A and B) Food intake was measured in female RIPCreSTAT3KO and control mice at 4 wks (A) and 12 wks (B) of age. Data represent the mean ± SEM for 8-10 animals of each genotype. Data represent the mean ± SEM for 8-10 animals of each genotype.

8.6 Response to fasting

The response to an overnight fast was studied in *RIPCreSTAT3KO* and control mice. Mice were fasted overnight and the feeding response monitored. At all time points there was no significant difference in food intake between *RIPCreSTAT3KO* and control mice for both males and females (Fig 8.8)

8.7 Response to leptin

Figure 8.9 shows that, at 4 weeks of age RIPCreSTAT3KO males are not significantly hyperleptinaemic compared with wild-type littermates. By 12 weeks of age RIPCreSTAT3KO mice have significantly higher leptin levels consistent with the increase in fat mass. RIPCreSTAT3KO and control males also responded to leptin treatment showing a decrease in food intake over three days of leptin treatment.

8.8 Glucose Homeostasis in RIPCreSTAT3KO mice

Fig 8.10shows that RIPCreSTAT3KO mice have normal fasting blood glucose levels after a 16h overnight fast at 4 and 12 weeks of age. Glucose tolerance tests were performed on male mice. After a 16h overnight fast mice were injected with 1.5g/kg D-glucose and the blood glucose levels measured via tail bleeds at the time points indicated. At both 4 weeks and 12 weeks of age RIPCreSTAT3KO mice show no impairment in glucose clearance, indicating that, in these mice, there are no defects in glucose homeostasis.

This was also seen in female RIPCreSTAT3KO females at the same ages (Fig 8.11)

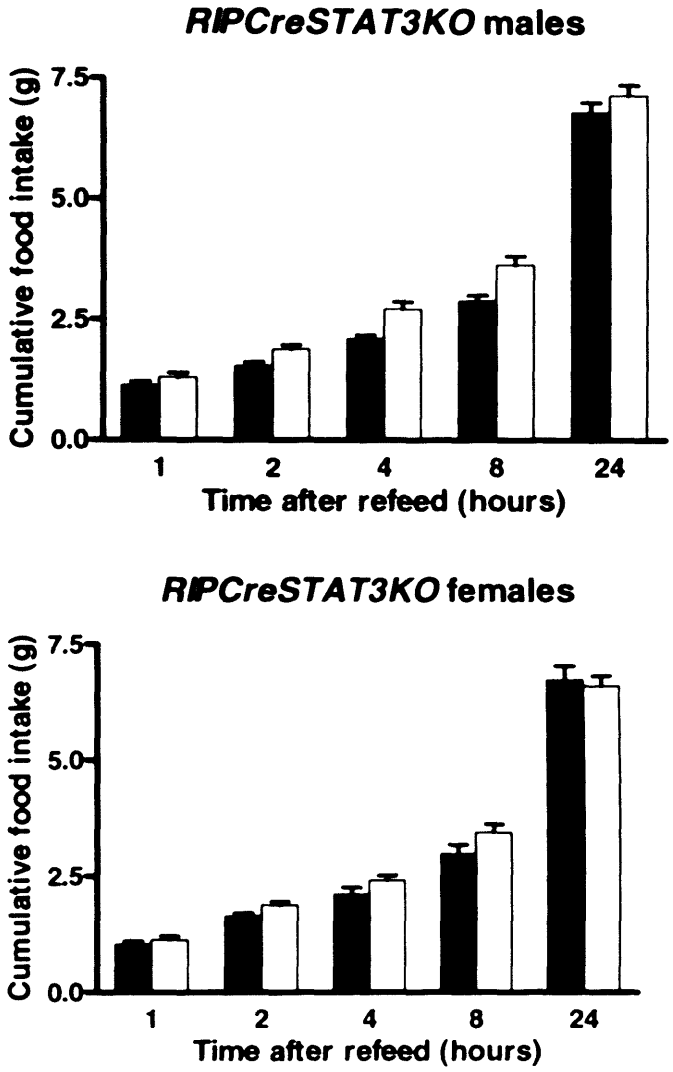

Figure.8.8. Response to fasting.

Male and female mice were fasted for 16 hours overnight and then refed with 50g food, and cumulative food intake measured in RIPCreSTAT3KO (black bars) and control (open bars) mice. Data represent mean ± SEM for 8-10 mice of each genotype.

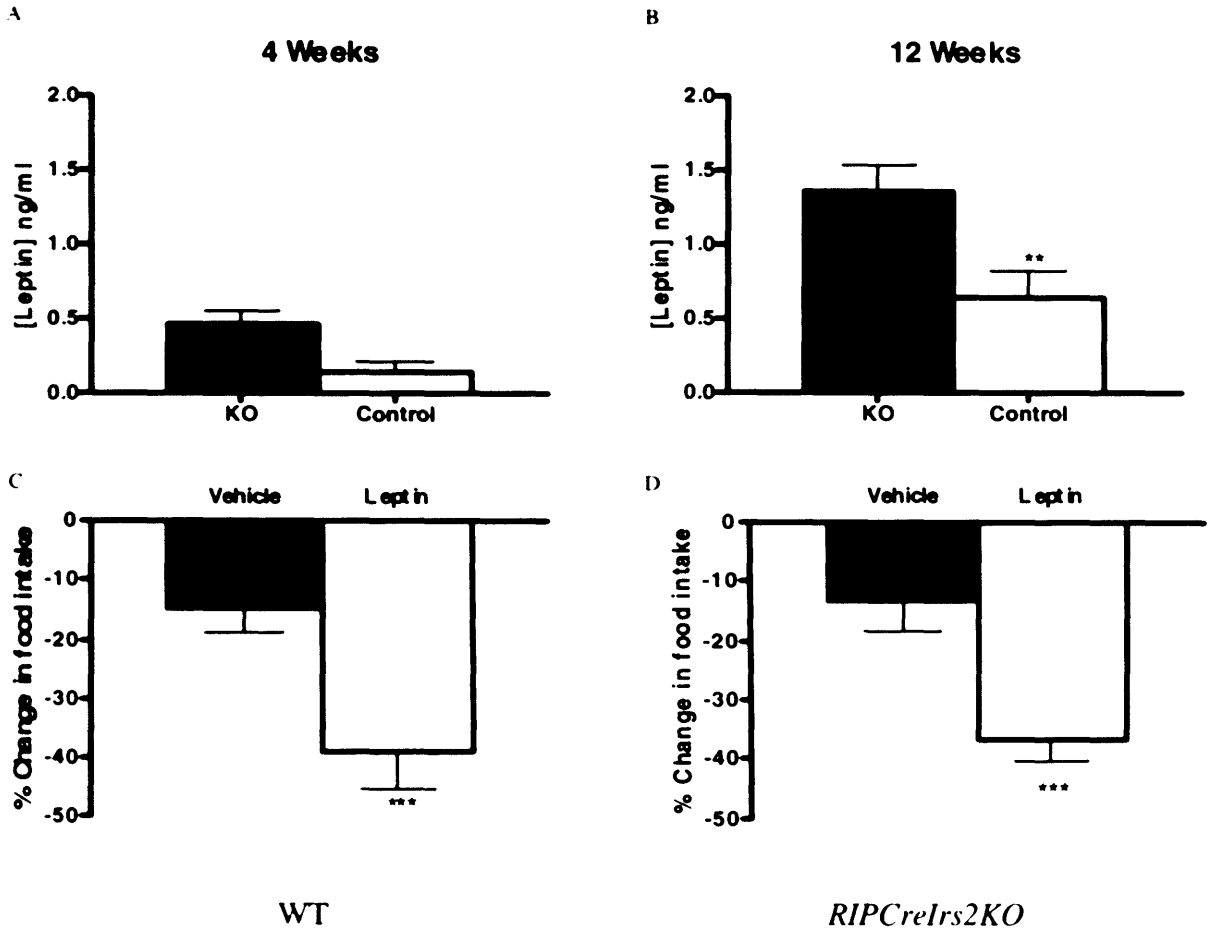

Figure8.9 Fasting leptin levels.

*Leptin levels were measured from serum of male RIPCreSTAT3KO (KO) and control mice at 4 wks (A) and 12 wks (B) of age after a 16 h overnight fast. Data represent the mean ± SEM for 8-10 animals of each genotype. (C and D) The response to 3 days of intraperitoneal leptin administration upon food intake was determined in acclimatized male control (C) and RIPCreSTAT3KO mice (D) at 8 wks of age. Mice received either leptin (5 mg/kg) or vehicle for three days in a cross-over design study and accumulative food intake was recorded. Data represent the mean ± SEM for 6-8 animals of each genotype. * $P < 0.05$ and ** $P < 0.01$.*

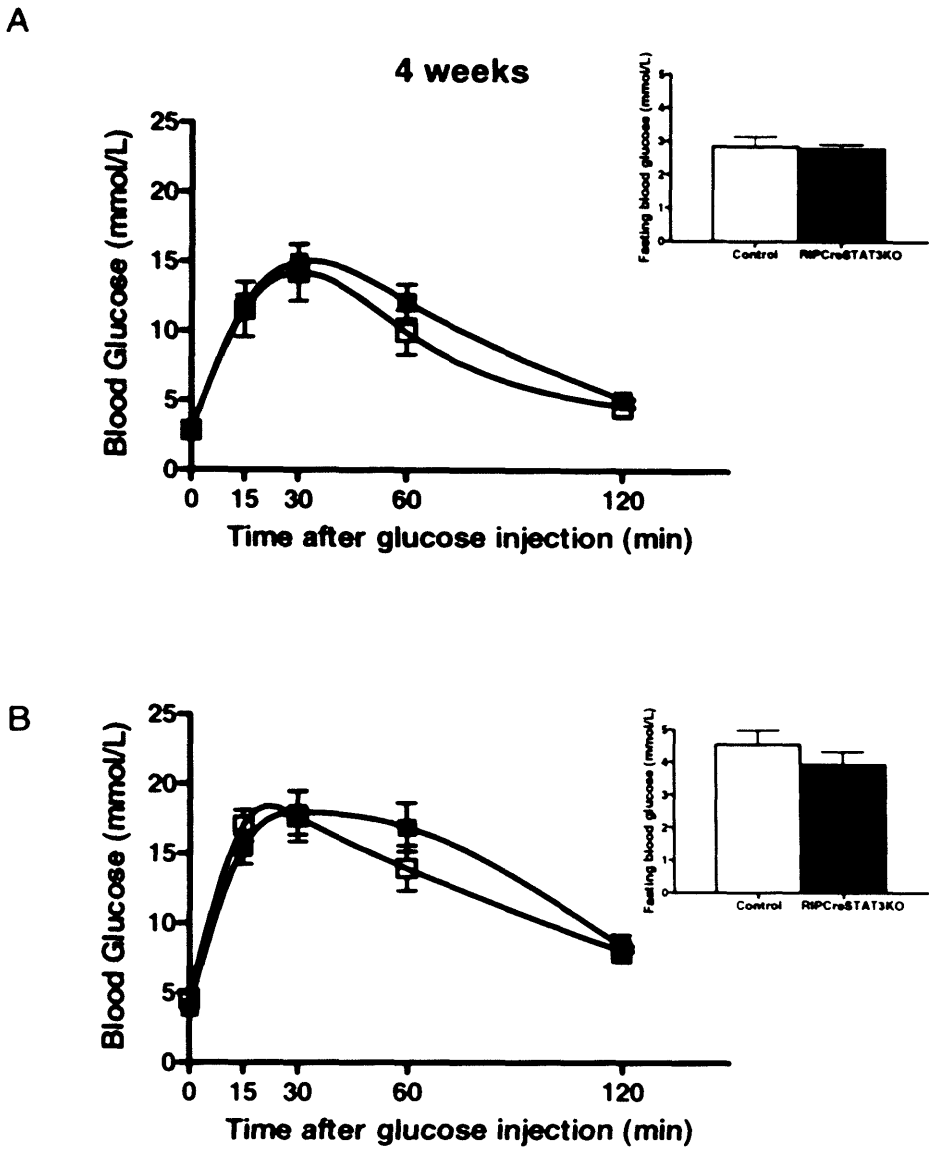

Figure 8.10 Glucose homeostasis in male RIPCreSTAT3KO and control mice.

Fasting blood glucose levels were measured on male RIPCreSTAT3KO and control mice at 4 wks (A) and 12 wks (B) of age after a 16 h overnight fast. Data represent the mean ± SEM for 8-10 animals of each genotype. Glucose tolerance tests were performed on male RIPCreSTAT3KO and control mice at 4 wks (A) and 12 wks (B) of age after a 16 h overnight fast. After intraperitoneal injection of D-glucose (1.5g/kg body weight) blood glucose was measured at the indicated time-points. Data presented are the mean ± SEM for 8-10 animals of each genotype.

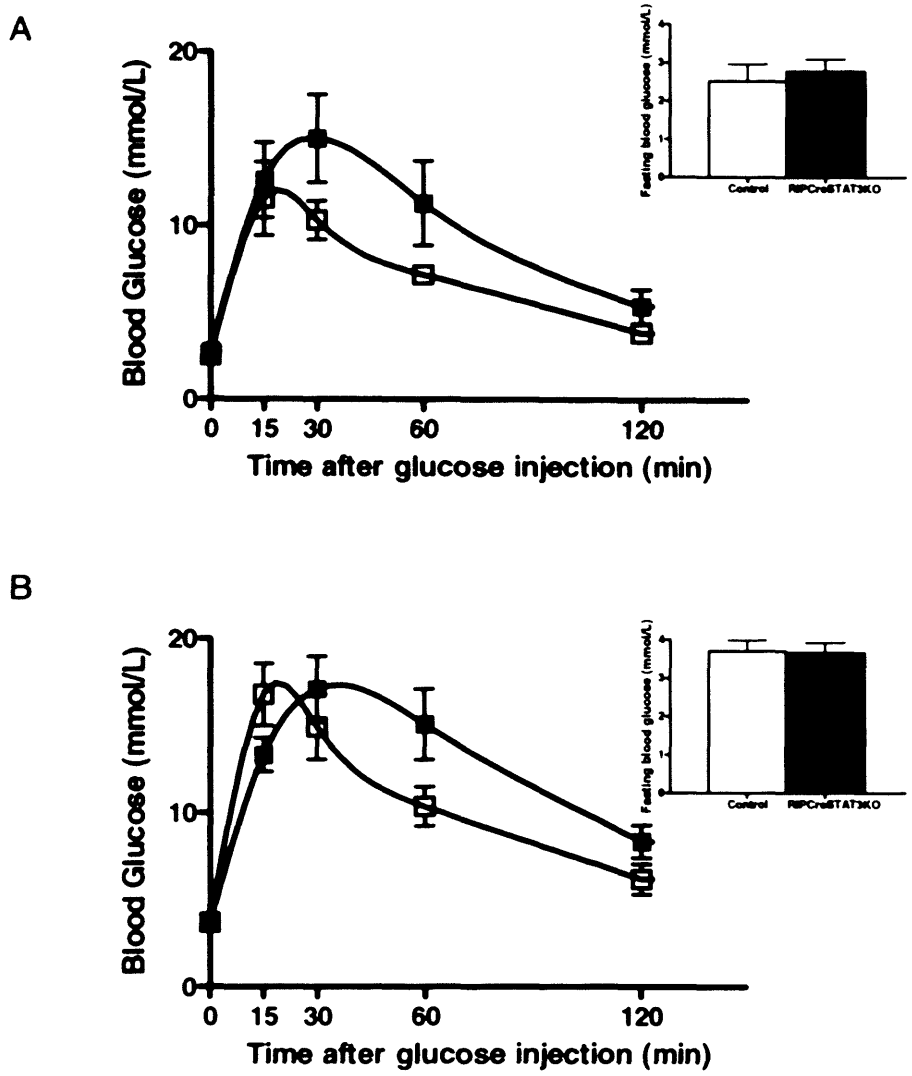

Figure 8.11 Glucose homeostasis in female RIPCreSTAT3KO and control mice.

Fasting blood glucose levels were measured on female RIPCreSTAT3KO and control mice at 4 wks (A) and 12 wks (B) of age after a 16 h overnight fast. Data represent the mean ± SEM for 8-10 animals of each genotype. Glucose tolerance tests were performed on female RIPCreSTAT3KO and control mice at 4 wks (A) and 12 wks (B) after a 16 h overnight fast. After intraperitoneal injection of D-glucose (1.5g/kg body weight) blood glucose was measured at the indicated time-points. Data presented are the mean ± SEM for 8-10 animals of each genotype. n-8 mice of each genotype.

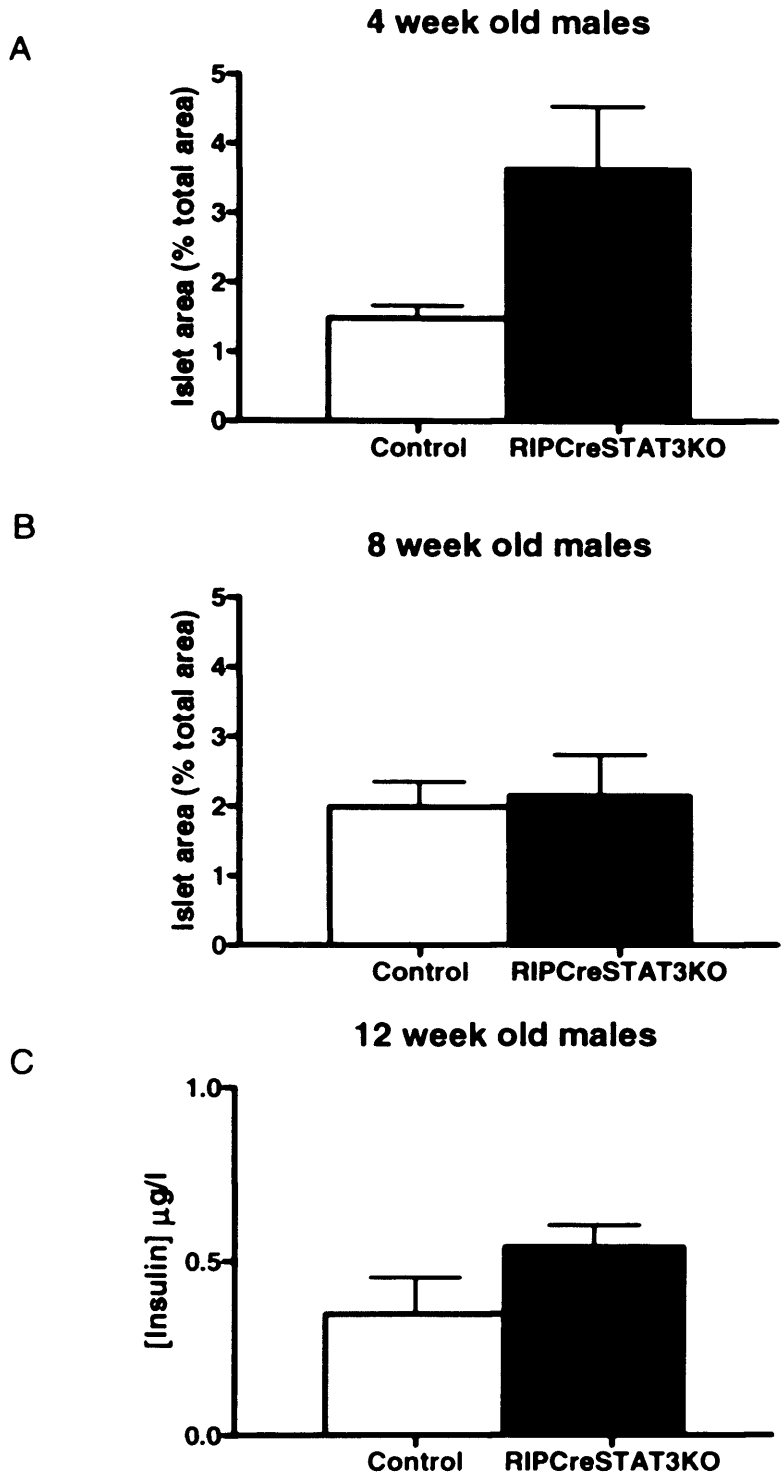

Figure 8.12 The percentage of the total pancreatic area occupied by beta cells.

(A) at 4 wks of age and (B) at 12 wks of age for male RIPCreSTAT3KO mice and control mice was calculated using insulin and glucagon stained pancreatic sections. Five pancreases were analysed per genotype at each time point and for each pancreas four sections were analysed. The data presented are mean ± SEM for five mice of each genotype. (C) fasting insulin was measured in RIPCreSTAT3KO and control mice at 12 weeks of aget. The data presented are mean ± SEM for 5 mice of each genotype.

8.9 Pancreatic mass and plasma insulin.

At 4 weeks of age the *RIPCreSTAT3KO* mice have an increased islet area and density compared to wild type mice, although the difference is not significant. However by 12 weeks of age the islet area is the same as in wild-type mice. At 12 weeks of age plasma insulin levels in *RIPCreSTAT3KO* mice are comparable to those of wild type mice (Fig 8.12).

8.10 Gene expression in hypothalami

Gene expression in 12 week old RIPCreSTAT3KO mice was anlysed using microfluidic gene cards at AstraZeneca. This allowed fold changes in gene expression in the hypothalamus to be determined for a range of genes (Table 8.2). Due to the limitations of the gene cards only a fold change of 2 or more can be considered a significant change. This is because each sample was run only once rather then in duplicate and no negative control samples were run. The changes seen were below significance which could be, in part, due to the fact that STAT3 was deleted in only a small proportion of hypothalamic neurones and therefore changes in gene expression may be too subtle to be detected using this method.

Gene	Fold change
Abcc8	1.0370 ± 0.0974
Abcc9	1.7605 ± 0.0242
Agrp	1.5583 ± 0.111
Akt1	**2.4501 ± 0.0342**
Cart	1.2716 ± 0.433
Dpp4	1.4414 ± 0.0307
Gck	1.5439 ± 0.0809
Glp1R	1.5585 ± 0.0482
Gpr119	1.2796 ± 0.2871
Gpr29	1.9507 ±0.059
Hsd11b1	1.6266 ± 0.0269
InsR	1.2548 ± 0.0678
Irs1	1.1708 ± 0.3475
Irs3	1.5985± 0.3654
Irs4	1.0162 ± 0.0804
Jak1	1.1789 ± 0.0599
Jak2	1.1910 ± 0.1456
Kcnj11	1.7580 ± 0.0808
Kcnj8	1.0954 ± 0.0431
LepR	1.9149 ± 0.0536
Mapk1	2.4074 ± 0.0398
Mc3R	**4.2239 ± 0.260**
Mc4R	1.2527 ± 0.0517
Npy1R	2.1342 ± 0.0909
Npy2R	1.2375 ± 0.1058
Npy5R	1.2615 ± 0.1232
Npy	1.0957 ± 0.0814
Pcsk1	1.001 ± 0.0472
Pcsk2	1.1679 ± 0.1846
Pik3R1	1.000 ± 0.0853
Pik3R2	1.3317 ± 0.0859
Pomc1	1.1058 ± 0.2444
Prkab1	1.4243 ± 0.0547
Prkag1	1.7970 ± 0.0484
Ptpn1	1.5184 ± 0.0516
Slc2a4	1.3485 ± 0.157
Stat3	1.3881 ± 0.0678
Wbsrc14	1.8077 ± 0.1133

Table 8.2 Fold changes in gene expression.

Gene cards determined fold changes in gene expression of RIPCreSTAT3KO mice compared to control mice. Increases in gene expression are shown in black and decreases in gene expression are shown in red. Data represents mean ± SEM for 6 mice of each genotype

RIPCreSTAT3KO mice display a prominent hypothalamic phenotype. At weaning body weight is normal, but by 12 weeks of age they are significantly heavier then control animals. Body composition studies indicate that this is due to a significant increase in fat mass as lean mass is normal at 12 weeks of age. Interestingly *RIPCreSTAT3KO* mice do not display hyperphagia at any of the ages studied, both in 24h food intake and in response to fasting. As would be expected with the increase in body fat *RIPCreSTAT3KO* mice are hyperleptinaemic, but respond normally to peripherally administered leptin.

Unlike the *RIPCreIrs2KO* mice *RIPCreSTAT3KO* mice have no defects in pancreatic function. Fasting blood sugar levels are normal, as is glucose tolerance at 4 and 12 weeks of age. At 4 weeks of age *RIPCreSTAT3KO* males showed an apparent increase in β-cell mass but this was non-significant. By 12 weeks of age β-cell mass in *RIPCreSTAT3KO* mice was comparable with that of control mice and these mice showed no changes in fasting insulin levels. This suggests that STAT3 signalling is not essential for β-cell growth and function.

9. Phenotype of *RIPCre* mice

As the studies described previously were nearing completion a paper was published in which it was claimed that the phenotype seen in *RIPCreIrs2KO* mice was a result of expression of *RIPCre* and that *RIPCre* mice alone were glucose intolerant (Lee *et al.*, 2006).

My initial studies had suggested that there was no difference between any of the control groups and so the data from all control groups has been pooled throughout these studies.

In light of this paper (Lee *et al.*, 2006). I re-analysed glucose tolerance test data from both *RIPCreIrs2KO* and *RIPCreSTAT3KO* mice.

9.1 Glucose tolerance test in RIPCreIrs2KO mice

RIPCreIrs2KO mice were compared with *RIPCre* control mice and also wild-type littermates at 4 weeks (Fig 9.1A) and 12 weeks (Fig9.1B) of age. It can be seen that at both of these ages *RIPCreIrs2KO* mice are glucose intolerant compared to wild-type littermates and also that there is no difference between wild-type mice and mice carrying the *RIPCre* transgene

9.2 Glucose tolerance in RIPCreSTAT3KO mice

Data from the *RIPCreSTAT3* cross was analysed separately from that from the *RIPCreIrs2* cross as the *STAT3 flox* mice were on a mixed genetic background.

The glucose tolerance of *RIPCre* mice resulting from the *RIPCreSTAT3* cross was also analysed (Fig 9.2) at 12 weeks of age where it is clear that again, there is no difference in glucose tolerance of *RIPCre* mice compared with that of wild-type control mice.

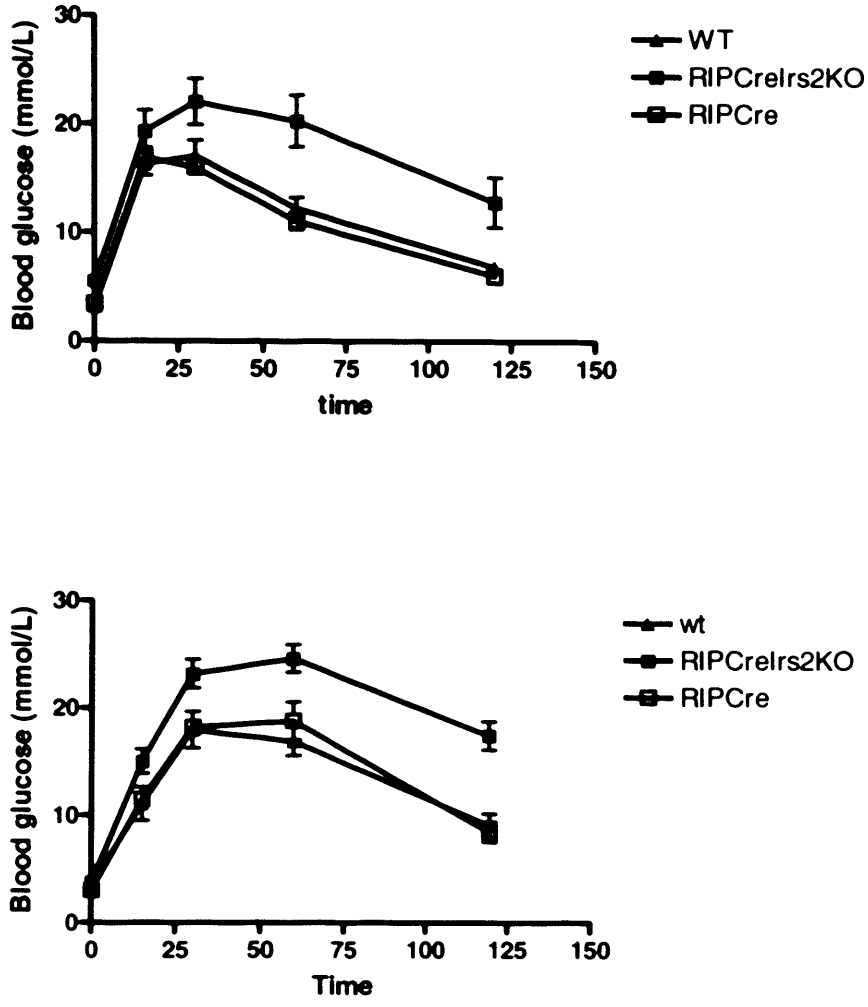

Fig 9.1 Glucose tolerance test in RIPCreIrs2 mice.

Glucose tolerance tests were performed on male RIPCreIrs2KO, RIPCre and wild-type mice at 4 wks (A) and 12 wks (B) of age after a 16 h overnight fast. Following an intraperitoneal injection of D-glucose (1.5g/kg body weight) blood glucose was measured at the indicated time-points. Data presented are the mean ± SEM for 15-20 animals of each genotype.

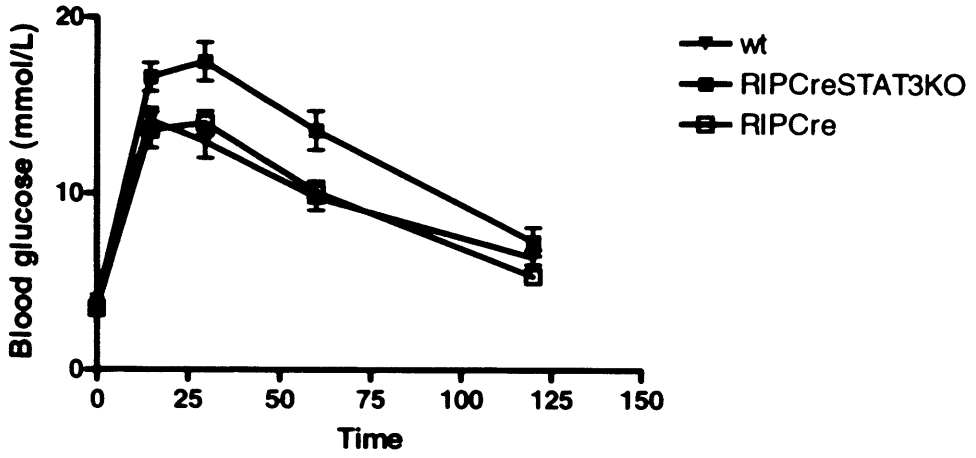

Fig 9.2 Glucose tolerance test in RIPCreSTAT3 mice.

Glucose tolerance tests were performed on male RIPCreSTAT3KO, RIPCre and wild-type mice at 12 weeks of age after a 16 h overnight fast. Following an intraperitoneal injection of D-glucose (1.5g/kg body weight) blood glucose was measured at the indicated time-points. Data presented are the mean ± SEM for 15-20 animals of each genotype.

From these studies it seems that mice carrying the *RIPCre* transgene alone do not display any glucose intolerance. In the *RIPCreIrs2* cross *RIPCre* mice do not show any differences in glucose tolerance to their wild-type littermates while the *RIPCreIrs2KO* mice are significantly glucose intolerant.

RIPCreSTAT3 mice were analysed separately as the *STAT3* mouse was on a mixed genetic background unlike the *RIPCreIrs2* mice which were maintained on a C57 Bl/6 background. Again the *RIPCre* mouse showed no differences in glucose tolerance compared to control mice while the *RIPCreSTAT3KO* mouse seemed slightly glucose intolerant compared to the control groups though this was not significant.

Therefore from these studies it is clear that the β-cell phenotype seen in the *RIPCreIrs2KO* mouse is due to deletion of Irs2 in the β-cell and not due to expression of Cre as the Cre positive controls in this cross have normal glucose tolerance and also all mice in the *RIPCreSTAT3* cross display normal glucose tolerance with even the *RIPCreSTAT3KO* mouse having only a mild β- cell phenotype.

10. Discussion

Global gene deletion has revealed that Irs2, through mediating the effects of insulin and IGF1 receptor function, has roles in the regulation of glucose metabolism, energy homeostasis, reproductive function and CNS development.

Previously, it has been shown that *Irs2* null mice display a progressive deterioration in glucose homeostasis due to a failure of β cell compensation accompanied by peripheral insulin resistance (Withers et al., 1998). In addition to this *Irs2* null mice also show increased body weight and resistance to leptin. While initial studies suggested that Irs2 might lie downstream of the IR or IGF1R in growth promotion and cell survival pathways, subsequent conditional gene targeting to produce β-cell specific deletion of these receptors has shown that neither mouse model has significant defects in β cell development, growth and survival (Kulkarni et al., 1999; Kulkarni et al., 2002). These findings challenge the idea that β cell autonomous Irs2 dependent signalling events alone are required for the normal maintenance of β cell mass and the response to insulin resistance.

The work described in this thesis was undertaken to elucidate the roles of Irs2 and STAT3 in the β-cell using conditional gene targeting.

Initially mice with a floxed allele of *Irs2* were intercrossed with mice expressing Cre recombinase under the control of the rat insulin 2 promoter. The offspring from this cross was then phenotyped with respect to growth, glucose homeostasis and β-cell function.

As expected *RIPCreIrs2KO* mice were hyperglycaemic and displayed glucose intolerance compared to control mice at 12 weeks of age. This hyperglycaemia and glucose intolerance progressively worsened with age but this phenotype was not as severe as that seen in the global *Irs2* null mouse although this was probably due to insulin resistance in other organs in the global knockout. Indeed, even by 12 months of age *RIPCreIrs2KO* mice showed no signs of overt diabetes. Analysis of fasting blood insulin levels showed that *RIPCreIrs2KO* mice were hyperleptinaemic at all ages studied demonstrating that, unlike the global knockout, *RIPCreIrs2KO* mice are able to increase insulin production to compensate for peripheral insulin resistance, thus explaining why these mice did not develop overt diabetes. It was reported by Lin *et al.* that the *RIPCreIrs2KO* mouse was hyperglycaemic and developed diabetes, which resolved itself at 6 – 10 months of age (Lin *et al.*, 2004). However in this study, *RIPCreIrs2KO* mice never developed diabetes and although the glucose intolerance did not progress to diabetes, no significant recovery in glucose tolerance was seen.

It has been reported that islet area in *RIPCreIrs2KO* mice at 4 weeks of age is normal (Kubota *et al.*, 2004; Lin *et al.*, 2004). Lin *et al.* also reported that islet area did not increase between 4 and 8 weeks of age. However relative β-cell mass had increased by 10 months of age (Lin *et al.*, 2004). In accordance with these two studies the data presented in this thesis shows a significant reduction in islet mass between 4 and 12 weeks of age in

the *RIPCreIrs2KO* mouse. By nine months of age, when Lin reported a reversal in the diabetic phenotype, islet area in *RIPCreIrs2KO* mice while still reduced compared to wild type mice, was significantly increased compared with 12 week old *RIPCreIrs2KO* mice.

This apparent recovery in islet mass in *RIPCreIrs2KO* mice explains why these mice do not develop progressive diabetes, as the increase in islet mass and therefore insulin secretion helps to offset the peripheral insulin resistance. However, it was not clear what the mechanism for this β-cell recovery was, or from what source the new islets were generated. Lin *et al.* attempted to address this question using PCR and reported a progressive increase in *Irs2flox* in β-cells, which mirrored a progressive decrease in *Cre* expression. Therefore it was suggested that β-cells arose from cells that only weakly expressed *Cre*, but the source of these cells was not known (Lin *et al.*, 2004).

In order to investigate the mechanism of β-cell recovery, we performed anatomical studies of recombination using the GFP indicator mouse crossed into *RIPCreIrs2KO* and control mice. This generated mice in which cells expressing *Cre recombinase* and therefore undergoing recombination also expressed GFP. These studies revealed that, even at 4 weeks of age a small proportion of β-cells did not express Cre, and therefore recombination would not occur in these cells. By 9 months of age a significant proportion of cells not expressing Cre had repopulated the islets, although there were still many GFP expressing cells undergoing recombination which would explain the persistent reduction in islet mass and the glucose intolerance still seen in *RIPCreIrs2KO* mice at this age.

Interestingly, the reduction in recombination occurs predominantly in the *RIPCreIrs2KOZeg* mouse suggesting that Irs2 signalling is needed for expression of the *RIPCre* transgene and therefore selection for cells with intact Irs2 signalling to repopulate the islets under conditions of insulin resistance.

It has also been suggested that new β-cells can arise from ductal precursor cells (Butler *et al.*, 2003a; Jones *et al.*, 2001). In the 9-month-old *RIPCreIrs2KOZeg* mouse no GFP expression was detected in the pancreatic ducts and so it is possible that the new β-cells could have arisen from ductal precursor cells. However no duct cell marker was detected in islets of 9-month-old *RIPCreIrs2KO* mice, nor was insulin expression detected in the ducts. This suggests that the β-cell phenotype seen in *RIPCreIrs2KO* mice results form a loss of *Irs2* in mature cells rather then precursor cells and that intrinsic β-cell Irs2 signalling pathways are important for islet function, and in particular for the development and maintenance of β-cell mass. In addition to this, Irs2 expression is required for the compensatory response to insulin resistance.

During the course of these studies it became apparent that these mice developed marked hypothalamic phenotypes, such as hyperphagia and obesity.

To examine the distribution of Cre recombinase in the CNS and pancreas in this study, RIPCre mice were intercrossed with Z/eg fluorescent indicator mice, generating mice in which tissues expressing Cre recombinase coexpressed GFP. This demonstrated that the

RIPCre transgene is expressed in the hypothalamus and pancreatic islets, resulting in Irs2 deletion in β cells and in a small population of hypothalamic neurons in *RIPCreIrs2KO* mice. Others have also recently confirmed this pattern of deletion but the hypothalamic neuronal population has remained poorly characterised (Cui et al., 2004).

Body weight analysis showed that *RIPCreIrs2KO* mice had a significant increase in body weight compared to control littermates. This increased body weight was significant at 4 weeks of age and continued throughout life. In addition to this increase in body weight, *RIPCreIrs2KO* mice were significantly longer (naso-anal distance) than control mice.

While both lean mass and fat mass were significantly increased in *RIPCreIrs2KO* mice, it appears that the increased fat mass is the major contributing factor. This suggests disordered energy homeostasis in *RIPCreIrs2KO* mice, which could result in either increased food intake or a reduction in metabolic rate.

Analysis of food intake showed that, from 4 weeks of age, *RIPCreIrs2KO* mice were significantly hyperphagic compared to control mice, and studies into the response to fasting showed that *RIPCreIrs2KO* mice exhibited long-term changes in food intake. Therefore it seems likely that the increase in body weight is due to an increase in food intake. This was supported by studies into metabolic rate which showed no differences in metabolic rate of *RIPCreIrs2KO* mice compared to control mice.

Two major arcuate neuronal populations have been implicated in the regulation of energy homeostasis, POMC and NPY neurons (Cowley, 2003). Injection of α-MSH into the brain reduces food intake, whereas NPY administration stimulates food intake (Schwartz et al., 2000). Leptin works by reducing NPY mRNA expression in the hypothalamus and lowers the electrical excitability of NPY expressing neurons (Cowley et al., 2001; van den Top et al., 2004), whereas leptin excites POMC neurons (Cowley et al., 2001) and elevates POMC mRNA levels (Thornton et al., 1997). Furthermore, NPY inhibits POMC neuronal activity (Cowley et al., 2001; Roseberry et al., 2004) and excites NPY neurons via a pre-synaptic autoreceptor. These dual actions of NPY have the net effect of inhibiting POMC release directly, and indirectly via increased inhibitory GABA tone provided by the synaptically connected NPY neuron (Cowley et al., 2001).

The increase in body weight and hyperphagia seen in *RIPCreIrs2KO* mice was also reported by Kubota *et al.* who also reported that these mice are leptin resistant and therefore proposed that *Irs2* was deleted in a proportion on POMC neurons in the hypothalamus (Kubota *et al.*, 2004).

RIPCreIrs2KO mice display a distinctive constellation of phenotypes including increased adiposity and body length, hyperphagia, hyperinsulinaemia and hyperleptinaemia but retained sensitivity to leptin. This group of phenotypes, following Irs2 selective deletion, closely resembles that of mice with MC-4 receptor deletion (Huszar et al., 1997), suggesting that RIPCre neurons could be POMC neurons.

Analysis of serum leptin levels showed that, consistent with the increased adiposity, *RIPCreIrs2KO* mice were significantly hyperleptinaemic at 12 weeks of age. Following three days of leptin treatment food intake was significantly reduced in *RIPCreIrs2KO* mice, which also exhibited a reduction in body weight. Therefore, *RIPCreIrs2KO* mice are not resistant to leptin suggesting that the hypothalamic phenotype in these mice is not due to defects in leptin signalling in these neurons.

Central melanocortin pathways have also been shown to regulate insulin secretion and peripheral insulin action (Fan *et al.*, 2000; Obici *et al.*, 2001; Obici *et al.*, 2002b). *RIPCreIrs2KO* mice display marked hyperinsulinaemia at an early age before onset of obesity, an important feature of MC4R null mice. These findings suggest that there is potentially a reciprocal regulation of insulin and melanocortin action and that RIPCre neurons are a component of this mechanism with a positive input coming from RIPCre neurons.

In order to further investigate this, *RIPCreIrs2KO* mice were treated with the melanocortin receptor agonist, melanotan II. MTII significantly reduced food intake in both *RIPCreIrs2KO* and control mice although the *RIPCreIrs2KO* mice seemed to be more sensitive to the anorectic action of MC4 activation by MTII than control mice.

Electrophysiological analysis of RIPCre neurons carried out by Dr Smith showed that, unlike POMC neurons, RIPCre neurons depolarise in response to both leptin and MTII,

suggesting that RIPCre neurons could be mediating the effects of Irs2 via a melanocortin-sensitive pathway.

In addition to this, leptin was found to have no electrophysiological effect on RIPCRe neurons, suggesting that this is not a leptin-sensitive neuronal population. This is also supported by immunocytochemistry, which showed that, while RIPCre and POMC neurons are closely associated, they do not colocalise.

The STAT3 signalling pathway is a parallel pathway downstream of the leptin receptor, and STAT3 has previously been shown to play an important role in body weight regulation (Cui *et al.*, 2004).

RIPCreSTAT3KO mice showed no difference in body weight at 4 weeks of age. By 12 weeks of age however, they weighed significantly more then control mice. This increase in weight was found to be due to a significant increase in body fat. However, unlike the *RIPCreIrs2KO* mouse, *RIPCreSTAT3KO* mice are not hyperphagic.

This suggests that STAT3 in RIPCre neurones is needed for regulation of body weight, but that STAT3 in the β-cell is not necessary for normal islet function. This finding is in contrast to the findings of Cui et al) who reported glucose intolerance and defects in insulin secretion in the *RIPCreSTAT3KO* mouse (Cui *et al.*, 2004). However Lee et al used PDX Cre to delete STAT3 specifically in β-cells and also found no defects in glucose tolerance (Lee *et al.*, 2005).

The use of conditional gene targeting has therefore revealed distinct roles for Irs2 signalling in β cell regulation and particularly in hypothalamic function. These studies also suggest caution in the interpretation of mouse phenotypes where the RIPCre transgenic mouse has been used with the intention of achieving β cell-specific deletion. However, a critical interplay between peripheral and central Irs2-dependent signalling events in the regulation of energy homeostasis has been demonstrated.

Another problem of conditional gene targeting was recently highlighted by Lee *et al* who claimed that the phenotypes seen in mice with genes deleted using the RIPCre transgene are due to the presence of the transgene, and not the actual deletion of the gene.

Initial studies on the mouse lines discussed in this thesis indicated that there were no differences between any of the control genotypes and therefore the control data presented represents equal numbers of all the control genotypes (*RIPCre, Irs2flox, wt*). In light of this paper, glucose tolerance data from both crosses was re-analysed, separating the genotypes. This showed that, in these studies the *RIPCre* and control data were indistinguishable, while the *RIPCreIrs2KO* still appeared to be glucose intolerant compared to the two control groups. In addition to this, in the *RIPCreSTAT3* cross showed similar results, although the *RIPCreSTAT3KO* mouse is not significantly glucose intolerant compared to either control group.

Therefore, in these studies it is clear that the phenotypes described result from deletion of either *Irs2* or *STAT3* and not simply a result of expression on the Cre transgene.

In summary, *Irs2* in the β-cell is vital for maintenance of islet mass and function while *STAT3* has no role in the β-cell under normal conditions. These studies have also demonstrated that CNS Irs2 pathways acting in a neuronal population distinct from POMC and NPY neurons regulate energy homeostasis and growth, while STAT3 pathways in the same neuronal population regulate energy homeostasis but not growth. These observations clarify the role of Irs2 in β-cell and hypothalamic function and suggest that Irs2 signalling pathways may be a useful target in the treatment of diabetes and obesity.

REFERENCES

AHIMA, R.S., PRABAKARAN, D., MANTZOROS, C., QU, D., LOWELL, B., MARATOS-FLIER, E. & FLIER, J.S. (1996). Role of leptin in the neuroendocrine response to fasting. *Nature*, **382,** 250-2.

ALBARADO, D.C., MCCLAINE, J., STEPHENS, J.M., MYNATT, R.L., YE, J., BANNON, A.W., RICHARDS, W.G. & BUTLER, A.A. (2004). Impaired coordination of nutrient intake and substrate oxidation in melanocortin-4 receptor knockout mice. *Endocrinology*, **145,** 243-52.

ALONZI, T., MARITANO, D., GORGONI, B., RIZZUTO, G., LIBERT, C. & POLI, V. (2001). Essential role of STAT3 in the control of the acute-phase response as revealed by inducible gene inactivation [correction of activation] in the liver. *Mol Cell Biol*, **21,** 1621-32.

ARAKI, E., LIPES, M.A., PATTI, M.E., BRUNING, J.C., HAAG, B., 3RD, JOHNSON, R.S. & KAHN, C.R. (1994). Alternative pathway of insulin signalling in mice with targeted disruption of the IRS-1 gene. *Nature*, **372,** 186-90.

BAE, S.S., CHO, H., MU, J. & BIRNBAUM, M.J. (2003). Isoform-specific regulation of insulin-dependent glucose uptake by Akt/protein kinase B. *J Biol Chem*, **278,** 49530-6.

BALTHASAR, N., COPPARI, R., MCMINN, J., LIU, S.M., LEE, C.E., TANG, V., KENNY, C.D., MCGOVERN, R.A., CHUA, S.C., JR., ELMQUIST, J.K. & LOWELL, B.B. (2004). Leptin receptor signaling in POMC neurons is required for normal body weight homeostasis. *Neuron*, **42,** 983-91.

BANKS, A.S., DAVIS, S.M., BATES, S.H. & MYERS, M.G., JR. (2000). Activation of downstream signals by the long form of the leptin receptor. *J Biol Chem*, **275,** 14563-72.

BARASH, I.A., CHEUNG, C.C., WEIGLE, D.S., REN, H., KABIGTING, E.B., KUIJPER, J.L., CLIFTON, D.K. & STEINER, R.A. (1996). Leptin is a metabolic signal to the reproductive system. *Endocrinology*, **137,** 3144-7.

BERNAL-MIZRACHI, E., FATRAI, S., JOHNSON, J.D., OHSUGI, M., OTANI, K., HAN, Z., POLONSKY, K.S. & PERMUTT, M.A. (2004). Defective insulin secretion and increased susceptibility to experimental diabetes are induced by reduced Akt activity in pancreatic islet beta cells. *J Clin Invest*, **114,** 928-36.

BERNARD-KARGAR, C. & KTORZA, A. (2001). Endocrine pancreas plasticity under physiological and pathological conditions. *Diabetes*, **50 Suppl 1,** S30-5.

BOUWENS, L. & ROOMAN, I. (2005). Regulation of pancreatic beta-cell mass. *Physiol Rev*, **85,** 1255-70.

BRUNING, J.C., GAUTAM, D., BURKS, D.J., GILLETTE, J., SCHUBERT, M., ORBAN, P.C., KLEIN, R., KRONE, W., MULLER-WIELAND, D. & KAHN, C.R. (2000). Role of brain insulin receptor in control of body weight and reproduction. *Science*, **289,** 2122-5.

BURKS, D.J., DE MORA, J.F., SCHUBERT, M., WITHERS, D.J., MYERS, M.G., TOWERY, H.H., ALTAMURO, S.L., FLINT, C.L. & WHITE, M.F. (2000). IRS-2 pathways integrate female reproduction and energy homeostasis. *Nature*, **407,** 377-82.

BUTLER, A.A. & CONE, R.D. (2002). The melanocortin receptors: lessons from knockout models. *Neuropeptides*, **36,** 77-84.

BUTLER, A.E., JANSON, J., BONNER-WEIR, S., RITZEL, R., RIZZA, R.A. & BUTLER, P.C. (2003a). Beta-cell deficit and increased beta-cell apoptosis in humans with type 2 diabetes. *Diabetes*, **52,** 102-10.

BUTLER, A.E., JANSON, J., SOELLER, W.C. & BUTLER, P.C. (2003b). Increased beta-cell apoptosis prevents adaptive increase in beta-cell mass in mouse model of

type 2 diabetes: evidence for role of islet amyloid formation rather than direct action of amyloid. *Diabetes*, **52,** 2304-14.

CAMPFIELD, L.A., SMITH, F.J., GUISEZ, Y., DEVOS, R. & BURN, P. (1995). Recombinant mouse OB protein: evidence for a peripheral signal linking adiposity and central neural networks. *Science*, **269,** 546-9.

CANTRELL, D.A. (2001). Phosphoinositide 3-kinase signalling pathways. *J Cell Sci*, **114,** 1439-45.

CHANDRA, J., ZHIVOTOVSKY, B., ZAITSEV, S., JUNTTI-BERGGREN, L., BERGGREN, P.O. & ORRENIUS, S. (2001). Role of apoptosis in pancreatic beta-cell death in diabetes. *Diabetes*, **50 Suppl 1,** S44-7.

CHENG, D. (2005). Prevalence, predisposition and prevention of type II diabetes. *Nutr Metab (Lond)*, **2,** 29.

CHO, H., THORVALDSEN, J.L., CHU, Q., FENG, F. & BIRNBAUM, M.J. (2001). Akt1/PKBalpha is required for normal growth but dispensable for maintenance of glucose homeostasis in mice. *J Biol Chem*, **276,** 38349-52.

COHEN, B., NOVICK, D. & RUBINSTEIN, M. (1996). Modulation of insulin activities by leptin. *Science*, **274,** 1185-8.

COWLEY, M.A. (2003). Hypothalamic melanocortin neurons integrate signals of energy state. *Eur J Pharmacol*, **480,** 3-11.

COWLEY, M.A., SMART, J.L., RUBINSTEIN, M., CERDAN, M.G., DIANO, S., HORVATH, T.L., CONE, R.D. & LOW, M.J. (2001). Leptin activates anorexigenic POMC neurons through a neural network in the arcuate nucleus. *Nature*, **411,** 480-4.

CUI, Y., HUANG, L., ELEFTERIOU, F., YANG, G., SHELTON, J.M., GILES, J.E., OZ, O.K., POURBAHRAMI, T., LU, C.Y., RICHARDSON, J.A., KARSENTY, G. & LI, C.

(2004). Essential role of STAT3 in body weight and glucose homeostasis. *Mol Cell Biol*, **24,** 258-69.

DEFRONZO, R.A. (1997). Pathogenesis of type 2 diabetes: metabolic and molecular implications for identifying diabetes genes. *Diabetes Reviews*, **5,** 177-268.

DEL ZOTTO, H., BORELLI, M.I., FLORES, L., GARCIA, M.E., GOMEZ DUMM, C.L., CHICCO, A., LOMBARDO, Y.B. & GAGLIARDINO, J.J. (2004). Islet neogenesis: an apparent key component of long-term pancreas adaptation to increased insulin demand. *J Endocrinol*, **183,** 321-30.

DHILLON, H., ZIGMAN, J.M., YE, C., LEE, C.E., MCGOVERN, R.A., TANG, V., KENNY, C.D., CHRISTIANSEN, L.M., WHITE, R.D., EDELSTEIN, E.A., COPPARI, R., BALTHASAR, N., COWLEY, M.A., CHUA, S., JR., ELMQUIST, J.K. & LOWELL, B.B. (2006). Leptin Directly Activates SF1 Neurons in the VMH, and This Action by Leptin Is Required for Normal Body-Weight Homeostasis. *Neuron*, **49,** 191-203.

DIABETES UK (2005). Type 2 Diabetes & Obesity: A Heavy Burden

DOR, Y., BROWN, J., MARTINEZ, O.I. & MELTON, D.A. (2004). Adult pancreatic beta-cells are formed by self-duplication rather than stem-cell differentiation. *Nature*, **429,** 41-6.

EIZIRIK, D.L. & DARVILLE, M.I. (2001). beta-cell apoptosis and defense mechanisms: lessons from type 1 diabetes. *Diabetes*, **50 Suppl 1,** S64-9.

FAN, W., DINULESCU, D.M., BUTLER, A.A., ZHOU, J., MARKS, D.L. & CONE, R.D. (2000). The central melanocortin system can directly regulate serum insulin levels. *Endocrinology*, **141,** 3072-9.

FANTIN, V.R., WANG, Q., LIENHARD, G.E. & KELLER, S.R. (2000). Mice lacking insulin receptor substrate 4 exhibit mild defects in growth, reproduction, and glucose homeostasis. *Am J Physiol Endocrinol Metab*, **278,** E127-33.

FAROOQI, I.S., JEBB, S.A., LANGMACK, G., LAWRENCE, E., CHEETHAM, C.H., PRENTICE, A.M., HUGHES, I.A., MCCAMISH, M.A. & O'RAHILLY, S. (1999). Effects of recombinant leptin therapy in a child with congenital leptin deficiency. *N Engl J Med*, **341,** 879-84.

FLIER, J.S. (2004). Obesity wars: molecular progress confronts an expanding epidemic. *Cell*, **116,** 337-50.

FREDERICH, R.C., HAMANN, A., ANDERSON, S., LOLLMANN, B., LOWELL, B.B. & FLIER, J.S. (1995). Leptin levels reflect body lipid content in mice: evidence for diet-induced resistance to leptin action. *Nat Med*, **1,** 1311-4.

FRIEDMAN, J. (2002). Fat in all the wrong places. *Nature*, **415,** 268-9.

FRIEDRICHSEN, B.N., RICHTER, H.E., HANSEN, J.A., RHODES, C.J., NIELSEN, J.H., BILLESTRUP, N. & MOLDRUP, A. (2003). Signal transducer and activator of transcription 5 activation is sufficient to drive transcriptional induction of cyclin D2 gene and proliferation of rat pancreatic beta-cells. *Mol Endocrinol*, **17,** 945-58.

FRÜHBECK, G. (2006). Intracellular signalling pathways activated by leptin. *Biochem J*, **393,** 7-20.

FRUMAN, D.A., MAUVAIS-JARVIS, F., POLLARD, D.A., YBALLE, C.M., BRAZIL, D., BRONSON, R.T., KAHN, C.R. & CANTLEY, L.C. (2000). Hypoglycaemia, liver necrosis and perinatal death in mice lacking all isoforms of phosphoinositide 3-kinase p85 alpha. *Nat Genet*, **26,** 379-82.

GROPP, E., SHANABROUGH, M., BOROK, E., XU, A.W., JANOSCHEK, R., BUCH, T., PLUM, L., BALTHASAR, N., HAMPEL, B., WAISMAN, A., BARSH, G.S., HORVATH, T.L. & BRUNING, J.C. (2005). Agouti-related peptide-expressing neurons are mandatory for feeding. *Nat Neurosci*, **8,** 1289-91.

HALAAS, J.L., GAJIWALA, K.S., MAFFEI, M., COHEN, S.L., CHAIT, B.T., RABINOWITZ, D., LALLONE, R.L., BURLEY, S.K. & FRIEDMAN, J.M. (1995). Weight-reducing effects of the plasma protein encoded by the obese gene. *Science*, **269,** 543-6.

HENNIGE, A.M., BURKS, D.J., OZCAN, U., KULKARNI, R.N., YE, J., PARK, S., SCHUBERT, M., FISHER, T.L., DOW, M.A., LESHAN, R., ZAKARIA, M., MOSSA-BASHA, M. & WHITE, M.F. (2003). Upregulation of insulin receptor substrate-2 in pancreatic beta cells prevents diabetes. *J Clin Invest*, **112,** 1521-32.

HETHERINGTON, A.W. (1983). Nutrition Classics. The Anatomical Record, Volume 78, 1940: Hypothalamic lesions and adiposity in the rat. *Nutr Rev*, **41,** 124-127.

HOLMAN, G.D. & KASUGA, M. (1997). From receptor to transporter: insulin signalling to glucose transport. *Diabetologia*, **40,** 991-1003.

HOORENS, A., VAN DE CASTEELE, M., KLOPPEL, G. & PIPELEERS, D. (1996). Glucose promotes survival of rat pancreatic beta cells by activating synthesis of proteins which suppress a constitutive apoptotic program. *J Clin Invest*, **98,** 1568-74.

HUSZAR, D., LYNCH, C.A., FAIRCHILD-HUNTRESS, V., DUNMORE, J.H., FANG, Q., BERKEMEIER, L.R., GU, W., KESTERSON, R.A., BOSTON, B.A., CONE, R.D., SMITH, F.J., CAMPFIELD, L.A., BURN, P. & LEE, F. (1997). Targeted disruption of the melanocortin-4 receptor results in obesity in mice. *Cell*, **88,** 131-41.

ITOH, Y., KAWAMATA, Y., HARADA, M., KOBAYASHI, M., FUJII, R., FUKUSUMI, S., OGI, K., HOSOYA, M., TANAKA, Y., UEJIMA, H., TANAKA, H., MARUYAMA, M., SATOH, R., OKUBO, S., KIZAWA, H., KOMATSU, H., MATSUMURA, F., NOGUCHI, Y., SHINOHARA, T., HINUMA, S., FUJISAWA, Y. & FUJINO, M. (2003). Free fatty acids regulate insulin secretion from pancreatic beta cells through GPR40. *Nature*, **422,** 173-6.

JONES, L.C. & CLARK, A. (2001). beta-cell neogenesis in type 2 diabetes. *Diabetes*, **50 Suppl 1,** S186-7.

KAHN, B.B. & FLIER, J.S. (2000). Obesity and insulin resistance. *J Clin Invest*, **106,** 473-81.

KAJI, H., TAI, S., OKIMURA, Y., IGUCHI, G., TAKAHASHI, Y., ABE, H. & CHIHARA, K. (1998). Cloning and characterization of the 5'-flanking region of the human growth hormone secretagogue receptor gene. *J Biol Chem*, **273,** 33885-8.

KENNEDY, G.C. (1953). The role of depot fat in the hypothalamic control of food intake in the rat. *Proc R Soc Lond B Biol Sci*, **140,** 578-96.

KIEFFER, T.J. & HABENER, J.F. (2000). The adipoinsular axis: effects of leptin on pancreatic beta-cells. *Am J Physiol Endocrinol Metab*, **278,** E1-E14.

KUBOTA, N., TERAUCHI, Y., TOBE, K., YANO, W., SUZUKI, R., UEKI, K., TAKAMOTO, I., SATOH, H., MAKI, T., KUBOTA, T., MOROI, M., OKADA-IWABU, M., EZAKI, O., NAGAI, R., UETA, Y., KADOWAKI, T. & NODA, T. (2004). Insulin receptor substrate 2 plays a crucial role in beta cells and the hypothalamus. *J Clin Invest*, **114,** 917-27.

KULKARNI, R.N., BRUNING, J.C., WINNAY, J.N., POSTIC, C., MAGNUSON, M.A. & KAHN, C.R. (1999). Tissue-specific knockout of the insulin receptor in

pancreatic beta cells creates an insulin secretory defect similar to that in type 2 diabetes. *Cell*, **96,** 329-39.

KULKARNI, R.N., HOLZENBERGER, M., SHIH, D.Q., OZCAN, U., STOFFEL, M., MAGNUSON, M.A. & KAHN, C.R. (2002). beta-cell-specific deletion of the Igf1 receptor leads to hyperinsulinemia and glucose intolerance but does not alter beta-cell mass. *Nat Genet*, **31,** 111-5.

KULKARNI, R.N., WANG, Z.L., WANG, R.M., HURLEY, J.D., SMITH, D.M., GHATEI, M.A., WITHERS, D.J., GARDINER, J.V., BAILEY, C.J. & BLOOM, S.R. (1997). Leptin rapidly suppresses insulin release from insulinoma cells, rat and human islets and, in vivo, in mice. *J Clin Invest*, **100,** 2729-36.

KUSHNER, J.A., CIEMERYCH, M.A., SICINSKA, E., WARTSCHOW, L.M., TETA, M., LONG, S.Y., SICINSKI, P. & WHITE, M.F. (2005). Cyclins D2 and D1 are essential for postnatal pancreatic beta-cell growth. *Mol Cell Biol*, **25,** 3752-62.

LAWLOR, M.A., MORA, A., ASHBY, P.R., WILLIAMS, M.R., MURRAY-TAIT, V., MALONE, L., PRESCOTT, A.R., LUCOCQ, J.M. & ALESSI, D.R. (2002). Essential role of PDK1 in regulating cell size and development in mice. *Embo J*, **21,** 3728-38.

LEE, J.Y. & HENNIGHAUSEN, L. (2005). The transcription factor Stat3 is dispensable for pancreatic beta-cell development and function. *Biochem Biophys Res Commun*, **334,** 764-8.

LEE, J.Y., RISTOW, M., LIN, X., WHITE, M.F., MAGNUSON, M.A. & HENNIGHAUSEN, L. (2006). RIP-Cre revisited, evidence for impairments of pancreatic beta-cell function. *J Biol Chem*, **281,** 2649-53.

LIN, X., TAGUCHI, A., PARK, S., KUSHNER, J.A., LI, F., LI, Y. & WHITE, M.F. (2004). Dysregulation of insulin receptor substrate 2 in beta cells and brain causes obesity and diabetes. *J Clin Invest*, **114,** 908-16.

LINGOHR, M.K., DICKSON, L.M., MCCUAIG, J.F., HUGL, S.R., TWARDZIK, D.R. & RHODES, C.J. (2002). Activation of IRS-2-mediated signal transduction by IGF-1, but not TGF-alpha or EGF, augments pancreatic beta-cell proliferation. *Diabetes*, **51,** 966-76.

LIU, L., KARKANIAS, G.B., MORALES, J.C., HAWKINS, M., BARZILAI, N., WANG, J. & ROSSETTI, L. (1998). Intracerebroventricular leptin regulates hepatic but not peripheral glucose fluxes. *J Biol Chem*, **273,** 31160-7.

LU, Y., HERRERA, P.L., GUO, Y., SUN, D., TANG, Z., LEROITH, D. & LIU, J.L. (2004). Pancreatic-specific inactivation of IGF-I gene causes enlarged pancreatic islets and significant resistance to diabetes. *Diabetes*, **53,** 3131-41.

MAEDA, N., SHIMOMURA, I., KISHIDA, K., NISHIZAWA, H., MATSUDA, M., NAGARETANI, H., FURUYAMA, N., KONDO, H., TAKAHASHI, M., ARITA, Y., KOMURO, R., OUCHI, N., KIHARA, S., TOCHINO, Y., OKUTOMI, K., HORIE, M., TAKEDA, S., AOYAMA, T., FUNAHASHI, T. & MATSUZAWA, Y. (2002). Diet-induced insulin resistance in mice lacking adiponectin/ACRP30. *Nat Med*, **8,** 731-7.

MANDRUP-POULSEN, T. (2001). beta-cell apoptosis: stimuli and signaling. *Diabetes*, **50 Suppl 1,** S58-63.

MEDINA-GOMEZ, G. & VIDAL-PUIG, A. (2005). Gateway to the metabolic syndrome. *Nat Med*, **11,** 602-3.

MIZUNO, T.M., MAKIMURA, H., SILVERSTEIN, J., ROBERTS, J.L., LOPINGCO, T. & MOBBS, C.V. (1999a). Fasting regulates hypothalamic neuropeptide Y, agouti-

related peptide, and proopiomelanocortin in diabetic mice independent of changes in leptin or insulin. *Endocrinology*, **140,** 4551-7.

MIZUNO, T.M. & MOBBS, C.V. (1999b). Hypothalamic agouti-related protein messenger ribonucleic acid is inhibited by leptin and stimulated by fasting. *Endocrinology*, **140,** 814-7.

MORA, A., KOMANDER, D., VAN AALTEN, D.M. & ALESSI, D.R. (2004). PDK1, the master regulator of AGC kinase signal transduction. *Semin Cell Dev Biol*, **15,** 161-70.

MYERS, M.G., JR. & WHITE, M.F. (1996). Insulin signal transduction and the IRS proteins. *Annu Rev Pharmacol Toxicol*, **36,** 615-58.

NISWENDER, K.D., MORTON, G.J., STEARNS, W.H., RHODES, C.J., MYERS, M.G., JR. & SCHWARTZ, M.W. (2001). Intracellular signalling. Key enzyme in leptin-induced anorexia. *Nature*, **413,** 794-5.

NOVAK, A., GUO, C., YANG, W., NAGY, A. & LOBE, C.G. (2000). Z/EG, a double reporter mouse line that expresses enhanced green fluorescent protein upon Cre-mediated excision. *Genesis*, **28,** 147-55.

OBICI, S., FENG, Z., KARKANIAS, G., BASKIN, D.G. & ROSSETTI, L. (2002a). Decreasing hypothalamic insulin receptors causes hyperphagia and insulin resistance in rats. *Nat Neurosci*, **5,** 566-72.

OBICI, S., FENG, Z., TAN, J., LIU, L., KARKANIAS, G. & ROSSETTI, L. (2001). Central melanocortin receptors regulate insulin action. *J Clin Invest*, **108,** 1079-85.

OBICI, S., ZHANG, B.B., KARKANIAS, G. & ROSSETTI, L. (2002b). Hypothalamic insulin signaling is required for inhibition of glucose production. *Nat Med*, **8,** 1376-82.

O'RAHILLY, S., BARROSO, I. & WAREHAM, N.J. (2005). Genetic factors in type 2 diabetes: the end of the beginning? *Science*, **307,** 370-3.

OTANI, K., KULKARNI, R.N., BALDWIN, A.C., KRUTZFELDT, J., UEKI, K., STOFFEL, M., KAHN, C.R. & POLONSKY, K.S. (2004). Reduced beta-cell mass and altered glucose sensing impair insulin-secretory function in betaIRKO mice. *Am J Physiol Endocrinol Metab*, **286,** E41-9.

OUCHI, N., KIHARA, S., FUNAHASHI, T., MATSUZAWA, Y. & WALSH, K. (2003). Obesity, adiponectin and vascular inflammatory disease. *Curr Opin Lipidol*, **14,** 561-6.

PEETERS, A., BARENDREGT, J.J., WILLEKENS, F., MACKENBACH, J.P., AL MAMUN, A. & BONNEUX, L. (2003). Obesity in adulthood and its consequences for life expectancy: a life-table analysis. *Ann Intern Med*, **138,** 24-32.

PENDE, M., KOZMA, S.C., JAQUET, M., OORSCHOT, V., BURCELIN, R., LE MARCHAND-BRUSTEL, Y., KLUMPERMAN, J., THORENS, B. & THOMAS, G. (2000). Hypoinsulinaemia, glucose intolerance and diminished beta-cell size in S6K1-deficient mice. *Nature*, **408,** 994-7.

PICK, A., CLARK, J., KUBSTRUP, C., LEVISETTI, M., PUGH, W., BONNER-WEIR, S. & POLONSKY, K.S. (1998). Role of apoptosis in failure of beta-cell mass compensation for insulin resistance and beta-cell defects in the male Zucker diabetic fatty rat. *Diabetes*, **47,** 358-64.

PORTE, D., JR., BASKIN, D.G. & SCHWARTZ, M.W. (2002). Leptin and insulin action in the central nervous system. *Nutr Rev*, **60,** S20-9; discussion S68-84, 85-7.

PREVIS, S.F., WITHERS, D.J., REN, J.M., WHITE, M.F. & SHULMAN, G.I. (2000). Contrasting effects of IRS-1 versus IRS-2 gene disruption on carbohydrate and lipid metabolism in vivo. *J Biol Chem*, **275,** 38990-4.

RHODES, C.J. (2005). Type 2 diabetes-a matter of beta-cell life and death? *Science*, **307,** 380-4.

ROSEBERRY, A.G., LIU, H., JACKSON, A.C., CAI, X. & FRIEDMAN, J.M. (2004). Neuropeptide Y-mediated inhibition of proopiomelanocortin neurons in the arcuate nucleus shows enhanced desensitization in ob/ob mice. *Neuron*, **41,** 711-22.

SALTIEL, A.R. & KAHN, C.R. (2001). Insulin signalling and the regulation of glucose and lipid metabolism. *Nature*, **414,** 799-806.

SCAGLIA, L., SMITH, F.E. & BONNER-WEIR, S. (1995). Apoptosis contributes to the involution of beta cell mass in the post partum rat pancreas. *Endocrinology*, **136,** 5461-8.

SCHUBERT, M., BRAZIL, D.P., BURKS, D.J., KUSHNER, J.A., YE, J., FLINT, C.L., FARHANG-FALLAH, J., DIKKES, P., WAROT, X.M., RIO, C., CORFAS, G. & WHITE, M.F. (2003). Insulin receptor substrate-2 deficiency impairs brain growth and promotes tau phosphorylation. *J Neurosci*, **23,** 7084-92.

SCHWARTZ, M.W., WOODS, S.C., PORTE, D., JR., SEELEY, R.J. & BASKIN, D.G. (2000). Central nervous system control of food intake. *Nature*, **404,** 661-71.

SHEPHERD, P.R., WITHERS, D.J. & SIDDLE, K. (1998). Phosphoinositide 3-kinase: the key switch mechanism in insulin signalling. *Biochem J*, **333 (Pt 3),** 471-90.

SHIMABUKURO, M., ZHOU, Y.T., LEVI, M. & UNGER, R.H. (1998). Fatty acid-induced beta cell apoptosis: a link between obesity and diabetes. *Proc Natl Acad Sci U S A*, **95,** 2498-502.

SHIMOMURA, I., MATSUDA, M., HAMMER, R.E., BASHMAKOV, Y., BROWN, M.S. & GOLDSTEIN, J.L. (2000). Decreased IRS-2 and increased SREBP-1c lead to

mixed insulin resistance and sensitivity in livers of lipodystrophic and ob/ob mice. *Mol Cell*, **6,** 77-86.

SPANSWICK, D., SMITH, M.A., MIRSHAMSI, S., ROUTH, V.H. & ASHFORD, M.L. (2000). Insulin activates ATP-sensitive K+ channels in hypothalamic neurons of lean, but not obese rats. *Nat Neurosci*, **3,** 757-8.

STRAUB, S.G. & SHARP, G.W. (2002). Glucose-stimulated signaling pathways in biphasic insulin secretion. *Diabetes Metab Res Rev*, **18,** 451-63.

TARTAGLIA, L.A., DEMBSKI, M., WENG, X., DENG, N., CULPEPPER, J., DEVOS, R., RICHARDS, G.J., CAMPFIELD, L.A., CLARK, F.T., DEEDS, J. & ET AL. (1995). Identification and expression cloning of a leptin receptor, OB-R. *Cell*, **83,** 1263-71.

TERAUCHI, Y., TSUJI, Y., SATOH, S., MINOURA, H., MURAKAMI, K., OKUNO, A., INUKAI, K., ASANO, T., KABURAGI, Y., UEKI, K., NAKAJIMA, H., HANAFUSA, T., MATSUZAWA, Y., SEKIHARA, H., YIN, Y., BARRETT, J.C., ODA, H., ISHIKAWA, T., AKANUMA, Y., KOMURO, I., SUZUKI, M., YAMAMURA, K., KODAMA, T., SUZUKI, H., KOYASU, S., AIZAWA, S., TOBE, K., FUKUI, Y., YAZAKI, Y. & KADOWAKI, T. (1999). Increased insulin sensitivity and hypoglycaemia in mice lacking the p85 alpha subunit of phosphoinositide 3-kinase. *Nat Genet*, **21,** 230-5.

THORNTON, J.E., CHEUNG, C.C., CLIFTON, D.K. & STEINER, R.A. (1997). Regulation of hypothalamic proopiomelanocortin mRNA by leptin in ob/ob mice. *Endocrinology*, **138,** 5063-6.

TSUKIYAMA, S., MATSUSHITA, M., MATSUMOTO, S., MORITA, T., KOBAYASHI, S., TAMURA, H., KAMACHI, H., OZAKI, M. & TODO, S. (2006). Transduction of

Exogenous Constitutively Activated Stat3 into Dispersed Islets Induces Proliferation of Rat Pancreatic beta-cells. *Tissue Eng.*

UEKI, K., OKADA, T., HU, J., LIEW, C.W., ASSMANN, A., DAHLGREN, G.M., PETERS, J.L., SHACKMAN, J.G., ZHANG, M., ARTNER, I., SATIN, L.S., STEIN, R., HOLZENBERGER, M., KENNEDY, R.T., KAHN, C.R. & KULKARNI, R.N. (2006). Total insulin and IGF-I resistance in pancreatic beta cells causes overt diabetes. *Nat Genet*, **38,** 583-8.

UM, S.H., FRIGERIO, F., WATANABE, M., PICARD, F., JOAQUIN, M., STICKER, M., FUMAGALLI, S., ALLEGRINI, P.R., KOZMA, S.C., AUWERX, J. & THOMAS, G. (2004). Absence of S6K1 protects against age- and diet-induced obesity while enhancing insulin sensitivity. *Nature*, **431,** 200-5.

UNGER, J.W. & BETZ, M. (1998). Insulin receptors and signal transduction proteins in the hypothalamo-hypophyseal system: a review on morphological findings and functional implications. *Histol Histopathol*, **13,** 1215-24.

UNGER, R.H. & ZHOU, Y.T. (2001). Lipotoxicity of beta-cells in obesity and in other causes of fatty acid spillover. *Diabetes*, **50 Suppl 1,** S118-21.

VAN DEN TOP, M., LEE, K., WHYMENT, A.D., BLANKS, A.M. & SPANSWICK, D. (2004). Orexigen-sensitive NPY/AgRP pacemaker neurons in the hypothalamic arcuate nucleus. *Nat Neurosci*, **7,** 493-4.

VANHAESEBROECK, B. & ALESSI, D.R. (2000). The PI3K-PDK1 connection: more than just a road to PKB. *Biochem J*, **346 Pt 3,** 561-76.

WEISS, R., DZIURA, J., BURGERT, T.S., TAMBORLANE, W.V., TAKSALI, S.E., YECKEL, C.W., ALLEN, K., LOPES, M., SAVOYE, M., MORRISON, J., SHERWIN, R.S. & CAPRIO, S. (2004). Obesity and the metabolic syndrome in children and adolescents. *N Engl J Med*, **350,** 2362-74.

WHITEHEAD, J.P., RICHARDS, A.A., HICKMAN, I.J., MACDONALD, G.A. & PRINS, J.B. (2006). Adiponectin--a key adipokine in the metabolic syndrome. *Diabetes Obes Metab*, **8,** 264-80.

WILD, S., ROGLIC, G., GREEN, A., SICREE, R., & KING, H. (2004). Global Prevalance of Diabetes.*Diabetes Care*, **27**, 1047-1053

WILLIAMS, M.R., ARTHUR, J.S., BALENDRAN, A., VAN DER KAAY, J., POLI, V., COHEN, P. & ALESSI, D.R. (2000). The role of 3-phosphoinositide-dependent protein kinase 1 in activating AGC kinases defined in embryonic stem cells. *Curr Biol*, **10,** 439-48.

WITHERS, D.J. (2001). Insulin receptor substrate proteins and neuroendocrine function. *Biochem Soc Trans*, **29,** 525-9.

WITHERS, D.J., GUTIERREZ, J.S., TOWERY, H., BURKS, D.J., REN, J.M., PREVIS, S., ZHANG, Y., BERNAL, D., PONS, S., SHULMAN, G.I., BONNER-WEIR, S. & WHITE, M.F. (1998). Disruption of IRS-2 causes type 2 diabetes in mice. *Nature*, **391,** 900-4.

WOODS, S.C., LOTTER, E.C., MCKAY, L.D. & PORTE, D., JR. (1979). Chronic intracerebroventricular infusion of insulin reduces food intake and body weight of baboons. *Nature*, **282,** 503-5.

YANG, Q., GRAHAM, T.E., MODY, N., PREITNER, F., PERONI, O.D., ZABOLOTNY, J.M., KOTANI, K., QUADRO, L. & KAHN, B.B. (2005). Serum retinol binding protein 4 contributes to insulin resistance in obesity and type 2 diabetes. *Nature*, **436,** 356-62.

YILDIZ, B.O. & HAZNEDAROGLU, I.C. (2005). Rethinking leptin and insulin action: Therapeutic opportunities for diabetes. *Int J Biochem Cell Biol.*

YOON, K.H., KO, S.H., CHO, J.H., LEE, J.M., AHN, Y.B., SONG, K.H., YOO, S.J., KANG, M.I., CHA, B.Y., LEE, K.W., SON, H.Y., KANG, S.K., KIM, H.S., LEE, I.K. & BONNER-WEIR, S. (2003). Selective beta-cell loss and alpha-cell expansion in patients with type 2 diabetes mellitus in Korea. *J Clin Endocrinol Metab*, **88,** 2300-8.

ZHANG, Y., PROENCA, R., MAFFEI, M., BARONE, M., LEOPOLD, L. & FRIEDMAN, J.M. (1994). Positional cloning of the mouse obese gene and its human homologue. *Nature*, **372,** 425-32.

ZHAO, A.Z., SHINOHARA, M.M., HUANG, D., SHIMIZU, M., ELDAR-FINKELMAN, H., KREBS, E.G., BEAVO, J.A. & BORNFELDT, K.E. (2000). Leptin induces insulin-like signaling that antagonizes cAMP elevation by glucagon in hepatocytes. *J Biol Chem*, **275,** 11348-54.

ZIMMET, P., ALBERTI, K.G. & SHAW, J. (2001). Global and societal implications of the diabetes epidemic. *Nature*, **414,** 782-7.

ZRAIKA, S., DUNLOP, M., PROIETTO, J. & ANDRIKOPOULOS, S. (2002). Effects of free fatty acids on insulin secretion in obesity. *Obes Rev*, **3,** 103-12.

Appendix 1

Abbreviations

Abbreviation	Full name
4EBP1	4E-binding protein-1
ADP	adenosine diphosphate
AgRP	agouti-related protein
ARC	arcuate nucleus
ATP	adenosine triphosphate
AUC	area-under-the-curve
CDNA	complementary DNA
CART	cocaine-amphetamine-regulated transcript
CNS	central nervous system
Cre	loxP-specific recombinase enzyme
DMH	dorsomedial hypothalamus
DMV	dorso-motor nucleus of the vagus
ELISA	enzyme-linked immuno-sorbent assay
FBG	fasted blood glucose
FFAs	free Fatty Acids
G6pc	glucose 6-phosphatase
Gab1	Grb2-associated binder-1
Glut	glucose transporter
Grb2	growth factor receptor-bound protein-2
Gsk3	glycogen synthase kinase-3

GTT	glucose tolerance test
HPO	horseradish peroxidase
ICV	intracerebroventricular
i.p.	intraperitoneal
Igf1	insulin-like growth factor-1
Igf1	rinsulin-like growth factor-1 receptor
Irs	insulin receptor substrate
JAK2	janus-kinase 2
K_{ATP} channel	ATP-activated potassium channel
KO	knockout
LHA	lateral hypothalamus
LoxP	locus of 'cross(x)-over'
MAPK	mitogen-activated protein kinase
MRNA	messenger RNA
MTOR	mammalian target of rapamycin
NPY	neuropeptide Y
NTS	nucleus of the solitary tract
ObRb	leptin long-form receptor
p70S6K	protein-70 S6 kinase
Pck1	phospho*enol*pyruvate carboxykinase, cytosolic isoform
PCR	polymerase chain reaction
Pdk1	phosphoinositide-dependent kinase-1
Pgc1	peroxisome proliferator-activated receptor-gamma coactivator-1
PH	pleckstrin homology

PI3K	phosphatidylinositol-3 kinase
PIP3	phosphatidylinositol triphosphate
PKA	protein kinase A
PKB	protein kinase B
PKC	protein kinase C
POMC	proopiomelanocortin
Pparg	peroxisome proliferator-activated receptor-gamma
PTB	phosphotyrosine binding
PVN	paraventricular nucleus
Rb	retinoblastoma protein
Rictor	rapamycin-insensitive companion of mTOR
RIP	rat insulin promoter
Ser	serine
SH2	src homology-2
Shc	SH2-containing protein
Shp2	SH2 domain phosphatase-2
Sos	son of sevenless
Srebp/f	sterol regulatory element-binding protein/factor
STAT	signal transducer and activators of transcription
TG	triglycerides
VMH	ventromedial hypothalamus

APPENDIX 2

Publications arising from this work:

The role of insulin receptor substrate 2 in hypothalamic and ß cell function.

Agharul I. Choudhury, **Helen Heffron**, Mark A. Smith, Hind Al-Qassab, Allison W. Xu, Colin Selman, Marcus Simmgen, Melanie Clements, Marc Claret, Gavin MacColl, David C. Bedford, Kazunari Hisadome, Ivan Diakonov, Vazira Moosajee, Jimmy D. Bell, John R. Speakman, Rachel L. Batterham, Gregory S. Barsh, Michael L.J. Ashford and Dominic J. Withers

Journal of Clinical Investigation 2005 Apr; 115(4): 940-50

Other Publications:

Liver-specific deletion of insulin receptor substrate 2 does not impair hepatic glucose and lipid metabolism in mice

M. Simmgen, C. Knauf, M. Lopez, A. I. Choudhury, M. Charalambous, J. Cantley, D. C. Bedford, M. Claret, M. A. Iglesias, **H. Heffron**, P. D. Cani[2], A. Vidal-Puig, R. Burcelin and D. J. Withers

Diabetologia, 2006 Mar; 49(3): 552-61